Integration of fermentation and cooling crystallisation to produce organic acids

Integration of fermentation and cooling crystallisation to produce organic acids

Proefschrift

ter verkrijging van de graad van doctor
aan de Technische Universiteit Delft,
op gezag van Rector Magnificus Prof.ir. K.C.A.M. Luyben,
voorzitter van het College voor Promoties,
in het openbaar te verdedigen op vrijdag 25 juni 2010 om 12:30 uur

door

Carol Andrea ROA ENGEL

Chemical Engineer and Bioprocess Designer
geboren te Bogotá, Colombia.

Dit proefschrift is goedgekeurd door de promotor:

Prof.dr. L.A.M. van der Wielen

Copromotor: Dr.ir. A.J.J. Straathof

Samenstelling promotie commissie:

Rector Magnificus	voorzitter
Prof.dr.ir. L.A.M. van der Wielen	Technische Universiteit Delft, promoter
Dr.ir. A.J.J. Straathof	Technische Universiteit Delft, copromotor
Prof. J. Woodley	Danmarks Tekniske Universitet
Prof.ir. J.P.M. Sanders	Wageningen Universiteit
Prof.dr.ir. A.I.Stankiewicz	Technische Universiteit Delft
Prof.dr.ir. J.J. Heijnen	Technische Universiteit Delft
Dr.ir. H. Noorman	DSM Biotechnology Center - Delft

Original picture of the cover taken by Leonie Marang

Diego,
you might find it boring to read this thesis,
but every word is written with all my love to you.

Contents

CHAPTER 1

Introduction

Fermentation has become a very important alternative in the production of different kinds of organic acids (Goldberg et al., 2006). Metabolic engineering and genetic tools have been used to improve fermentation titers and make fermentation technologies very competitive for industrial purposes (Goldberg et al., 2006, Zelle et al., 2008; van Maris et al., 2004). However, many times high fermentation titers lead to problems during fermentation, caused by product inhibition, which affects the performance of the strain (Freeman et al., 1993; Woodley et al., 2007). Because the competitive pressure of the industrial development, it is necessary to solve inhibition problems during fermentation, which might also improve cost, quality, environmental impact, safety, and process yields in order to make bioprocesses feasible (Stark and von Stockar 2003; Woodley et al., 2007). Additionally, for many bioprocesses a large cost factor in manufacture is in the downstream process where product separation and purification is carried out (Schügerl and Hubbuch, 2005). In situ product recovery (ISPR) has been studied for different processes giving promising results in the reduction of product inhibition and the number of downstream steps, and might therefore reduce cost and environmental impact of biotechnology processes.

The choice of the right ISPR technique depends of the nature of the product to be recovered and the conditions in the fermentation (Freeman et al., 1993). Furthermore, the configurations of the ISPR should be evaluated according to the location and purpose of the recovery unit (Freeman et al., 1993; Stark and von Stockar, 2003). A more detailed explanation of ISPR will be given in the following section. In the case of organic acids, precipitation has been applied extensively as a recovery and purification technique but leading waste salts production (Ling and Ng, 1989). In this thesis crystallisation as a recovery unit within ISPR framework will be addressed to recover an organic acid reducing waste salts formation. The integration of crystallisation and fermentation will be described for the model systems under study.

1   In situ product recovery as a process integration tool

In situ product recovery or removal (ISPR) has been also called extractive fermentation or bioconversion (biotransformation). The objective of ISPR is to take a product from its producing cell or production environment (Woodley et al., 2007). ISPR is characterised by product accumulation and its removal from the cell or enzyme vicinity (Freeman et al., 1993; Stark and von Stockar 2003). Therefore, ISPR is designed to improve yield and productivities of a process via the following strategies (Freeman et al., 1993):

- Minimisation of product after is being produced, allowing continuous expression of maximal production level
- Reduction of product losses
- Reduction in the number of the downstream steps

The potential of ISPR is not only to improve a process but also to open options for the introduction of new processes depending on ISPR.

Different configurations for ISPR process have been presented (Freeman et al., 1993; Stark and von Stockar 2003; Woodley et al., 2007). These configurations are mainly divided into two categories: internal and external product removal. For each of these two categories, direct and indirect contact with the production vessel can be designed (Figure 1).

The Internal configuration implies the integration in one vessel of the fermentation/reaction unit with the product recovery unit. For the external configuration, the units work separately. As the name suggest, direct contact involves immediate contact of the media containing the cells or enzyme with the recovery unit, which is not the case for indirect contact. Despite of the process configuration, ISPR is a useful strategy to overcome inhibition/toxicity problems via integration of the reaction (or fermentation) with the first step of the downstream process.

The success of the ISPR process does not depend only in the appropriately chosen configuration but also in the appropriate recovery technique and unit. Five principal product properties have been proposed to help choose the most favourable ISPR technique (Freeman et al., 1993). These properties are: Volatility (boiling point < 80 $^{\circ}$C), hydrophobicity (Log P_{oct} > 0.8), size (molecular weight < 1000 Da), charge (positive, negative, neutral) and specific binding properties. From these properties one can select the appropriate ISPR technique. The ISPR techniques have been classified in different groups as is shown in Table 1.

However, crystallisation has not been widely considered as a recovery technique in the cited literature. When crystallisation is suitable as a recovery technique, it provides the desired product in the crystal form, which might avoid auxiliary phases. Furthermore, subsequent purification units can be minimised if the product is recovered in the crystal form.
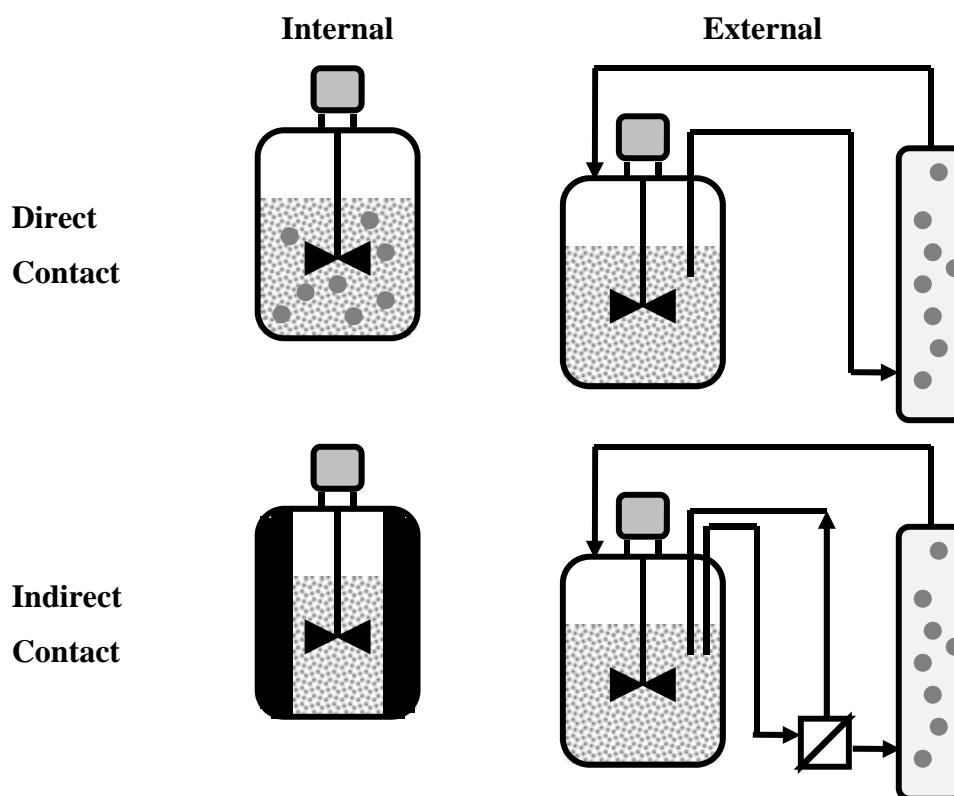
Figure 1: Configurations for the application of ISPR techniques (adapted from Woodley et al., 2007)

Table 1: ISPR techniques classification. (Stark and von Stockar, 2003)

ISPR technique	
Evaporation	Stripping, distillation, pervaporation, transmembrane distillation
Extraction	Organic solvent, supercritical fluid, reactive
Permeation	Dialysis, electrodialysis, reverse osmosis, nanofiltration
Immobilisation	Hydrophobic adsorption, ion-exchange, affinity adsorption.
Precipitation	

2   In situ product recovery of fermentation products by cooling crystallisation

As reviewed by Stark and von Stockar (2003), all the techniques listed in Table 1 have been used as recovery techniques for ISPR configurations. Although crystallisation was recognised as a recovery technique; it had not been studied/applied so much yet (Stark and von Stockar, 2003). Nevertheless, a recent study conducted by Buque-Taboada et al. (2006) presented the feasibility of using cooling crystallisation in an ISPR configuration to produce 6R-dihydro-oxoisophorone. The

microbial formation was suffering from product inhibition, which was overcome by external product crystallisation including a cell retention unit. Moreover, L-phenylalanine recovery by cooling crystallisation from fermentation media has been investigated to reduce product inhibition and increase the general process productivity (Cuellar Soares, 2008).

When the fermentation product titer is very close to the solubility limit (products with an aqueous solubility between about 0.0003 and 0.2 M (Straathof, 2003)), the potential to apply ISPR by crystallisation increases (Straathof, 2003). The product solution can be taken from the fermentor and after cells have been removed, the product can be crystallised. In the specific case of organic acid production by fermentation the pH has to be controlled at a value where the strain is capable to keep producing the acid. With the integration of crystallisation and fermentation not only inhibition might be reduced but also consumption of neutralising agents. This is due to the fact the direct product recovery from the fermentor could avoid high acid concentrations titers and then the use of neutralising agents, which are used to keep the pH at desired values would be less. This will avoid production of waste salts. Furthermore, after crystals removed from the mother liquor of the crystallisation, which can contain nutrients and neutralising compounds, the mother liquor can be reused in the fermentation. This might improve yields and process productivities.

3 Model systems

3.1 Fumaric acid

Fumaric has become a very interesting compound in the biotechnology field (Werpy and Petersen, 2004). Among the different food applications of fumaric acid, this one can be used as starting material in the bio-polymer industry. Nowadays, fumaric acid is produce via chemical conversion of maleic anhydride. However, this process involves the use of petrochemical raw materials (Lohbeck et a., 1990). Therefore, the fermentation route to produce fumaric acid has been attracting interest not only because the use of renewable raw materials but also for the potential of using CO_2 as an additional carbon source (Zhou, 1999). The following equation indicates the theoretical fumaric acid production by *Rhizopus* species.

$$C_6H_{12}O_6 + 2CO_2 \rightarrow 2C_4H_4O_4 + 2H_2O$$
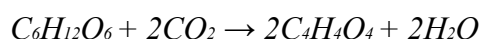
The potential of using fermentative produced fumaric acid is presented in a detailed review in Chapter 2 of this thesis. Because of the low solubility of fumaric acid (7 g L^{-1} (Stephen, 1965)),

recovery from fermentation broth by cooling crystallisation presents a very good option for process integration and for reduction of inorganic bases required to neutralise the produced fumaric acid. Figure 2 presents the aimed process scheme to produce fumaric acid via the integration of fermentation and cooling crystallisation.
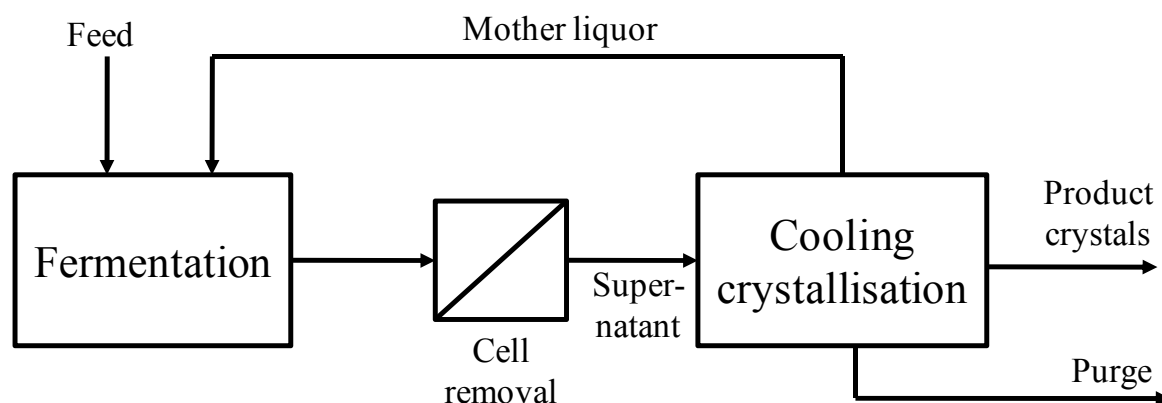

Figure 2: Process scheme to produce fumaric acid via integration of fermentation and cooling crystallisation.

3.2 7-Aminodeacetoxycephalosporanic and 6-aminopenicillanic acids

An increasing number of bacterial strains have become resistant to Pen G, which was phased out of clinical use in the late 1960s. Since then, a large range of alternative β-lactam antibiotics has been developed, which are very effective against bacterial diseases. These consist of penicillins and cephalosporins, for which the β-lactam nuclei 6-aminopenicillanic acid (APA) and 7-aminodeacetoxycephalosporanic acid (ADCA) are the major starting materials (Bruggink, 2001). The processes to produce these two acids include solvent extraction units that involve the use of aromatic compounds and also require many downstream process steps (Diender et al., 2002). These two acids are chosen because their conversion titers are very close to the solubility limit of the compound to be crystallised by cooling. Furthermore, to reduce the number of units operations ISPR configurations will be studied to produce 6-APA and 7-ADCA. The concept applied for fumaric acid production will also be studied for 6-APA and 7-ADCA production (Figure 2), but the latter processes also involve an enzymatic conversion step. This offers the possibility to integrate the crystallisation and conversion steps and also the possibility to integrate fermentation and conversion steps (Schroën et al., 2002). ISPR techniques will be applied here to integrate the production units with the crystallisation unit.

4   Strategy and outline of the thesis

As mentioned before, the use of crystallisation as a recovery technique within the framework of ISPR configurations has been little investigated, although crystallisation has been proven to be a feasible technique to overcome product inhibition problems. In the case of organic acids, fermentation/conversion processes should minimise the use of inorganic bases that are required to neutralise the fermentation broth because of the low pH achieved when the acid concentration is increasing. When neutralising agents are used at pH values where the acid is completely dissociated, the production of waste salts is stoichiometric to the production of the acid, adding in this way an environmental problem to the process. This thesis presents a study on crystallisation for recovery of organic acids, to overcome problem inhibition and use of neutralising agent in the fermentation/conversion units. Fumaric and 7-aminodeacetoxycephalosporanic acids can be used as model systems since their solubility values are quite low (fumaric acid 7 g L^{-1} and 7-ADCA 2.8 g L^{-1} (Stephen, 1965; Roa Engel et al., 2009). We expect to achieve during fermentation production/conversion higher values than the solubility ones at low temperatures (0 – 5 ^{o}C) and then be able to use of cooling crystallisation as recovery technique. Furthermore, the strains used for these fermentations can be cultivated easily in batch and fed-batch mode.

The aim of this thesis is to strengthen the understanding of using crystallisation as a recovery unit in the framework of ISPR configurations for further applications to other organic production systems. The questions of how the units can be integrated and how the product can be recovered are answered by addressing windows of operation, low pH fermentations/conversions, and limitations in the cooling crystallisation system. The outcome of this study is presented in this thesis as follows:

Chapters 2-5 cover the study concerned to fumaric acid and its production via the integration of fermentation and crystallisation. In this section, **Chapter 2** gives a detailed review of the production of fumaric acid via fermentation. After studying the potential of producing fumaric acid by fermentation the possibilities of integrating fermentation and crystallisation become clearer. **Chapter 3** focuses on the experimental study of fumaric acid fermentation. First, an experimental study to produce *R. oryzae* pellets is conducted in shake flasks to determine the conditions to produce *R. oryzae* pellets between 1 – 1.5 mm in 700 - 1000 mL shake flask working volume. Moreover, the effect of pH during the fermentation of *R. oryzae* is studied using glucose and carbon dioxide as carbon sources, and sodium hydroxide as a neutralising agent. In **Chapter 4**, through an analysis of multicomponent phase diagrams, the operating conditions for the integration of the fermentation and crystallisation to produce fumaric acid crystals is studied. The window of operation

shows that the integrated system has to work at pH 3.5. **Chapter 5** describes the integration of fermentation and cooling crystallisation to produce fumaric acid crystals. The integration is evaluated experimentally and the production of fumaric acid crystals is achieved on laboratory scale.

Chapter 6 focuses on the feasibility to produce 7-ADCA via the application of ISPR configurations. Here a detailed mathematical model is used to simulate the production of 7-ADCA by the integration of fermentation and deacylation together with cooling crystallisation as a recovery technique. **Chapter 7** contains the concluding remarks and outlook of the thesis.

References

Bruggink, A (2001) Synthesis of β-lactam antibiotics. Chemistry, biocatalysis and process integration. Kluwer Academic Publishers. Dordrecht, The Netherlands.

Buque-Taboada EM, Straathof AJJ, Heijnen JJ, van der Wielen LAM (2006) In situ product recovery (ISPR) by crystallization: basic principles, design, and potential applications in whole-cell biocatalysis. Appl Microbiol Biotechnol (71) 1.

Cuellar Soares MC (2008) Towards the integration of fermentation and crystallization. A study on the production of L-phenylalanine. PhD Thesis. TU Delft, Delft, The Netherlands. pp163.

Diender M, Straathof AJJ, Van der Does T, Ras C, Heijnen JJ (2002) Equilibrium modelling of extractive enzymatic hydrolysis of penicillin G with concomitant 6-aminopenicillanic acid precipitation. Biotechnol Bioeng (78) 395.

Freeman A, Woodley JM, Lilly MD (1993) In situ product removal as a tool for bioprocessing. Bio/technology (11) 1007.

Goldberg I, Rokem JS, Pines O (2006) Organic acids: old metabolites, new themes. J Chem Tech Biotechnol (81) 1601.

Ling LB and Ng TK (1989) Fermentation process for carboxylic acids. US4877731.

Lohbeck K, Haferkorn H, Fuhrmann W, Fedtke N (1990) Maleic and fumaric acids. Ullmann's Encyclopedia of Industrial Chemistry, 5th ed., Vol. A16, VCH., 53-62. Weinheim, Germany.

Roa Engel CA, Straathof AJJ, van Gulik WM, van de Sandt EJAX, van der Does T, van der Wielen LAM (2009) Conceptual Process Design of Integrated Fermentation, Deacylation and Crystallization in the Production of β-Lactam Antibiotics. Ind Eng Chem Res (48) 4352.

Schroën CGPH, Nierstrasz VA, Bosma, R, Kroon PJ, Tjeerdsma PS, de Vroom E, van der Laan JM, Moody HM, Beeftink HH, Janssen AE, Tramper J (2002) Integrated reactor concepts for the enzymatic kinetic synthesis of Cephalexin. Biotechnol Bioeng (80) 144.

Schugerl K, Hubbuch J (2005) Integrated bioprocesses. Curr Opin Biotech (8) 294.

Stephen WI (1965) Solubility and pH calculations. Anal Chim Acta (33) 227.

Stark D, von Stockar U (2003) In situ product removal (ISPR) in whole cell biotechnology during the last twenty years. Adv Biochem Eng Biotechnol (80) 149.

Straathof AJJ (2003) Auxiliary phase guidelines for microbial biotransformations of toxic susbtrate into toxic product. Biotechnol Prog (19) 755.

van Maris AJA, Konings WN, van Dijken JP, Pronk JT (2004) Microbial export of lactic and 3-hydroxypropanoic acid: implications for industrial fermentation processes. Metab Eng (6) 245.

Werpy T and Petersen G (2004) Topten value added chemicals from biomass feedstocks. U.S. Department of Energy. USA.

Woodley JM, Bisschops M, Straathof AJJ, Ottens M (2007) Perspective. Future directions for in situ product removal. J Chem Tech Biotechnol (83) 121.

Zelle RM, de Hulster E, van Winden WA, de Waard P, Dijkema C, Winkler AA, Geertman JMA, van Dijken JP, Pronk JT, van Maris AJA (2008) Malic acid production by *Saccharomyces cerevisiae*: Engineering of pyruvate carboxylation, oxaloacetate reduction, and malate export. Appl Environ Microbiol 74 (9) 2766.

Zhou Y (1999) Fumaric acid fermentation by *Rhizopus oryzae* in submerged system. Thesis dissertation. Purdue University. La Fayette, Indiana, USA. pp149.

SECTION 1

Fumaric acid

CHAPTER 2

Fumaric acid production by fermentation

The potential of fumaric acid as a raw material in the polymers industry and the increment of cost of petroleum-based fumaric acid raises interest in fermentation processes for production of this compound. Although petroleum-based fumaric acid production has a higher yield (112 %w/w) than fermentative production based on renewable resources (85 %w/w), the fact that the fermentation fumaric acid production fixes CO_2 and uses a glucose as a raw material, brings the attention back to the fermentation process. Moreover, current petroleum-based fumaric acid production uses maleic anhydride, which is three times more expensive than the fermentation process raw material, glucose. Production of fumaric acid by *Rhizopus* species and the involved metabolic pathways are reviewed. Submerged fermentation systems coupled with product recovery techniques seem to have achieved economically attractive yields and productivities. Future prospects for improvement of fumaric acid production include metabolic engineering approaches in order to achieve low pH fermentations.

1   Introduction

Fumaric acid (Figure 1) is a naturally occurring organic acid. It was first isolated from the plant *Fumaria officinalis*, from which it derives its name. Many microorganisms produce fumaric acid in small amounts, as it is a key intermediate in the citrate cycle. Fumaric acid is also known as (*E*)-2-butenedioic acid or *trans*-1,2-ethylenedicarboxylic acid. Sometimes the term "fumarates" is also used. In this review this general term is not used to describe fumaric acid esters like dimethyl fumarate but only to describe the salts of fumaric acid (sodium fumarate, calcium fumarate).

Currently, fumaric acid is produced chemically from maleic anhydride, which in turn is produced from butane. However, as petroleum prices are rising rather quickly, maleic anhydride as a petroleum derivative has increased in price as well (Anonymous, 2007). This situation has caused a renewed interest in the fumaric acid production by fermentation that was operational during the 1940s (Goldberg et al., 2006), but was discontinued and replaced by petrochemical processes. The fermentation process is also interesting because it involves carbon dioxide fixation, as will be discussed later. Fungi are known for their organic acid producing capability and have been used in fermentation processes for fumaric acid production.

Production by filamentous fungi of organic acids, including fumaric acid, has recently been reviewed (Magnuson and Lasure, 2004; Goldberg et al., 2006). These reviews focused on the microorganisms with their associated metabolic pathways. In contrast, the current review focuses on development of fumaric acid production processes. After summarising fumaric acid properties, applications and production, metabolic pathways for fumaric acid production will be discussed only briefly before turning to fermentation performance of the most prominent fumaric acid producing strains. Furthermore, different methods that have been studied in order to optimise fermentation processes will be mentioned and future prospects for process development will be discussed.

2   Properties and applications of fumaric acid

Because of its structure (a carbon-carbon double bond and two carboxylic acid groups), fumaric acid has many potential industrial applications (Figure 1). It can act as starting material for polymerisation and esterification reactions (www.the-innovation-group.com/ChemProfiles/ Fumaric%20Acid.htm; 10/06/07).
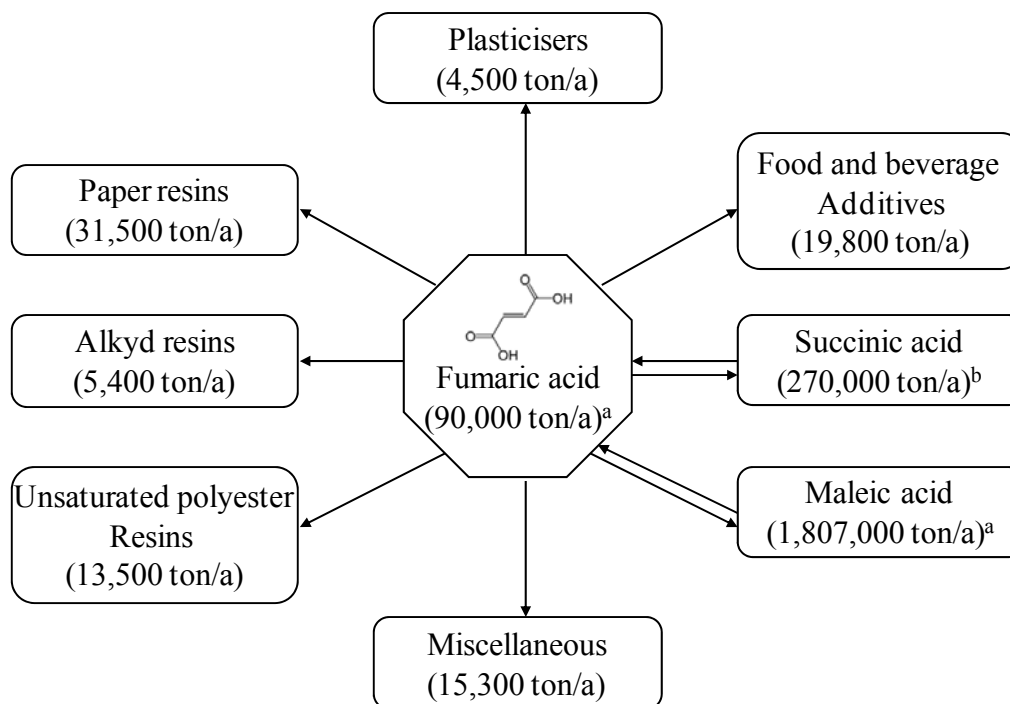
Figure 1: Current applications of fumaric acid production. Miscellaneous include: lubricating oil, inks, lacquers, carboxylating agent for styrenebutadiene rubber, personal care additives. a) Anonymous, 2007; b) Willke and Vorlop, 2004.

As raw material for polymerisation, especially in the production of unsaturated polyester resins, maleic anhydride is currently preferred to fumaric acid because maleic anhydride (1.46 - 1.63 $/kg; (Anonymous, 2007)) is cheaper than fumaric acid, the latter historically being around 10% more expensive than maleic anhydride (http://www.chemweek.com/inc/articles /t/2007/04/04/04/022.html). However, fumaric acid could be a better option for the polymers industry among other carboxylic acids or their derivatives, because of its non-toxic nature. In addition special properties like greater hardness in the polymer structure can be achieved when fumaric acid is used (www.the-innovation-group.com/ChemProfiles/Fumaric%20Acid.htm; 10/06/07). In addition to polymerisation, there are two potentially new applications for fumaric acid and both require a different grade of purity of it. The first is as a medicine to treat psoriasis, a skin condition (Altmeyer et al., 1994; Mrowietz et al., 1998). Psoriatic individuals are unable to produce fumaric acid in their body (which is not the case in normal individuals) due to a certain bio-chemical defect that interferes with adequate fumaric acid production in the skin. Therefore, psoriatic individuals need to take orally fumaric acid in form of fumaric acid monoethyl or dimethyl ester to treat their disease. The second potential application of fumaric acid is as supplement in cattle feed. Recent studies indicate that a large reduction in the methane emissions of cattle can be achieved (up to 70%), if this cattle receives fumaric acid based additive as a supplement in their diet (Mcginn et

al., 2004). This could greatly reduce the total emission of methane, as farm animals are responsible for 14 % of the methane emission caused by human activity.

Fumaric acid, together with the related succinic and malic acids, has been identified as one of the top ten building block chemicals that can be produced from sugars via biological or chemical conversion (Werpy and Petersen, 2004). As compared to these other dicarboxylic acids, fumaric acid has a low aqueous solubility (7 g/kg at 25 $^{\circ}$C; 89 g/kg at 100 $^{\circ}$C (Stephen, 1965)) and low pK_a values (3.03 and 4.44 (Lohbeck et al., 2005)), which are properties that can be exploited for product recovery.

3   Fumaric acid production by petrochemical routes

Fumaric acid is currently produced by isomerisation of maleic acid, which is produced from maleic anhydride. Maleic anhydride, in turn, is industrially produced by catalytic oxidation of suitable hydrocarbons in the gas phase. Benzene used to be the predominant starting material, but oxidation of n-butane or n-butane-n-butene mixtures has become more important in recent years (Lohbeck et al., 2005). The butane oxidation reaction that produces maleic anhydride and the subsequently conversion of maleic anhydride to fumaric acid are as follows:

$$C_4H_{10} + 3.5\ O_2 \rightarrow C_4H_2O_3 + 4\ H_2O$$
$$C_4H_2O_3 + H_2O \rightarrow C_4H_4O_4$$
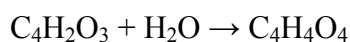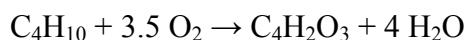
In the most common maleic anhydride process, the catalyst is embedded in fixed bed tubular reactors. The catalysts applied in this process are based on vanadium and phosphorus oxides. In this process, water is formed as a by-product and a fairly small amount of it can be directly liquefied from the reaction gas by partial condensation. Organic solvents absorb maleic anhydride contained in the reaction gas. More than 98% of the anhydride can be absorbed in this way. The solvent–anhydride mixture is then subjected to fractional distillation to separate maleic anhydride from the solvent and the latter is returned to the absorption column (Lohbeck et al., 2005). The thus obtained pure maleic anhydride is then hydrolysed into maleic acid.

Subsequently, the maleic acid is converted almost quantitatively by thermal or catalytic cis-trans isomerisation into fumaric acid (Lohbeck et al., 2005). The most common catalysts used are mineral acids, peroxy compounds and thiourea. The crude fumaric acid obtained in this way is purified by

crystallisation from water (Figure 2). As will be shown later, a comparable purification may be used for fermentative fumaric acid production.
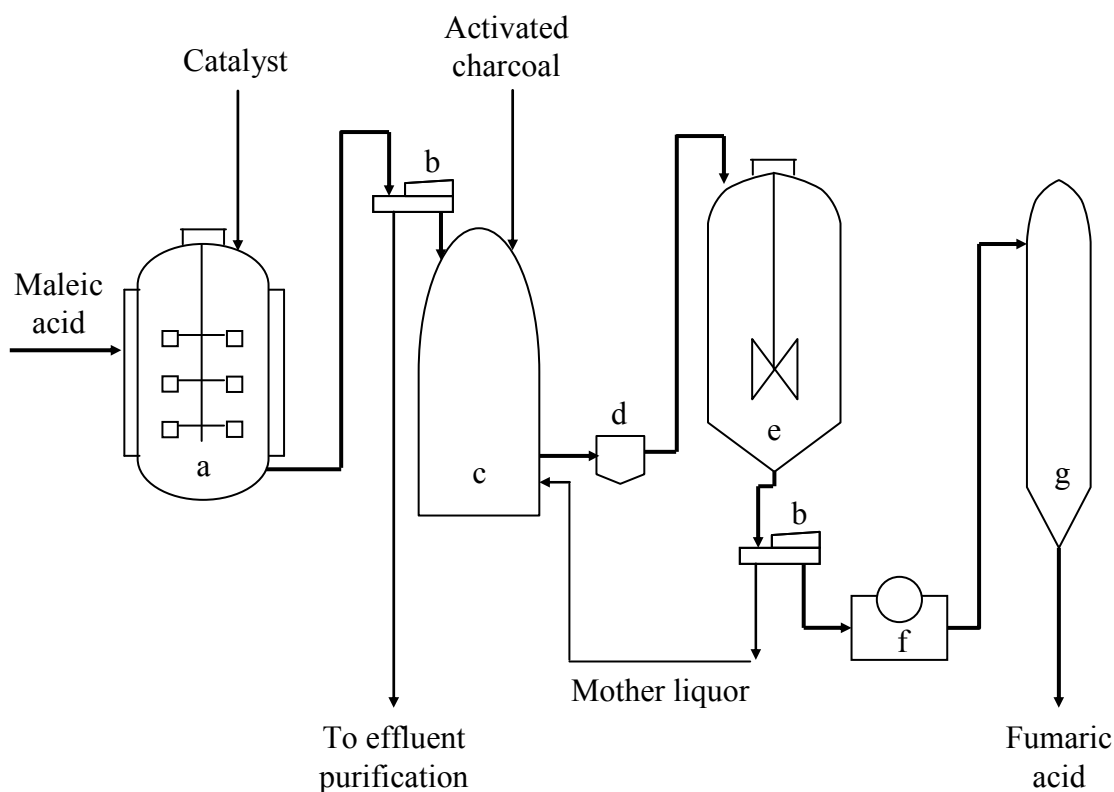
Figure 2: Plant for fumaric acid production from malic acid. a) Isomerisation vessel; b) Centrifuge; c) Dissolving tank; d) Filter; e) Crystalliser; f) Dryer. (Adapted from Felthouse et al. 2001).

Production capacity of maleic anhydride in 2007 was about 1,807,000 ton/a (Anonymous, 2007), with around 3% of this being used for fumaric acid production (http://chemicalmarketreporter.com /home/Default.asp?type=17&liArticleID=2015643...;18/04/2007) corresponding to 90,000 ton/a.

4   Enzymatic conversion of maleic acid into fumaric acid

In the aforementioned chemical isomerisation of maleic acid into fumaric acid, the conversion yield is restricted by the reaction equilibrium. This chemical conversion is occurring at high temperatures that causes formation of byproducts from maleic and fumaric acids and as a consequence yields are below the equilibrium yields (Goto et al., 1998). This problem was the main motivation to look for a good enzyme that would facilitate isomerisation. Equilibrium mixture is obtained without formation of by-products.

It is known that the enzyme maleate isomerase (maleate cis-trans-isomerase) isomerises maleic acid into fumaric acid. Microorganisms that produce maleate isomerase are *Pseudomonas* species (Otsuka, 1961), *Alcaligenes faecalis* (Takamura et al., 1969) and *Pseudomonas fluorescens* (Scher and Lennarz, 1969). However, maleate isomerase is unstable even at moderate temperatures (Takamura et al., 1969) and therefore a heat-stable maleate isomerase is desired. Thermo-stable maleate isomerases derived from *Bacillus stearothermophilus*, *Bacillus brevis* and *Bacillus sp. MI-105* were reported by Goto et al. (1998) and according to the authors, the use of enzymes from these bacteria can improve the fumaric acid production process.

Furthermore, in a more recent study using *Pseudomonas alcaligenes* XD-1 high rates of conversion of maleic acid into fumaric acid (6.98 g L^{-1} h^{-1}) were reported (NakajimaKambe et al., 1997). This organism does not normally accumulate fumaric acid, but by heat treatment of the cells (70°C for 1 h), they lost their fumarase activity, which otherwise would be responsible for a conversion of fumaric acid into L-malic acid. This heat treatment did not affect the maleate isomerase activity. In addition, when calcium ions were added during the conversion step the thermal stability of maleate isomerase was increased. With the use of *Pseudomonas alcaligenes* XD-1, the highest reported conversion yield, 95%, was achieved in the conversion of maleic acid to fumaric acid (Ichikawa et al., 2003). Immobilisation of the heat-treated cells is currently under investigation.

5 Microbial production of fumaric acid

Fumaric acid production by fermentation was operated in the United States during the 1940s but later this process was discontinued and replaced by chemical synthesis from petrochemical feedstocks, the latter being explained in a previous section. Nevertheless, the continuous increase of the petroleum prices has brought back the interest in fumaric acid production by submerged fermentation (Goldberg et al., 2006). Fumaric acid production by fermentation using *Rhizopus* species has been patented occasionally (Waksman, 1943; Kane, 1943; Lubowitz and La Roe, 1958; Le Roe, 1959; Goldberg and Stieglitz, 1986). In 1989, DuPont patented an improved fermentation process producing carboxylic acids (fumaric, succinic, malic and mixtures thereof) by controlling dissolved oxygen levels between 30 and 80% (Ling and Ng, 1989).

In the field of fumaric acid production by fermentation, there are many aspects determining the productivity of the fermentation process, such as the applied microbial strain and its morphology, the

use of a neutralising agent and the applied feedstock. Those aspects are reviewed and analysed in more detail in the following sections.

5.1   Fumaric acid producing strains

After the discovery of fumaric acid production in *Rhizopus nigricans* by Felix Ehrlich in 1911, Foster et al. (1939) screened 41 strains from eight different genera in order to identify high fumarate producing strains. The fumarate producing genera identified were *Rhizopus, Mucor, Cunninghamella*, and *Circinella* species. Among these strains, *Rhizopus* species (*nigricans, arrhizus, oryzae* and *formosa)* were the best producing ones, yielding fumaric acid under aerobic and anaerobic conditions (Foster and Waksman, 1939; Rhodes et al, 1959; Kenealy et al., 1986; Cao et al., 1996; Carta et al., 1999). Table 1 lists these fungi and as is shown there *R. arrhizus* NRRL 2582 and *R. oryzae* ATCC 20344 gave the highest volumetric productivity, product titer and product yield values (Gangl et al., 1990; Cao et al., 1996).

Despite the fact that the aforementioned experimental studies involve fungi, the use of bacteria has been considered as well. Donnelly et al. (2001) have suggested using a *Lactobacillus* host strain that lacks the malolactate enzyme, fumarase and fumarate dehydrogenase. Introducing the maeA gene for the malic enzyme from *Escherichia coli* would result in a pathway from pyruvate to malate and hence in a malic acid producing mutant. Additional genetic engineering would result in fumaric acid production.

Genetic modification of microorganisms has hardly been explored for fumaric acid production but offers a potentially useful approach solution for improving yields and rates in fermentation.

5.2   Metabolic pathways to fumaric acid

Fumaric acid is primarily an intermediate of the citrate cycle, but is also involved in other metabolic pathways. In 1939, it was suggested a fumarate biosynthesis pathway involving a C-2 plus C-2 condensation in *Rhizopus* species (Foster and Waksman, 1939). The reactions in this pathway seemed to be similar to those of the glyoxylate bypass (Foster et al., 1949). Years after, the glyoxylate bypass mechanism was ruled out because the theoretical molar yield for this pathway of 100% was not in agreement with the experimental yield of 140% (Rhodes et al., 1959; Romano et

al., 1967). However, the main evidence for rejecting the glyoxylate bypass mechanism is that the key enzyme of the glyoxylate pathway, isocitrate-glyoxylate lyase, was repressed when high glucose concentrations were present like in the experiments used for fumaric acid production (Romano et al., 1967).

It was discovered that a C_3 plus C_1 mechanism involving CO_2 fixation catalysed by pyruvate carboxylase under aerobic conditions explained the high molar yields in fumarate production (Overman and Romano, 1969). This CO_2 fixation leads to oxaloacetic acid formation (Osmani and Scrutton, 1985), so that C_4 citrate cycle intermediates can be withdrawn for biosynthesis during the growth phase under aerobic conditions. When nitrogen becomes limiting and the growth phase stops, the metabolism of glucose and CO_2 fixation could continue and lead to an accumulation of C_4 acids (Romano et al., 1967). The maximal theoretical yield in a non-growth situation is 2 moles of fumaric acid per mole of glucose consumed, upon fixation of 2 moles of CO_2 via reductive pyruvate carboxylation. However, if the reductive pyruvate carboxylation would be the sole pathway, no ATP would be produced for maintenance or transport purposes. Therefore, the citrate cycle is also active during fumaric acid production (Rhodes et al., 1959; Kenealy et al., 1986).

The CO_2 carboxylation enzyme, pyruvate carboxylase, is known to be localised exclusively in the cytosol, together with NAD-malate dehydrogenase and fumarase (that are present in the cytosol and in the mitochondria), leading to fumaric acid synthesis in this cell compartment (Osmani and Scrutton, 1985). Studies performed by Peleg et al. (1989) indicated higher activities of these enzymes (especially the cytosolic isoenzymes) during fumaric acid production. Kenealy et al. (1986) used mitochondrial inhibitors to investigate their role in fumarate accumulation and found no direct involvement of such inhibitors of the citrate cycle in fumarate production. However, carbon-labeling studies have demonstrated the simultaneous utilisation of both the citrate cycle and the reductive pyruvate carboxylation pathways under aerobic conditions (Figure 3).

Table 1: Literature data on fumaric acid production by different *Rhizopus* genera.

Strain	Fermenter	Substrate	Product Titer (g l⁻¹)	Yield (g g⁻¹)	Vol. Prod. (g l⁻¹h⁻¹)	Time (h)	Final pH	Reference
R. nigricans 45	Shake flask	Glucose	14.7	0.50	-	168	6.5	Foster & Waksman. 1938
	Shake flask	Glucose	20.0	0.66	0.25	80	6.5	Romano et al. 1967
R. arrhizus NRRL 2582	Stirred tank	Glucose	90.0	0.70	1.22	72	6.0	Rhodes et al. 1962
	Stirred tank	Glucose	107.0	0.82	2.00	53	6.0	Ng et al. 1986
	Stirred tank	Glucose	73.0	0.72	0.50	147	5.5	Gangl et al. 1990
R. arrhizus NRRL 1526	Shake flask	Glucose	97.7	0.81	1.02	96	6.0	Kenealy et al. 1986
	Fluidised bed	Molasses	17.5	0.36	0.36	48	6.0	Petruccioli et al. 1996
	Stirred tank	Glucose	38.0	0.33	0.46	82	5.5	Riscaldati et al. 2000
R. oryzae ATCC 20344	RBC[1] plus	Glucose	92.0	0.85	4.25	24	4.5	Cao et al. 1996
	Stirred tank	Glucose	65.0	0.65	0.90	72	5.0	Cao et al. 1996
	RBC[1]	Glucose	75.5	0.75	3.78	24	5.0	Cao et al. 1997
	10-l air lift	Glucose	37.8	0.75	0.81	46	5.0	Du et al. 1997
	Stirred tank	Glucose	35.8	0.60	0.90	40	5.5	Zhou. 1999
	Bubble column	Glucose	37.2	0.53	1.03	36	5.0	Zhou et al. 2002
R. formosa MUCL 28422	Stirred tank	Cassava bagasse	21.3	-	-	-	6.5	Carta et al. 1999

[1] Rotatory Biofilm Contactor
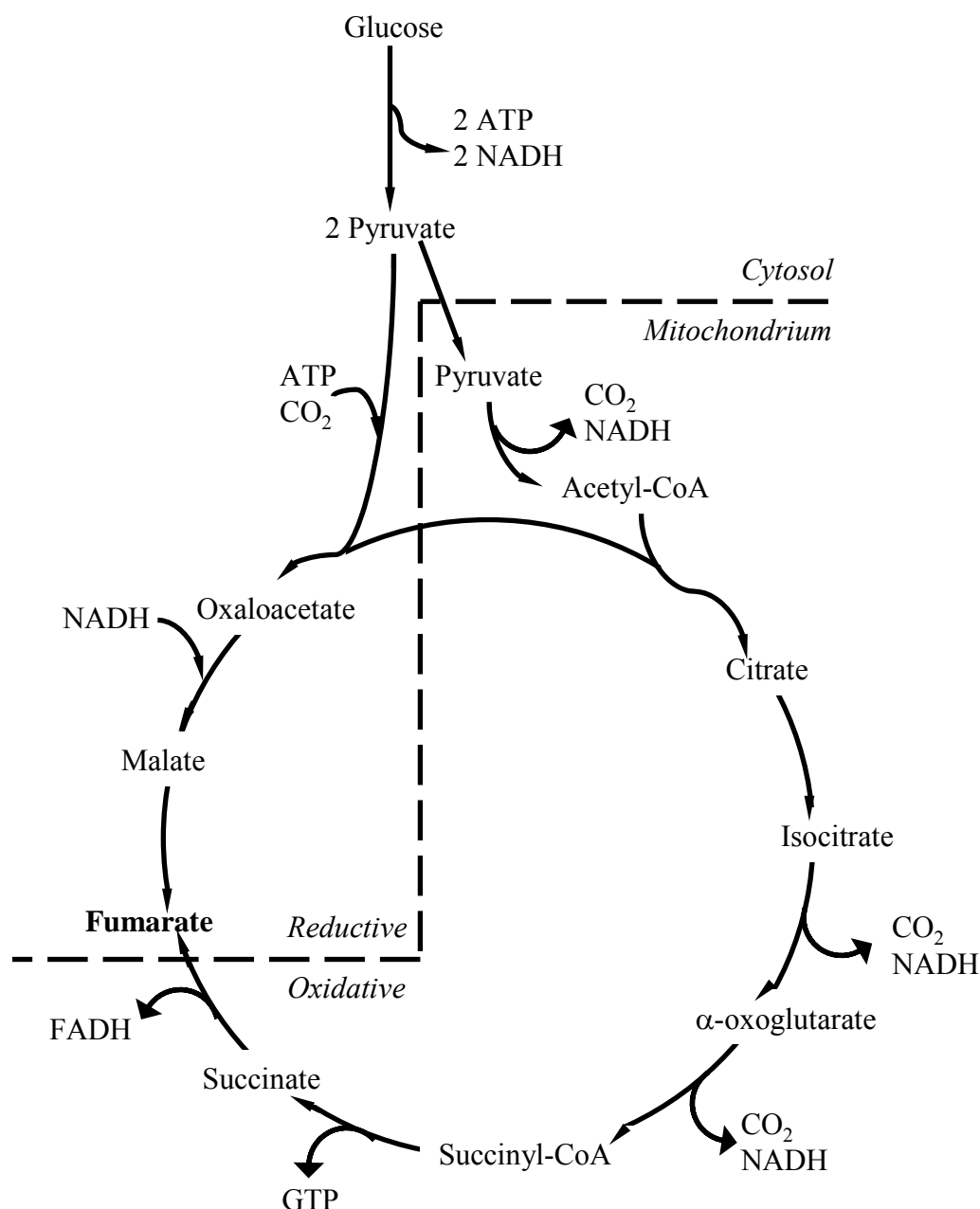
Figure 3: Citrate cycle pathway and reductive carboxylation pathway leading to fumaric acid accumulation (Adapted from Kenealy et al., 1986). The ratio between the two pathways is not 1:1 as suggested by this figure.

Besides the localisation of fumarase isoenzymes, it was also found that addition of cycloheximide virtually eliminated the cytosolic isoenzyme and therefore caused a large decrease in the amount of fumaric acid produced by *R. oryzae* (Peleg et al., 1989). The carboxylation of pyruvate has been studied in more detail for the analogous microbial succinate production, but the understanding of the different metabolic fluxes involved is still incomplete (McKinlay et al., 2007).

High producing fumaric acid strains of *Rhizopus* not only produce fumaric acid but also other carboxylic acids like malic, lactic, acetic, succinic and citric in smaller amounts than fumaric acid production (Rhodes et al., 1959; Carta et al., 1999). Sometimes ethanol is also produced, for example for the high producing strain *R. oryzae* ATCC 20344 (Cao et al., 1996). However, it was found that ethanol production can be reduced by a sufficient supply of oxygen to the culture (Cao et al., 1996).

5.3   Fumaric acid transport across the cell membrane

The transport mechanism of fumaric acid in fungi has not been studied yet. However, transport of L-malic acid and other dicarboxylic acids, including fumaric acid, has been studied in yeasts like *Schizosaccharomyces pombe, Candida utilis, Candida sphaerica* and *Hansenula anomala* (Corte-Real et al., 1989; Corte-Real and Leao, 1990; Saayman et al., 2000). These microorganisms may be comparable to fumaric-producing fungi. These studies showed that the initial uptake of malic acid was accompanied by disappearance of extracellular protons suggesting that the anionic form of the acid was transported by an accumulative dicarboxylate proton symporter. As fumaric acid seems to be a competitive inhibitor of L-malic acid uptake, it was suggested that fumaric acid uses the same import system.

On the other hand, these studies showed that undissociated dicarboxylic acid entered the cells slowly by simple diffusion. In addition it was revealed that the rate of diffusion of the undissociated acid across the plasma membrane is subjected to opposite pH influences: an increase due to the relative increase of undissociated acid with decreasing pH and a decrease due to a decrease of the permeability of the cell membrane for the undissociated acid at decreasing pH (Corte-Real and Leao, 1990). Increasing the number or activity of the dicarboxylic acid transporters could lower the intracellular fumarate concentration and could therefore have a positive effect on the production yield (van Maris et al., 2004).

5.4   Alternative fermentation feedstocks

Glucose has not been the only carbon source used for fumaric acid producing strains. The use of xylose with immobilised *R. arrhizus* was studied, but the highest obtained volumetric productivity was only 0.087 g l^{-1} h^{-1} (Kautola and Linko, 1989). Also sucrose has been considered as a raw

material in fumaric acid production processes (Kautola and Linko, 1989; Zhang et al., 2007) but sucrose has the disadvantage of being poorly metabolised by *R. oryzae* compared to glucose (Bulut et al., 2004).

Starch containing materials were also screened as feedstock for the fumaric acid production. Potato flour was used as feedstock for *R. arrhizus* and although fumaric acid was the main metabolic product, a volumetric productivity of only 0.35 g l^{-1} h^{-1} was achieved (Moresi et al., 1991). On the other hand, it was found that the highest yields of fumaric acid were obtained from acid hydrolysates of starch-based materials (Moresi et al., 2002). The same feedstock was used by Federici et al. (1993) in studies on the effect of agitation speed and applied neutralising agent. The tested neutralising agent was a combination of $CaCO_3$ and KOH/KCO_3 and it was concluded that comparable fumaric acid yields were obtained using these neutralising agents and starch-base materials (Federici et al., 1993). Carta et al. (1999) optimised the fumaric acid production by *R. formosa* MUCL 28422 by using enzymatic hydrolysates of cassava bagasse, a high starch containing waste product. The productivity was not improved with respect to a fermentation where glucose was used as a feedstock, but the fact that these feedstocks are cheap and abundant makes these optimised fermentations economically attractive.

5.5   Nutrient requirements

Physical and nutritional requirements for fumaric acid fermentation have been studied in *Rhizopus arrhizus* (Rhodes et al., 1959; Rhodes et al., 1962). As *Rhizopus* species should enter a phase of limited growth during the fermentation, which can be achieved by nitrogen limitation, these studies showed that in order to achieve high yields during fumaric acid fermentation, the most critical parameter is the ratio of glucose to nitrogen. For example, a yield of fumaric acid on glucose of 85% (w/w) was obtained using an initial C:N molar ratio of 200:1 for *R. arrhizus* 2582. When nitrogen limitation is not desired, phosphorus limitation can be used instead (Riscaldati et al., 2000). Trace metal concentrations of 500 ppm, 4 ppm, and 100 ppb for Mg^{++}, Zn^{++}, and Fe^{++}, respectively, were found optimal for the formation of small (1 mm) spherical pellets that produced high concentrations of fumaric acid (36 g L^{-1}) (Zhou, 1999).

Because CO_2 is needed for the oxaloacetate formation from pyruvate by pyruvate carboxylase the addition of calcium carbonate ($CaCO_3$), which is used in many cases as a neutralising agent, seems also important as a CO_2 source during the production phase of the fermentation. However, in case

that no CO_2 or carbonate is added, the complete catabolism of a mole of glucose via the citrate cycle provides 6 moles of CO_2 that may be used for pyruvate carboxylation (see Figure 3). In this case the maximum theoretical yield would be 1.5 mole of fumaric acid per mole of glucose. This theoretical value is close to the value of 1.32 mole of fumaric acid per mole of glucose reported by Cao et al. (1996), who optimised a fermentation process without CO_2 or carbonate feeding.

5.6   Neutralising agents

Continuous neutralisation of the pH has been necessary to obtain optimal yields in fumaric acid production by fermentation. Preferably $CaCO_3$ has been used as a neutralising agent but at the same time this compound is causing viscosity problems due to the low aqueous solubility of calcium fumarate (21 g/l at 30 ^{o}C (Gangl et al., 1990)) that precipitates as a fermentation product. Furthermore the cells can interact with the precipitated product, as has been found for *R. oryzae*, resulting in a highly viscous suspension. This has a detrimental effect on the rate of oxygen transfer which can be achieved and hence the fermentation might fail due to oxygen limitation problems. Therefore, replacement of $CaCO_3$ by other neutralising agents like Na_2CO_3, $NaHCO_3$, $Ca(OH)_2$ and $(NH_4)_2CO_3$ has been studied by different authors (Gangl et al., 1990; Riscaldati et al., 2000; Zhou et al., 2002). However, these studies showed that the fumarate production rates are the highest when $CaCO_3$ is used as a neutralising agent.

Because of the high solubility of sodium fumarate, fermentative production of fumarate using Na_2CO_3 as neutralising agent leads to cheaper downstream processing than when $CaCO_3$ is used. This is due to the fact that the fermentation product, sodium fumarate, has a higher solubility than $CaCO_3$ and hence there is no need of heating to recover the fermentation product (see Figure 4). In addition, cells can be reused (Gangl et al., 1990; Zhou et al., 2002). A similar situation was obtained when *Rhizopus* growth was limited by phosphorus so that $(NH_4)_2CO_3$ could be used as neutralising agent (Riscaldati et al., 2000). Nevertheless, it has been argued that a fermentation process without the use of neutralising agents and at the same time preventing product inhibition, will improve the economics of the general process (Gangl et al., 1990). However, when a high yield process is developed without a carbonate as neutralising agent, the required CO_2 must be supplied by other sources. Fumaric acid fermentation systems without the use of neutralising agents have been studied in the past and will be discussed in the following sections.

With respect to fumarate salts inhibition, Rhodes et al. (1961) reported that production of soluble sodium or potassium fumarates was inhibited when the concentration of fumarate reached values of $34 - 40$ g L^{-1} using *R. arrhizus* as a producer strain. Nonetheless, Gangl et al. (1990) found that addition of sodium fumarate (71.3 g L^{-1}) was not inhibiting the same strain although the cells needed 35 hours to adapt to the high sodium fumarate concentrations. On the other hand, the free fumaric acid does inhibit its own production because the accumulated protons in the production medium decrease the pH, thus exerting a progressive inhibitory effect on fumaric acid production (Riscaldati et al., 2000). At low pH, excreted fumaric acid will passively diffuse back through the plasma membrane of the fungus decreasing its intracellular pH and due to this phenomenon the fermentation fails. Proposed methods to enable carboxylic acid fermentation at low pH are: genetic engineering of acid tolerant organisms such as yeasts and in situ product removal techniques (Cao et al., 1996; Schügerl, 2000; van Maris et al., 2004).

5.7 Morphology and oxygen transfer problems

One of the difficulties of fermenting *Rhizopus* species is the morphology of these fungi. *Rhizopus* species tend to grow on the walls and on the stirrer of the reactor and sometimes clumps are formed. Therefore, the fermentation can suffer from oxygen limitation in particular when calcium fumarate is present. One way to solve this problem is to control the growth of the fungi and their morphology.

A way to minimise oxygen mass transfer limitation to the cells is to stimulate formation of small spherical cell pellets (Zhou, 1999). Small pellets can reduce clumps formation during fermentation and even if $CaCO_3$ is present, the viscosity of the broth can be reduced. Moreover, pellets can facilitate the performance of a biomass retention system. For *R. oryzae* low initial pH values for the cultivation media favored pellet formation and good fumaric acid yields have been reached (Zhou et al., 2000).

In another morphology improvement study, Cao et al. (1997*)* used a rotary biofilm contactor (RBC) as fermentor with immobilised *R. oryzae* to produce fumaric acid. $CaCO_3$ was used as neutralising agent during this experiment. During the fermentation, the discs with immobilised cells were rotating, moving the cells from the gas phase of the fermentor to the liquid phase and back again (Cao et al., 1997). When the cells are exposed to the air, high oxygen transfer rates can be reached, while the cells can take up substrate and excrete the produced fumaric acid when they are submerged. In this system additional agitation was not needed. The volumetric productivity was very

high, as compared to the volumetric productivity of an equivalent stirred vessel fermentor setup (see Table 1). A disadvantage of this system could be the scalability potential of the RBC fermentor.

Immobilisation techniques for *Rhizopus* species have been investigated in order to open the possibility of a continuous operation mode for fumaric acid production and to reduce oxygen transfer problems as well. Buzzini et al. (1993) searched for the most suitable support for cell immobilisation in fluidised-bed reactors during fumaric acid fermentation. Cork, expanded polystyrene, expanded clay and wood shavings were investigated. With 6 mm pieces of cork the highest titer, 24.1 g fumaric acid l^{-1} in 144 h, was achieved, which is comparable to the titer of 37.7 g l^{-1} after 166 h under conventional submerged conditions (Buzzini et al., 1995). The performance of a semi-continuous process was investigated with *R. arrhizus* immobilised on 5 mm cubic particles made of polyurethane sponge (Petruccioli et al., 1996). These particles were used in repeated batch fermentations in a fluidised-bed reactor (48 h, 8 times). In the optimised process the fumaric acid titer was 12.3 g l^{-1} and the volumetric productivity 0.256 g l^{-1} h^{-1}.

Furthermore, as the oxygen mass transfer resistance through the boundary layer on the liquid side of the gas-liquid interface can affect the interfacial oxygen transfer from the gas phase to the liquid phase, pressure pulsation was applied in a stirred tank fermentor using *R. oryzae* (Zhou, 1999) in order to reduce this resistance. Mass yield and volumetric productivity of fumarate were 70.1% and 0.99 g L^{-1} h^{-1}, respectively, which were higher than for traditional stirred tank fermentations. The same organism was studied in an airlift loop reactor as a fermentation system for fumaric acid production (Du et al., 1997). Here the airlift loop reactor with porous sparger produced favorable conditions for mass transfer and also higher yields and productivities were reached than in stirred tank fermentations.

5.8 Integrated fermentation and recovery of fumaric acid

Figure 4 presents a flow scheme proposed for fumaric acid production by batch fermentation (Gangl et al., 1990). Glucose and mineral salts are fed to the fermentor. The nitrogen source solution, $(NH_4)_2SO_4$, is sterilised separately and fed to the cooled fermentor. The harvested broth containing sodium fumarate (cells and trace amounts of Na_2CO_3) is filtered in order to remove the cells and then acidified by H_2SO_4 to pH 1. After acidification, fumaric acid precipitates out of the solution and is sent to a rotary dryer to be completely recovered (Gangl et al., 1990). When $CaCO_3$ is used as a neutralising agent instead of Na_2CO_3, additional heating after the fermentation was

supposed to be required to dissolve calcium fumarate and the excess of $CaCO_3$ that usually stick to the cells. This problem leads to a tedious and expensive downstream processing.
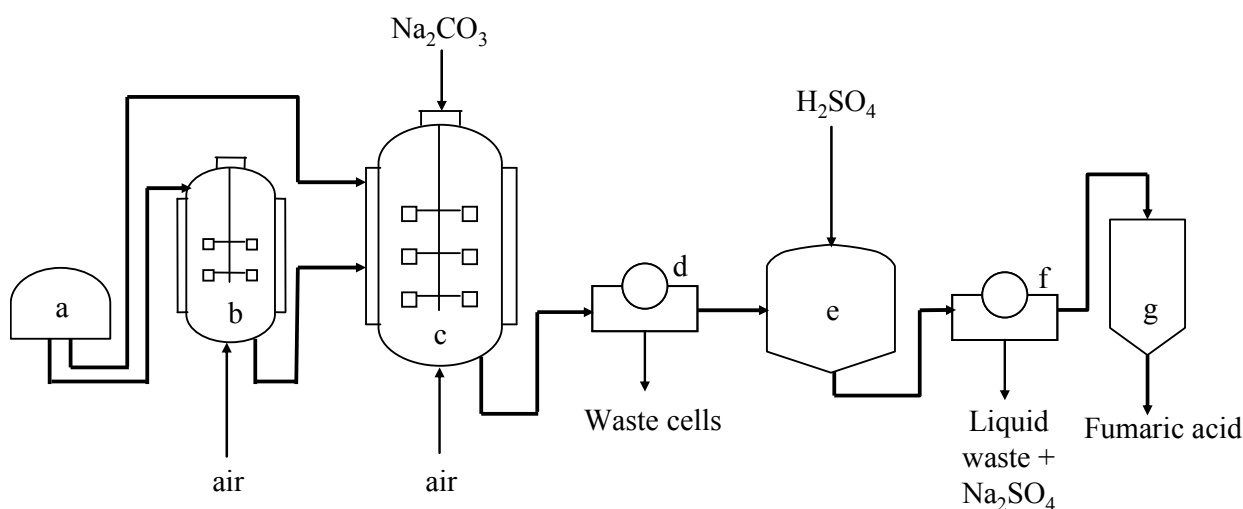

Figure 4: Flow-sheet for fumaric acid production via fermentation. a) Formulation tanks containing glucose and nutrients; b) Seed fermentor; c) Production fermentor; d) Filter; e) Acidification tank; f) Filter; g) Rotary dryer. (Adapted from Gangl et al. 1990).

In the downstream processing field, recovery techniques have not so much been studied for fumaric acid producers in submerged cultivations as it has been done for related fermentation products like succinic acid (Zeikus et al., 1999), citric acid (Heinzle et al., 2006) and lactic acid (Joglekar et al., 2006). Recovery systems like reactive extraction and membrane electrodialysis have not been studied yet. However, simultaneous fermentation and adsorption have been studied in order to remove of fumaric acid during its formation to control fermentation pH at desired values and avoid product inhibition (Cao et al., 1996; Zhou, 1999).

Cao et al. (1996) used a rotary biofilm contactor (RBC) setup as fermentor for *R. oryzae*, in combination with an adsorption column. The produced fumaric acid was removed from the broth by the adsorption column in a recycle loop, reducing product inhibition and thus increasing the production rate and sustaining cell viability. Polyvinyl pyridine (PVP) anion exchange resin in the hydroxide form was selected as adsorbent because it yielded the highest loading capacity for fumaric acid (0.31 g g^{-1} dry wt). The RBC, coupled with the adsorption column, increased the fumaric acid productivity significantly, to 4.25 g l^{-1} h^{-1}, because the total fermentation time was much less than in traditional stirred tank fermentations (see Table 1). This volumetric productivity and the yield are the highest reported in literature. In this integrated system the constant removal of the fumarate produced and the liberation of OH$^-$ from the adsorption column kept the fermentation pH at 4.5. The

fumarate was desorbed from the adsorption resin by using 0.4 M NaOH so additional processing will be necessary to convert the sodium fumarate into neutral fumaric acid. Addition of extra CO_2 was not necessary due to the fact that during the production stage, the biofilm was exposed to sterile air that was present in the headspace of the RBC enhancing the opportunity for CO_2 fixation by the biofilm.

A novel product recovery process by an ion exchanger resin was developed by Zhou (1999). Fumarate was recovered from the fermentation broth without the use of neutralising agents while keeping the pH at 5, by cycling the broth over a column of a resin (Amberlite IRA-900 with OH$^-$ as counterion). After eluting the loaded column with ammonium hydroxide, ammonium fumarate solution was obtained. This was passed through a Y-zeolite column that retained the ammonium and liberated the fumaric acid. The ammonium hydroxide solution can be recovered and recycled by thermal regeneration of the zeolite (Zhou, 1999). However, this integrated process did not surpass yield values obtained in a stirred tank fermentor when fumaric acid fermentation was controlled by $CaCO_3$ under pressure pulsation (see previous section), but a higher productivity value of 1.09 g L^{-1} h^{-1} was reached (Zhou et al., 2000).

6 Economics of fumaric acid production

In a theoretical study, Gangl et al. (1990) compared a fermentation and a benzene-based petrochemical process with respect to economy. The fermentation process taken for this has been described in the beginning of the previous section. Although Na_2CO_3 was assumed as a neutralising agent in this study, the productivity (2 g l^{-1} h^{-1}) and yield (0.82 g g^{-1}) of the fumaric acid fermentation with $CaCO_3$ obtained in a previous study were used (Ng et al., 1986).

This economic evaluation showed that the fermentation route was less favorable than the petrochemical route (economic evaluation included upstream and downstream sections). In particular, the raw material costs were higher for the fermentation process than for the petrochemical route. It was concluded that the fermentation route could become competitive with the petrochemical route if oil prices were around 61 $/barrel. The latter price has been reached in the recent years (http://tonto.eia.doe.gov/dnav/pet/xls/PET_PRI_WCO_K_W.xls), while the productivity of the fermentation process has been improved significantly as is shown in Table 1. Besides, one can roughly calculate from Gangl's study that the assumed sugar price was around 0.6 $/kg of glucose, which is high compared to the current price (see Table 2). Therefore, if the current glucose price is

assumed in the calculations of Gangl's study one can expect lower raw material costs for the fermentation route. On the other hand, the petrochemical route has also been improved significantly, now using butane instead of benzene. This will be reflected in the current maleic anhydride price, which is shown in Table 2.

The simple comparison of petrochemical and fermentation routes for fumaric acid production given in Table 2 suggests that the lower raw material price of the fermentative production might compensate the higher yields of the petrochemical production from maleic anhydride and fermentation may become an economically viable alternative.

Table 2: Comparison between petrochemical and fermentation route for fumaric acid production.

Parameter	Petrochemical route	Fermentation route
Raw material	Maleic anhydride	Glucose
Reaction temperature (°C)	90-100	35
Raw material price ($/kg)	1.46 - 1.63 (Anonymous, 2007)	0.46[a]
Product yield (% w/w)	112 (Lohbeck et al., 2005)	85 (Cao et al., 1996)

a: http://www.ers.usda.gov/briefing/sugar/data.htm; for 4th quarter of 2006

7 Conclusions and future prospects

Due to increasing prices of fossil feedstock, fermentatively produced fumaric acid could become a cheaper alternative to the petrochemically based maleic acid as unsaturated dibasic acid in polyester resins in the nearby future. Based on the available literature the micro-organism with the highest productivity and yield of fumaric acid appears to be *Rhizopus oryzae*. This organism produces fumaric acid via a combination of the citrate cycle and reductive pyruvate carboxylation. In addition, the fumaric acid production by fermentation can be improved if the use of neutralising agents is reduced or avoided and the morphology of the fungi is optimised. However, avoiding the use of neutralising agent will lead to product inhibition; therefore, it would be useful if metabolic engineering is applied to achieve fumaric acid production in suspended, acid-resistant microorganisms such as yeast. Another way to solve product inhibition problems is applying in-situ removal of fumaric acid during the fermentation.

Acknowledgements

References

Altmeyer PJ, Matthes U, Pawlak F, Hoffmann K, Frosch PJ, Ruppert P, Wassilew SW, Horn T, Kreysel HW, Matthes U, Pawlak F, Rietzschel I, Joshi RK (1994) Antipsoriatic effect of fumaric acid derivatives – Results of multicenter double blind study in 100 patients. J Am Acad Dermatol (30) 977.

Anonymous (2007) Product focus: Maleic anhydride. Chem Week 39

Bulut S, Elibol M, Ozer D (2004) Effect of different carbon sources of L(+)-lactic acid production by *Rhizopus oryzae*. Biochem Eng J (21) 33.

Buzzini P, Gobbetti M, Rossi J, Ribaldi M (1995) Comparison in different unconventional supports for the immobilization of *Rhizopus arrhizus* cells to produce fumaric acid on grape must. Ann Microbiol Enzim (43) 53.

Cao NJ, Du JX, Chen CS, Gong CS, Tsao GT (1997) Production of fumaric acid by immobilized *Rhizopus* using rotary biofilm contactor. Appl Biochem Biotech 63 (5) 387.

Cao NJ, Du JX, Gong CS, Tsao GT (1996) Simultaneous production and recovery of fumaric acid from immobilized *Rhizopus oryzae* with a rotary biofilm contactor and an adsorption column. Appl Environ Microbiol (62) 2926.

Carta FS, Soccol CR, Ramos LP, Fontana JD (1999) Production of fumaric acid by fermentation of enzymatic hydrolysates derived from cassava bagasse. Bioresource Technol (68) 23.

Corte-Real M, Leao C (1990) Transport of malic acid and other carboxylic acids in the yeast *Hansenula anomala*. Appl Environ Microbiol (56) 1109.

Corte-Real M, Leao C, van Uden N (1989) Transport of L-malic acid and other dicarboxylic acids in the yeast *Candida sphaerica*. Appl Microbiol Biot (31) 551.

Donnelly M, Millard CS, Stols L (2001) Mutant *E. Coli* strain with increased succinic acid production. USRE37393

Du JX, Cao NJ, Gong CS, Tsao GT, Yuan NJ (1997) Fumaric acid production in airlift loop reactor with porous sparger. Appl Biochem Biotech (63-65) 541.

Federici F, Moresi M, Parente E, Petruccioli M, Piccioni P (1993) Effect of stirring rate and neutralising agent on fumaric acid production by *Rhizopus arrhizus*. Ital J Food Sci (4) 387.

Felthouse TR, Burnett JC, Horrell B, Mummey MJ and Kuo YJ (2001) Maleic anhydride, maleic acid, and fumaric acid. Kirk-Othmer encyclopedia of chemical technology, 4th ed., (15) 1.

Foster JW and Waksman SA (1938) The specific effect of zinc and other heavy metals on growth and fumaric acid production by *Rhizopus*. J Am Chem Soc (37) 599.

Foster JW, Carson SF, Anthony DS, Davis JB, Jefferson WE, Long MV (1949) Aerobic formation of fumaric in the mold *Rhizopus nigricans* – Synthesis by direct C-2 condensation. P Natl Acad Sci USA (35) 663.

Foster JW, Waksman SA (1949) The production of fumaric acid by molds belonging to the genus *Rhizopus*. J Am Chem Soc (61) 127.

Gangl IC, Weigand WA, Keller FA (1990) Economic comparison of calcium fumarate and sodium fumarate production by *Rhizopus arrhizus*. Appl Biochem Biotech (24 -25) 663.

Goldberg I, Rokem JS, Pines O (2006) Organic acids: old metabolites, new themes. J Chem Tech Biotech (81) 1601.

Goldberg I, Stieglitz B (1986) Fermentation process for production of carboxylic acids. US4564594

Goto M, Nara T, Tokumaru I, Fugono N, Uchida Y, Terasawa M, Yukawa H (1998) Method of producing fumaric acid. US5783428

Heinzle E, Biwer AP, Cooney CL (2006) Development of sustainable bioprocess – Modelling and assetment. Wiley. Chichester.

Ichikawa S, Iino T, Sato S, Nakahara T, Mukataka S (2003) Improvement of production rate and yield of fumaric acid from maleic acid by heat treatment of *Pseudomonas alcaligenes* strain XD-1. Biochem Eng J (13) 7.

Joglekar HG, Rahman I, Babu S, Kulkarni BD, Joshi A (2006) Comparative assessment of downstram processing options for lactic acid. Sep Purif Technol 52: 1-17

Kane JH (1943) Production of fumaric acid. US2327191

Kautola H, Linko YY (1989) Fumaric acid production from xylose by immobilized *Rhizopus arrhizus* cells. Appl Microbiol Biot (31) 448.

Kenealy W, Zaady E, Dupreez JC, Stieglitz B, Goldberg I (1986) Biochemical aspects of fumaric acid accumulation by *Rhizopus arrhizus*. Appl Environ Microbiol (52) 128.

La Roe EG (1959) Fumaric acid fermentation process. US2912363

Ling LB and Ng TK (1989) Fermentation process for carboxylic acids. US4877731

Lohbeck K, Haferkorn H, Fuhrmann W, Fedtke N (2005) Maleic and Fumaric Acids. Ullmann's Encyclopedia of Industrial Chemistry, 5th ed., Vol. A16, VCH., 53-62. Weinheim, Germany

Lobowitz HR and La Roe EG (1958) Fumaric acid fermentation process. US2861922

Magnuson JK and Lasure LL (2004) Organic acid production by filamentous fungi. Advances in fungal biotechnology for industry, agriculture and medicine. Edited by JS Tracz and L Lange. Chapter 12, 307-.340. Kluwer Academic/Plenum Publishers.

Mcginn SM, Beauchemin KA, Coates T, Colombatto D (2004) Methane emissions from beef cattle: Effects of monensin, sunflower oil, enzymes, yeast and fumaric acid. J Anim Sci (82) 3346.

McKinlay JB, Vieille C, Zeikus JG (2007) Prospects for a bio-based succinate industry. Appl Microbiol Biotechnol (76) 727.

Moresi M, Ceccantoni B, Lo Presti S (2002) Modelling of ammonium fumarate recovery from model solutions by nanofiltration and reverse osmosis. J Membrane Sci (209) 405.

Moresi M, Parente E, Petruccioli M, Federici F (1991) Optimization of fumaric acid production from potato flour by *Rhizopus arrhizus*. Appl Microbiol Biot (36) 35.

Mrowietz U, Christophers E, Altmeyer P (1998) Treatment of psoriasis with fumaric acid esters: results of a prospective multicentre study. Brit J Dermatol (138) 456.

NakajimaKamber T, Nozue T, Mukouyama M, Nakahara T (1997) Bioconversion of maleic acid to fumaric acid by *Pseudomonas alcaligenes* strain XD-1. J Ferment Bioeng (84) 165.

Ng TK, Hesser RJ, Stieglitz B, Griffiths BS, Ling LB (1986) Production of tetrahydrofuram/1,4 butanediol by a combined biological and chemical process. Biotech Bioeng Symp (17) 344.

Osmani SA, Scrutton MC (1985) the sub-cellular localization and regulatory properties of pyruvate carboxylase from *Rhizopus arrhizus*. Eur J Biochem (147) 119.

Otsuka K (1961) Cis-trans isomerase – Isomerisation from maleic acid to fumaric acid. Agr Biol Chem (25) 726.

Overman SA, Romano AH (1969) Pyruvate carboxylase of *Rhizopus nigricans* and its role in fumaric acid production. Biochem Bioph Res Co (37) 457.

Peleg Y, Battat E, Scrutton MC, Goldberg I (1989) Isoenzyme pattern and subcellular localization of enzymes involved in fumaric acid accumulation by *Rhizopus oryzae*. Appl Microbiol Biot (32) 334.

Petruccioli M, Angiani E, Federici F (1996) Semi continuous fumaric acid production by *Rhizopus arrhizus* immobilized in polyurethane sponge. Process Biochem (31) 463.

Rhodes RA, Lagoda AA, Jackson RW, Misenhei TJ, Smith ML, Anderson RF (1962) Production of fumaric acid in 20 liter fermentors. Appl Microbiol (10) 9.

Rhodes RA, Moyer AJ, Smith ML, Kelley SE (1959) Production of fumaric acid by *Rhizopus arrhizus*. Appl Microbiol (7) 74.

Riscaldati E, Moresi M, Federici F, Petruccioli M (2000) Direct ammonium fumarate production by *Rhizopus arrhizus* under phosphorous limitation. Biotechnol Lett (22) 1043.

Romano AH, Bright MM, Scott WE (1967) Mechanism of fumaric acid accumulation in *Rhizopus nigricants*. J Biotech (93) 600.

Saayman M, van Vuuren HJJ, van Zyl WH, Viljoen-Bloom M (2000) Differential uptake of fumarate by *Candida utilis* and *Schizosaccharomyces pombe*. Appl Microbiol Biot (54) 792.

Scher M, Lennarz WJ (1969) Maleate Isomerase. J Biol Chem (244) 1878.

Schügerl K (2000) Integrated processing of biotechnology products. Biotechnol Adv (18) 581.

Stephen WI (1965) Solubility and pH calculations. Anal Chim Acta (33) 227.

Takamura Y, Takamura T, Soejima M, Uemura T (1969) Studies on induced synthesis of maleate cis-trans isomerase by malonate. Purification and properties of maleate cis-trans isomerase indiced by malonate. Agr Biol Chem (33) 718.

van Maris AJA, Konings WN, van Dijken JP, Pronk JT (2004) Microbial export of lactic and 3-hydroxypropanoic acid: implications for industrial fermentation processes. Metab Eng (6) 245.

Waksman SA (1943) Process for the production of fumaric acid. US2326986

Werpy T and Petersen G (2004) Topten value added chemicals from biomass feedstocks. U.S. Department of Energy. USA

Willke T, Vorlop K-D (2004) Industrial bioconversion of renewable resources as an alternative to conventional chemistry. Appl Microbiol Biotechnol (66) 131.

Zeikus JG, Jain MK, Elankovan P (1999) Biotechnology of succinic acid production and markets for derived industrial products. Appl Microbiol Biot (51) 545.

Zhang ZY, Jin B, Kelly JM (2007) Production of lactic acid and byproducts from waste potato starch by *Rhizopus arrhizus*: role of nitrogen sources. World J Microb Biot (23) 229.

Zhou Y, Du J, Tsao GT (2002) Comparison of fumaric acid production by *Rhizopus oryzae* using different neutralizing agents. Bioproc Biosyst Eng (25) 179.

Zhou Y, Du JX, Tsao GT (2000) Mycelial pellet formation by *Rhizopus oryzae* ATCC 20344. Appl Biochem Biotech (84-86) 779.

CHAPTER 3

Development of a low pH fermentation strategy for fumaric acid production by *Rhizopus oryzae*

Due to the fact that petrochemical resources will become scarcer, dicarboxylic acids produced from renewable resources are interesting feedstocks for the polymers industry. Amongst the most common carboxylic acids, fumaric acid is a very interesting one, not only because of its low toxicity to microbial cells but also because of its low aqueous solubility, which facilitates product recovery. A low pH for fumaric acid fermentation will avoid excessive waste salt production during downstream processing and hence be beneficial. Studying the influence of pH, working volume and shaking frequency on cell cultivation helped us to identify the best conditions to obtain a proper pellet morphology of a wild type strain of *Rhizopus oryzae* capable of producing high amounts of fumaric acid. Moreover, the effects of cultivation pH and CO_2 addition were studied to determine the best conditions to produce fumaric acid in *R oryzae* fermentations under nitrogen limited conditions with glucose as carbon source. These included fermentation performance analysis at constant cultivation pH as well as during pH profiles. Significant differences in productivity were observed when lowering the fermentation pH and increasing the CO_2 content of the inlet air above 10%, both negatively affecting the final fermentation productivities and titers. However, switching off the pH control during the batch phase did not affect the fermentation productivity and allowed achieving pH of 3.6. Remarkably, the results of this work indicated that after productivities reached the maximum value the effect of the pH was less pronounced from that point to the end of the batch. A concentration of 20 g L^{-1} of fumaric acid was obtained at pH 3.6 while the average cell-mass specific productivity was not at pH 5.0.

1   Introduction

Fumaric acid has been identified as one of the so-called top 12 chemicals to be produced by industrial fermentation (Werpy and Petersen, 2004). Fumaric acid is an interesting compound because of its numerous applications, not only in the food industry but also in polymers industry. The current production of fumaric acid involves chemical conversion of petrochemical maleic anhydride. However, as petroleum is becoming scarcer, fermentation routes for fumaric acid production are receiving more attention (Roa Engel et al., 2008).
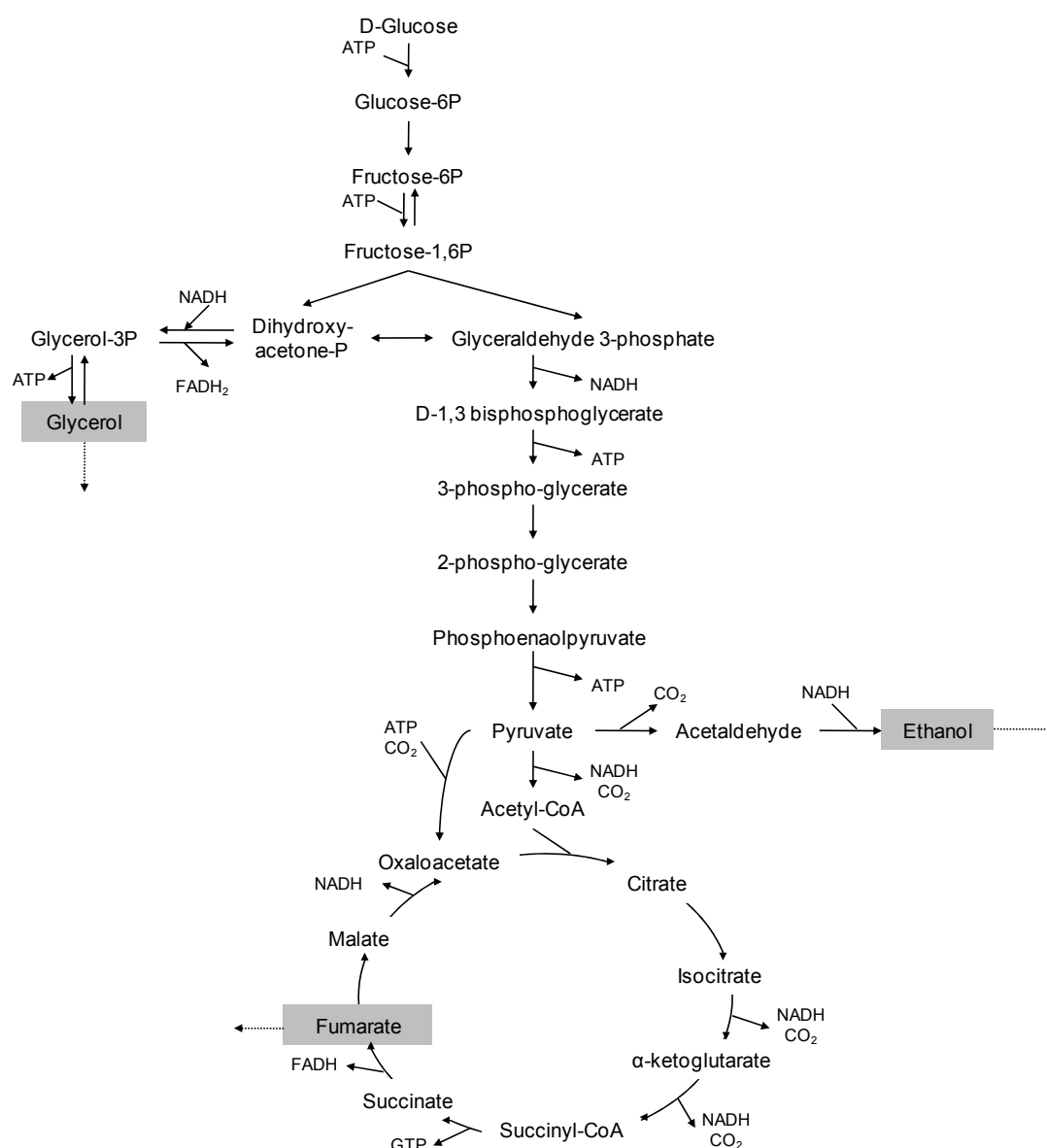

Figure 1: Metabolic pathways in *Rhizopus oryzae* leading accumulation of fumaric acid, ethanol and glycerol.

Fumaric acid production by fermentation has usually been carried out with *Rhizopus oryzae* around neutral pH values, leading to fumarate salts because the dissociation constants for fumaric acid are $pKa_1 = 3.02$ and $pKa_2 = 4.38$ (Lohbeck et al., 1990). After cell removal, fumaric acid can be recovered by precipitation from the broth upon acidification, due to the low solubility of the undissociated acid. Nevertheless, this process leads to high consumption of base (to control the fermentation pH) and acid for precipitation and as a consequence a lot of waste salts are produced (Roa Engel et al., 2008). This situation would be improved when the fermentation could be performed at a lower pH. This is due to the fact that at lower pH larger fractions of the undissociated form of the acid and the monohydrogen salt will be present. Undissociated fumaric acid has a low solubility so its separation by crystallisation from the broth may become feasible. Other separation processes like extraction and absorption, may also become easier when a larger amount of the undissociated form of the acid would be present (Joglekar et al., 2006). Therefore, to minimise mineral acid and base consumption and waste salt production, a fermentation strategy to produce fumaric acid at low pH has to be studied. Another important aspect is the supply of extra carbon dioxide (CO_2), which is consumed if fumaric acid is produced via the carboxylation of pyruvate (Figure 1). Usually CO_2 has been supplied as carbonate salt ($CaCO_3$, Na_2CO_3) but it is known that air enriched by CO_2 also helps to improve the fumaric acid production by fermentation of *R. oryzae* (Zhou et al., 2000).

When cultivated in a stirred tank bioreactor (STR) *R. oryzae* has the tendency to grow in clumps or pellets. Pellets are often the preferred morphology in industrial fermentation processes; however, the pellet size should be kept below a certain critical value to prevent oxygen limitation, resulting in suboptimal production rates (Rhodes et al., 1959; Zhou et al., 2000). Furthermore, the cell mass removal after fermentation will be easier if the pellet form is used. Pellet formation varies from one microorganism to another and is strongly determined by the growth conditions (Dinesen and Nielsen, 2003). For the high fumarate producing *R. oryzae* ATCC 20344 strain used in the current study, the influence of initial pH (2.5 to 5.5) and nutrient concentrations (Zn^{++}, Mg^{++}, Fe^{++} and Mn^{++}) have been studied previously (Zhou et al., 2000). Furthermore, in the same study it was concluded that a pellet size of 1 mm is ideal for fumaric acid production, being the maximum diameter that oxygen can still penetrate through the entire pellet (Zhou et al., 2000). Moreover, a multiple logistic regressed model was tested and validated for this strain to find the best conditions for pH, agitation, spore concentration, temperature and nutrients concentration in the pellets cultivation (Liu et al., 2007). However, the optimal working volume combined with pH, shaking frequency and hydrodynamic conditions to produce pellets have not yet been optimised for this strain.

This chapter addresses the feasibility of fumaric acid production by fermentation at low pH (< 5.0) where the acid is not completely dissociated. To achieve low pH, CO_2 was supplied as gas rather than carbonate salt. Cultivating sufficient suitable *R. oryzae* pellets is a prerequisite for the fermentation and therefore, the influence of working volume; pH and rotation frequency on the formation of *R. oryzae* pellets in shake flasks was also investigated.

2   Materials and Methods

2.1   Microorganism and growth conditions

R. oryzae ATCC 20344 was obtained from the American Type Culture Collection (Rockville, Md.). The culture was grown at 37 ^{o}C on YMP agar plates, containing of 0.3% yeast extract, 0.3% malt extract, 0.3% peptone, 2% glycerol and 2% agar in distilled water, to produce spores. After four days of sporulation the spores were washed with a glycerol (10% v/v) and Tween 80 (0.05% v/v) solutions. This solution contained approx. 10^{6} spores per mL and was collected in vials of 2 mL and stored at −80 ^{o}C.

2.2   Preculture conditions

1 L shake flasks containing 200 mL of growth medium were inoculated with two vials (2 mL each) of spore suspension. The composition of the growth medium was (per 1000 mL) 10 g of glucose, 2.0 g of urea, 0.6 g of KH_2PO_4, 0.25 g of $MgSO_4 \cdot 7H_2O$, and 0.088 g of $ZnSO_4 \cdot 7H_2O$. The pH of the medium was, if necessary, adjusted by adding HCl (10% v/v). The medium, without the glucose, was heat sterilised (20 min at 121 ^{o}C). The glucose solution was sterilised separately (20 min at 110 ^{o}C). Pre-cultures were carried out at 35°C and 200 rpm in a gyratory incubator-shaker for 2 days. The shake flasks were covered with cotton. After cultivation, the obtained mycelium pellets were washed for one hour with 1 L of new fresh media free of glucose and urea. The pellets were transferred immediately after the washing into a fermentor containing the production medium (see later).

2.3   Shake flask cultivations

To study the effect of the pH, shake flask volume and shaking speed on pellet formation, shake flask cultivations were carried out at five different volumes: 200, 300, 500, 700 and 1000 mL of cultivation medium (same compositions as for the pre-cultures) in flat bottom shake flasks (ISO 1773) with a volume of 1, 1, 2, 3 and 4 L respectively. In the experiments to determine the combined effect of pH and volume on the morphology of *R. oryzae*, incubation was carried out for 48 h, in a rotary shaker (Certomat® BS-1) at 35ºC and 200 rpm. The initial pH was varied between 2.8 and 6.3. The experiments to determine the combined effect of agitation speed and volume on the morphology of *R. oryzae* were all performed at an initial pH of 3.2. These incubations were also carried out for 48 h, in a rotary shaker (Certomat® BS-1) at 35ºC, but the agitation frequency was subsequently changed to 150, 175 and 225 rpm. All the experiments were performed in duplicate.

2.4   Fermentation conditions for fumaric acid production

The production medium to which the produced pellets were transferred aseptically was nitrogen free. The salt composition of the production medium was the same as of the inoculation medium. Glucose concentrations are listed in Tables 4 and 5. Batch fermentations were performed at 35 °C in 2 L fermentors (Applikon, Schiedam, The Netherlands), with a working volume of 1.4 L. NaOH (25 % w/w) was used to control the pH at desired values. The fermentation medium was stirred at 600 rpm to keep homogeneity with an aeration rate of 1.0 L L^{-1} min^{-1} for ~165 h. Samples were taken periodically and the oxygen and carbon dioxide contents in the off-gas from the fermentor was monitored using a NGA200 gas analyser (Rosemount Analytics, USA). It also analyses the composition of the gas coming into the vessel. pH was continuously monitored and data archived using MFCS applications. Similarly, the additions of NaOH were also monitored on-line.

2.5   O$_2$ profile in pellets

To determine the O$_2$ profile within *R. oryzae* pellets, a miniaturised Clark-type oxygen sensor with a tip-diameter of about 25 μm (Unisense OX25 Aarhus, Denmark. www.unisense.com) was used. The O$_2$ concentration was measured every 50 μm, from 200 μm outside the pellet to 400 μm inside the pellet. The O$_2$ concentration outside the pellets was set to 100%.

2.6 Analytical methods

Fumaric acid, glucose, ethanol and glycerol concentrations were quantified by HPLC with a Bio-Rad Aminex HPX-87H ion-exclusion column (300 x 7.8 mm) with a refractive index detector (Waters 2414) and U.V. detector at 210 nm (Waters 2489). The column was eluted with dilute phosphoric acid (1.5 mmol/L in Milli-Q water) at a column temperature of 59 $^{\circ}$C and a flow rate of 0.6 mL/min. The final cell mass was filtered on pre-weighed Whatman, GF/C, diameter 47 mm filter paper. The solid fraction was washed completely with deionised water, dried at 70°C for 24 h, and weighed to yield the final dry weight.

3 Results and discussion

Preliminary experiments showed that cultivating *R. oryzae* from spores in 2 L stirred fermentors led to the formation of large clumps. Therefore, pre-cultivations were carried out in shake flasks, thereby attempting to find cultivation conditions that would result in large amounts of small uniform pellets (< 1 mm) with a high specific activity for fumaric acid production.

3.1 Effect of pH and shake flask volume on pellet formation

All morphologies observed during the cultivation of *R. oryzae* in different volumes and at different initial pH values but at a fixed shaking frequency, are summarised in Table 1. This table also contains information about the diameter and the characteristics of the obtained pellets. Figure 2 illustrates the terms used to describe the pellet surfaces. It was found that the observed morphology depended much more on the shake flask volume than on initial pH. The experiments performed in 1 L shake flasks mostly resulted in pellets, both after 24 and after 48 h of growth. Cultivation in 2 or 3 L flasks, however, resulted mainly in the dispersed growth of mycelia during the first 24 h. Very large pellets were formed in the 4 L shake flasks. It was visually observed that, for fixed shaking frequency, shaking in the 4 L flasks was much less intense than in the other flasks, and apparently this led to much larger pellets in the 4 L flasks.

Table 1: Overview of the observed morphology of *R. oryzae* after 48 h of growth in different working volumes and initial pH values. (200 rpm, 35 °C).

Volume (mL)	pH	Morphology	Pellet diameter (mm)		Pellet characteristics	Cell dry mass (g L⁻¹)
			Average	*Size range*		
200 (in 1 L flask)	2.8	Little growth	-	-	-	0.01
	3.0	Pellets	1.0	0.5 – 2.0	Little cell mass	0.07
	3.2	Pellets	1.3	0.4 – 3.2	Hairy	0.71
	4.7	Pellets	1.4	0.4 – 2.7	Very hairy, sticking together	0.63
	5.9	Pellets	1.2	0.5 – 2.1	Smooth	0.26
	6.3	Strands & Pellets	3.0	2.5 – 3.8	Smooth, hollow	0.53
300 (in 1 L flask)	2.8	Little growth	-	-	-	0.01
	3.0	Pellets	0.8	0.4 – 2.2	Little cell mass	0.06
	3.2	Pellets	1.9	0.7 – 6.7	Hairy	0.68
	4.7	Pellets	1.0	0.4 – 2.3	Very hairy, sticking together	0.65
	5.9	Clumps & pellets	1.6	1.2 – 2.4	Smooth	0.26
	6.3	Clumps & pellets	2.3	1.6 – 3.7	Smooth, hollow	0.53
500 (in 2 L flask)	2.8	Little growth	-	-	-	0.002
	3.0	Pellets	1.0	0.4 – 1.6	Little cell mass	0.08
	3.2	Pellets	0.9	0.3 – 3.3	Smooth, little cell mass	0.07
	4.7	Sparse mycelium	-	-	-	0.05
	5.9	Sparse & pellets	0.9	0.4 – 1.5	Very hairy	0.25
	6.3	Clumps	-	-	-	0.39
700 (in 3 L flask)	3.0	Sparse & pellets	0.6	0.4 – 1.2	Little cell mass	0.02
	4.7	Pellets	1.0	0.3 – 2.9	Smooth	0.08
	6.3	Clumps & pellets	1.2	0.4 – 2.4	Smooth	0.44
1000 (in 4 L flask)	3.0	Pellets	7.2	4.2 – 10.4	Large, hollow, fluffy	0.35
	3.2	Pellets	7.4	3.5 – 10.9	Large, hollow, fluffy	0.24
	4.7	Pellets	6.2	3.8 – 8.1	Large, hollow, fluffy	0.27
	6.3	Pellets	7.6	3.7 – 12.0	Large, hollow, fluffy	0.37

Not only the morphology but also the final cell dry mass concentration clearly varied with shake flask volume. The formation of dispersed mycelia during growth of *R. oryzae*, which was observed in the cultivations with 2 and 3 L flasks, had a disastrous effect on the cell mass yield. Even when the morphology changed to pellets during the second 24 h of the cultivation, the final cell dry mass concentration was less than 0.1 g L⁻¹.
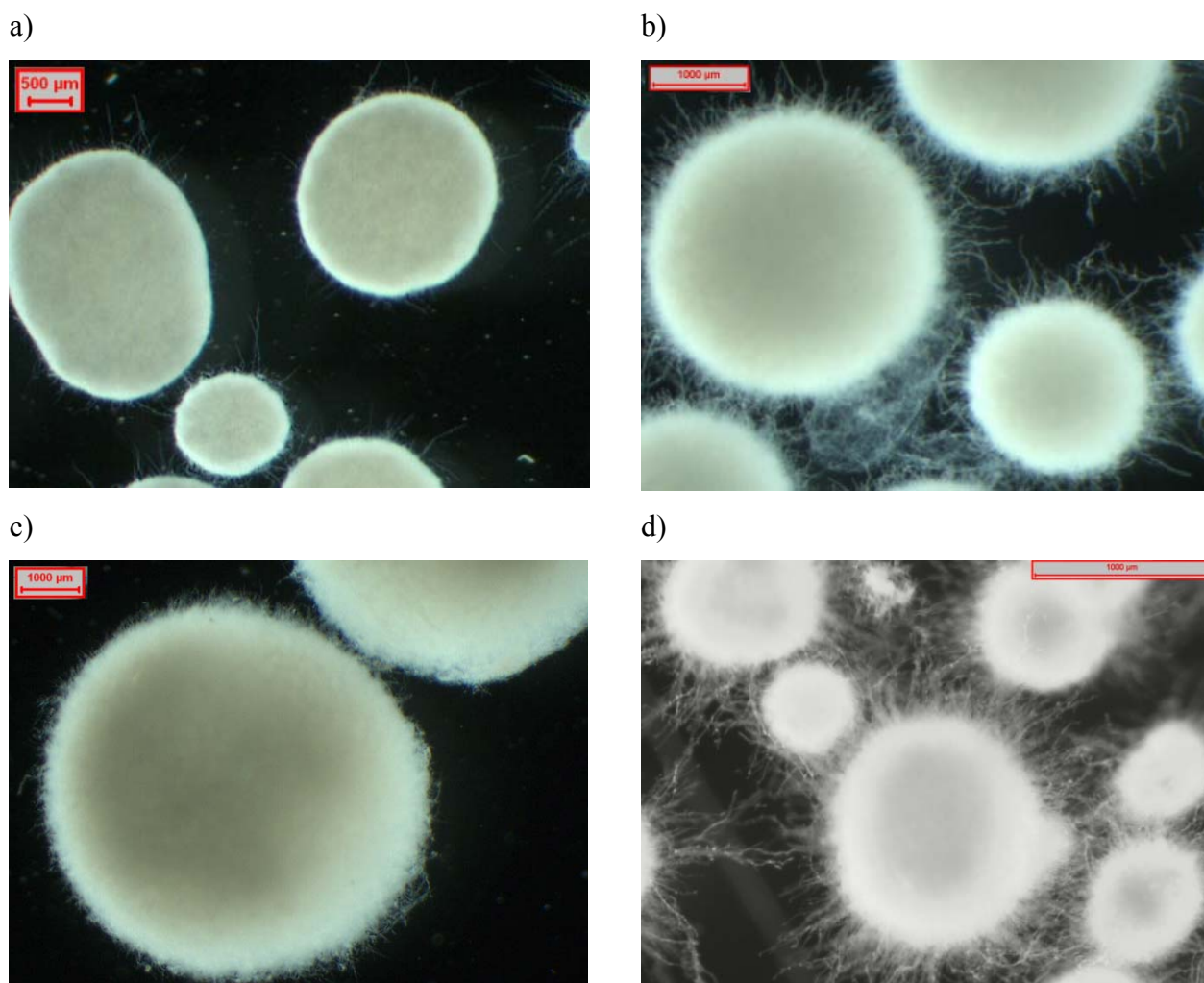
a)

b)

c)

d)

Figure 2: Examples illustrating descriptions of pellet characteristics used in Table 1. a) Smooth pellets, cultivation in 200 mL at pH 6.3 and 200 rpm; b) Hairy pellets, cultivation in 300 mL at pH 3.2 and 150 rpm; c) Fluffy pellets, cultivation in 1000 mL at pH 3.0 and 200 rpm; d) Very hairy pellets, cultivation in 300 mL at pH 4.7 and 200 rpm.

In the range from pH 3.2 to 6.3 the final cell mass concentration in the 1 L shake flasks increased with decreasing initial pH. A maximal final cell dry mass concentration of 0.7 g L^{-1} was obtained by the cultivation of *R. oryzae* in 1 L flask at pH 3.2. When the initial pH was lowered further, the final cell mass concentration dropped to less than 0.1 g L^{-1}. The average pellet diameter decreased slightly with decreasing initial pH. Also, clumps and strands of mycelia were formed more often at higher initial pH values. These observations are in agreement with those of Zhou et al., (2000) and Liu et al., (2008).

During the growth phase, HPLC analysis (data not shown) showed that the highest fumaric acid concentration is obtained after cultivation in 1 L flasks at an initial pH of 4.7. On the other hand, less ethanol resulted than in the cultivations at pH 3.2. However, the cell mass concentration was slightly

lower and the formed pellets were very hairy and sticking together. Therefore, pH 3.2 was selected as the best initial pH for the formation of small pellets. This value is in line with the optimal pH value of 3.1, found by Zhou et al., (2000).

3.2 Shaking frequency and shake flask volume effect on pellet formation

The previous results indicate that the hydrodynamic conditions in the flask are important for the morphology obtained. Therefore, the effect of shaking frequency was studied in combination with flask volume. Within each of the tested volumes four different stages of shaking could be distinguished while the shaking frequency increased (see Figure 3). At low shaking frequency (100-125 rpm) the mixing was very calm and slow. At 150 rpm good shaking was achieved for all volumes, from 1 to 4 L shake flasks. The height reached by the liquid on the flask wall oscillated and the experiments in the first part had shown that small pellets were formed under these conditions. When the shaking frequency was further increased (see Figure 3), the shaking became more intense and the liquid level on the wall no longer oscillated, but remained at a uniform height. From the experiments at different initial pH values it was concluded, that this flow regime promotes dispersed mycelial growth.

For these shaking frequencies the liquid movement was 'in-phase' with the shaking frequency: the liquid followed the movement of the flask. At higher shaking frequencies however, the behaviour of the liquid became 'out-of-phase' and a chaotic flow with splashing was observed. At one point in the transition from fast 'in-phase' shaking to 'out-of-phase' behaviour, hardly any movement of the liquid was observed. This situation was seen during the cultivations in the 4 L shake flasks at 200 rpm and resulted in the formation of large, fluffy pellets. The 'out-of-phase' phenomenon has been described by Büchs et al., (2000) and it was said to occur mostly in large volumes or when the viscosity of the liquid was elevated. This is in agreement with our observations, because the 'out-of-phase' behaviour was only observed at high shaking frequencies in the larger shake flask volumes (2 L or more).

rpm	Working volume (ml)				
	200	300	500	700	1000
100					
125					
150					
175					
200					
225					
250					

slow shaking
good shaking
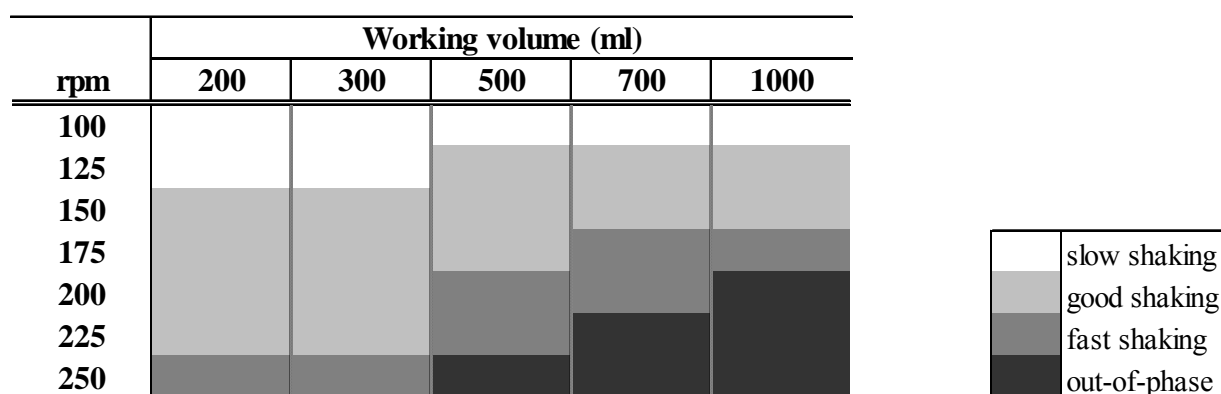fast shaking
out-of-phase

Figure 3: Flow regimes observed for different working volumes and shaking frequencies.

As described above, the shaking frequency at which transition to 'out-of-phase' behaviour occurs, decreases with increasing flask volume. This is also supported by the observation that the velocity of the liquid increased with increasing flask volume, when all flasks were shaken at the same frequency. This is explained by the larger diameter, and thus perimeter, of the bigger shake flasks.

3.2.1 Morphology and Pellet Diameter

Pellets were obtained in all the cultivations performed at different working volumes and shaking frequencies at pH 3.2. Though, the cultivation in 3 L flasks at 175 rpm led partially to disperse mycelial growth. Table 2 gives an overview of the size and characteristics of these pellets. For each flask volume, the average pellet diameter decreased with increasing shaking frequency. The range of the measured diameters, however, was more or less constant (0.5-3.5 mm), but the pellets became less uniform. This effect is illustrated in Figure 4 for the pellets formed during the cultivation in 300 mL medium at 150 and 225 rpm.

The same is observed for a fixed shaking frequency: the average pellet diameter decreases with increasing volume, but the uniformity of the pellets also decreases. To obtain uniform small pellets like formed in the 1 L shake flasks at 200 rpm on a larger scale, the hydrodynamic conditions in the flasks have to be similar. This means that the shaking frequency has to be lowered. From the experiments in large volumes performed in this work the best pellets were obtained after the cultivation in 3 L shake flasks with 700 mL medium at pH 3.2 and 150 rpm (~1-2 mm). The cell mass amount (concentration times volume) was also the highest for this case. The pellets obtained in the 4-L shake flasks at the same shaking speed were smaller, less uniform and lower amounts were obtained.

Table 2: Overview of the observed morphology of *R. oryzae* after 48 h of growth in different working volumes and shaking frequency (pH = 3.2, 35 $^{\circ}$C).

Volume (mL)	rpm	Morphology	Pellet diameter (mm)		Pellet characteristics	Cell dry mass (g L^{-1})
			Average	*Size range*		
200 (in 1 L flask)	150	Pellets	2.5	0.8 – 3.8	Large, hairy	0.81
	175	Pellets	0.9	0.5 – 3.4	Smooth, little cell mass	0.24
	200	Pellets	1.3	0.4 – 3.2	Hairy	0.71
	225	Pellets	0.9	0.3 – 3.3	Small, hairy	0.49
300 (in 1 L flask)	150	Pellets	2.2	0.9 – 3.3	Large, hairy	0.77
	175	Pellets	1.0	0.4 – 2.9	Smooth	0.38
	200	Pellets	1.9	0.7 – 6.7	Hairy	0.68
	225	Pellets	0.9	0.3 – 2.8	Small, hairy	0.54
500 (in 2 L flask)	150	Pellets	1.5	0.3 – 5.9	Hairy	0.53
	175	Pellets	0.9	0.5 – 3.2	Small, hairy	0.61
	200	Pellets	0.9	0.3 – 3.3	Smooth, little cell mass	0.07
700 (in 3 L flask)	150	Pellets	1.7	0.6 – 3.0	Small, hairy	0.66
	175	Dispersed & pellets	0.7	0.5 – 2.3	Smooth, little cell mass	0.08
1000 (in 4 L flask)	150	Pellets	1.0	0.3 – 4.7	Small, hairy	0.38
	200	Pellets	7.4	3.5 – 10.9	Large, hollow, fluffy	0.24
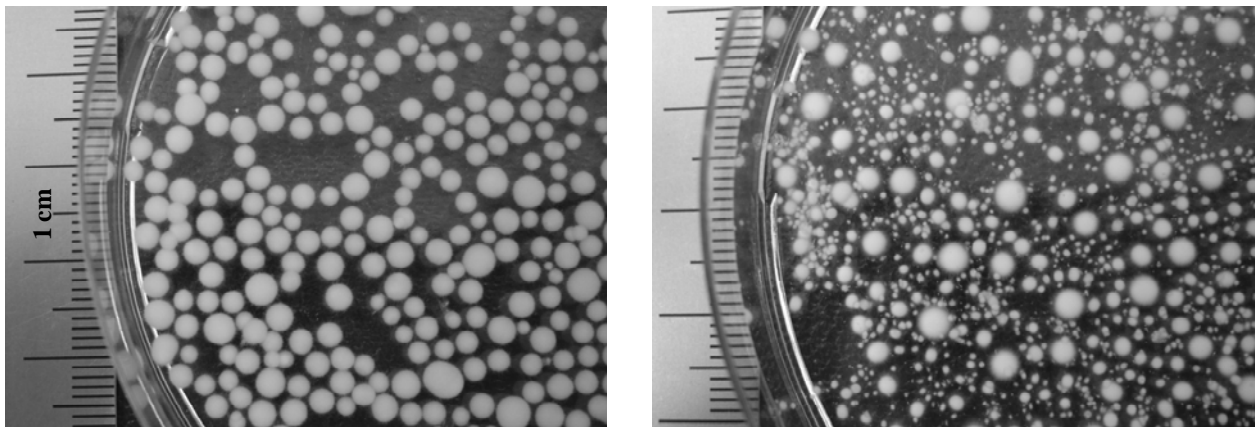
Figure 4: Close-up of the pellets formed in the 1 L shake flask with 300 mL medium after 48 h of growth at 150 rpm (left hand side) and 225 rpm (right hand side) (pH 3.2, 35 $^{\circ}$C).

Additionally, it was confirmed that 'fast shaking' (as observed in cultivations in 3 L at 175 rpm and in 2 L at 200 rpm) results in dispersed growth of mycelia, very little cell mass and very high concentrations of residual glucose.

3.2.2 O$_2$ Profiles

All experiments with a high final cell mass concentration and a pellet diameter larger than ~1 mm during the growing phase also had a high final ethanol concentration (data not shown). This suggested that the centres of the pellets were anaerobic. To determine the critical diameter, above which the pellet centre becomes anaerobic, two O$_2$ profiles were determined.

A pellet obtained by cultivation in 500 mL medium at pH 3.2 and 150 rpm was compact and had a diameter of 1.6 mm. When the sensor was 0.25 mm inside the pellet, the O$_2$ level was less than 5% of the O$_2$ concentration outside the pellet. The second pellet was large (3.7 mm) and fluffy, and was obtained by cultivation in 1000 mL medium at pH 3.2 and 200 rpm. Again the O$_2$ concentration inside the pellet quickly dropped and the O$_2$ level was less than 5% of the O$_2$ concentration outside the pellet when the sensor was 0.30 mm inside the pellet. The results confirmed that both pellets had an anaerobic core. The slope of the O$_2$ profile of the fluffy pellet was slightly less steep than that of the compact pellet, but the difference is very small. It was concluded that, in air-saturated broth, anaerobic conditions may occur in the core of the pellet if the diameter exceeds 0.5 mm. Such anaerobic conditions might lead to ethanol rather than fumaric acid production.

3.3 Fumaric acid production by fermentation at low pH

Initially, to determine the pH effect on fumaric acid production by fermentation, fermentation experiments at pH values from 3.0 to 5.0 were studied. Table 3 provides the initial glucose concentration, yield of fumarate in glucose ($Y_{p/s}$), final product and by-product concentrations, cell mass specific fumaric acid production rate (q_p) and final cell dry mass of all fermentations performed for studying the pH effect. It was observed that the pH value quickly dropped from 5.0 to ~ 2.0 in the first 20 h if it was not controlled. Then, fumaric acid production was very low and the low ethanol production and $Y_{p/s}$ value suggests that glucose was consumed mainly for maintenance purposes. Other experiments showed that the final titers of fumaric acid were decreasing when the pH was fixed at low values (Table 3). The same is observed for $Y_{p/s}$ and q_p, so at lower pH values the performance of the fermentation is lower, which was expected since high concentrations of the acid cause low production (Du et al., 1997; Gangl et al., 1990). Furthermore, a higher glycerol/fumarate ratio was observed when the fermentation pH value was going down. Glycerol production consumes NADH (see Figure 1) and may compensate the decreased NADH consumption by the respiration and

cytosolic pathways at low pH to maintain the proper NAD/NADH ratio. In addition, as the initial glucose concentrations were high, the fungi were exposed to a quite high osmotic pressure environment and probably producing glycerol as a stress response (Mager and Siderius, 2002).

The time course of fermentative production of fumaric acid by *R. oryzae* at pH 5.0 (which is an optimal pH value for fumaric acid production (Zhou et al., 2000)) is shown in Figure 5a. The profiles in this Figure illustrate glucose consumption and fumaric acid and ethanol production. The production of fumaric acid starts to increase rapidly after around 24 h. This is probably due to the fact that during the first hours of the batch *R. oryzae* pellets have to adjust to their new condition and switch from growing phase to production phase.

The ethanol profiles of Figures 5a show that ethanol production reached its maximum value at about 70 h and then remained relatively constant. However, because ethanol is a volatile compound, its evaporation rate from a solution of 5 g L^{-1} of ethanol in water was measured using the same bioreactor set up and conditions used for the fermentation experiments (35 $^{\circ}$C and 600 rpm). The measured ethanol evaporation rate was 0.09 g L^{-1} h^{-1}, so the ethanol values in Figures 5a – 5d are underestimated by 30-40 %. Moreover, it has been reported that when glucose is being depleted, *R. oryzae* consumes ethanol as an alternative carbon source (Cao et al., 1996). This phenomenon was also observed during some experiments performed in this study (data not shown). Therefore, it was not possible to quantify the total amount of ethanol produced during fermentation.

On Figures 5c and 5d the profiles and glucose consumption and fumaric acid and ethanol production are illustrated for experiments were the pH control was switched off. Instead of keeping the pH low during the whole fermentation time, changing the pH during the fermentation could be a better strategy to achieve a low final pH (where more undissociated acid is formed) in the fermentation without compromising the fumarate production too much. It was therefore decided to initially control the pH at 5.0 and stop the pH control after a certain time resulting in a decrease of the pH as a result of fumaric acid production (see Figure 5b). When the pH control was stopped at 120 h (Figure 5c), the performance was very similar to the fermentation that was controlled at pH 5.0 during the entire cultivation period (Figure 5a). However, terminating the pH control at 120 h did not lead to very low final pH values (pH = 4.1).

Table 3: Experimental data from *R. oryzae* fermentations carried out at different pH values (at 10% (v/v) CO_2).

Initial pH	3.0	3.5	4.0	5.0	5.0	5.0	5.0
Time of pH control off	-	-	-	-	0	120	90
Final pH	3.00	3.50	4.00	5.00	2.42	4.10	3.60
Initial glucose (g L^{-1})	93.06 ± 7.16	111.96 ± 6.05	89.03 ± 4.82	118.00 ± 6.42	118.80 ± 6.46	126.00 ± 6.85	118.80 ± 9.20
Final cells dry mass (g)	4.44 ± 1.52	3.74 ± 0.90	3.40 ± 1.11	3.71 ± 0.89	2.28 ± 0.55	3.57 ± 0.86	2.36 ± 0.79
Final fumaric acid (g L^{-1})	9.39 ± 2.81	19.84 ± 4.12	24.54 ± 5.89	30.21 ± 6.38	2.92 ± 0.62	29.05 ± 6.14	20.45 ± 7.74
Final ethanol (g L^{-1})	5.88 ± 1.85	5.82 ± 1.29	5.96 ± 0.96	7.17 ± 1.59	0.00 ± 0.00	5.76 ± 1.28	8.30 ± 2.10
Final glycerol (g L^{-1})	3.17 ± 1.60	6.59 ± 2.27	4.57 ± 2.02	4.63 ± 1.65	2.07 ± 0.74	7.13 ± 2.54	3.05 ± 2.22
q_p (g g^{-1} h^{-1})	0.02 ± 0.01	0.04 ± 0.01	0.06 ± 0.01	0.06 ± 0.02	0.01 ± 0.00	0.06 ± 0.02	0.07 ± 0.03
$Y_{p/s}$ (g g^{-1})	0.13 ± 0.04	0.19 ± 0.04	0.26 ± 0.06	0.28 ± 0.06	0.09 ± 0.02	0.27 ± 0.06	0.25 ± 0.09
Total NaOH added (g)	13.00 ± 3.96	17.81 ± 3.69	21.83 ± 3.90	27.53 ± 5.93	0.00 ± 0.00	25.15 ± 5.40	12.45 ± 4.58

When the pH control was stopped at 90 h (Figure 5d) the final fermentation pH was around 3.6 but the fumaric acid titers were ~30% lower than for fermentation at pH 5.0 and for the fermentation where the pH control was terminated at 120 h. However, before 90 h where the pH was switched off, the fumaric acid production was not as high at that time as for the experiments at pH 5.0 and when the control was off at 120 h (Figures 5a and 5c). This implies that the production of fumaric acid in the experiments where the pH control was off at 90 h was going to be anyway lower compared to the profiles of experiments at pH 5.0 and control off at 120 h. Therefore, it seems that switching off the pH at 90 h did not affect strongly the fumaric acid production.
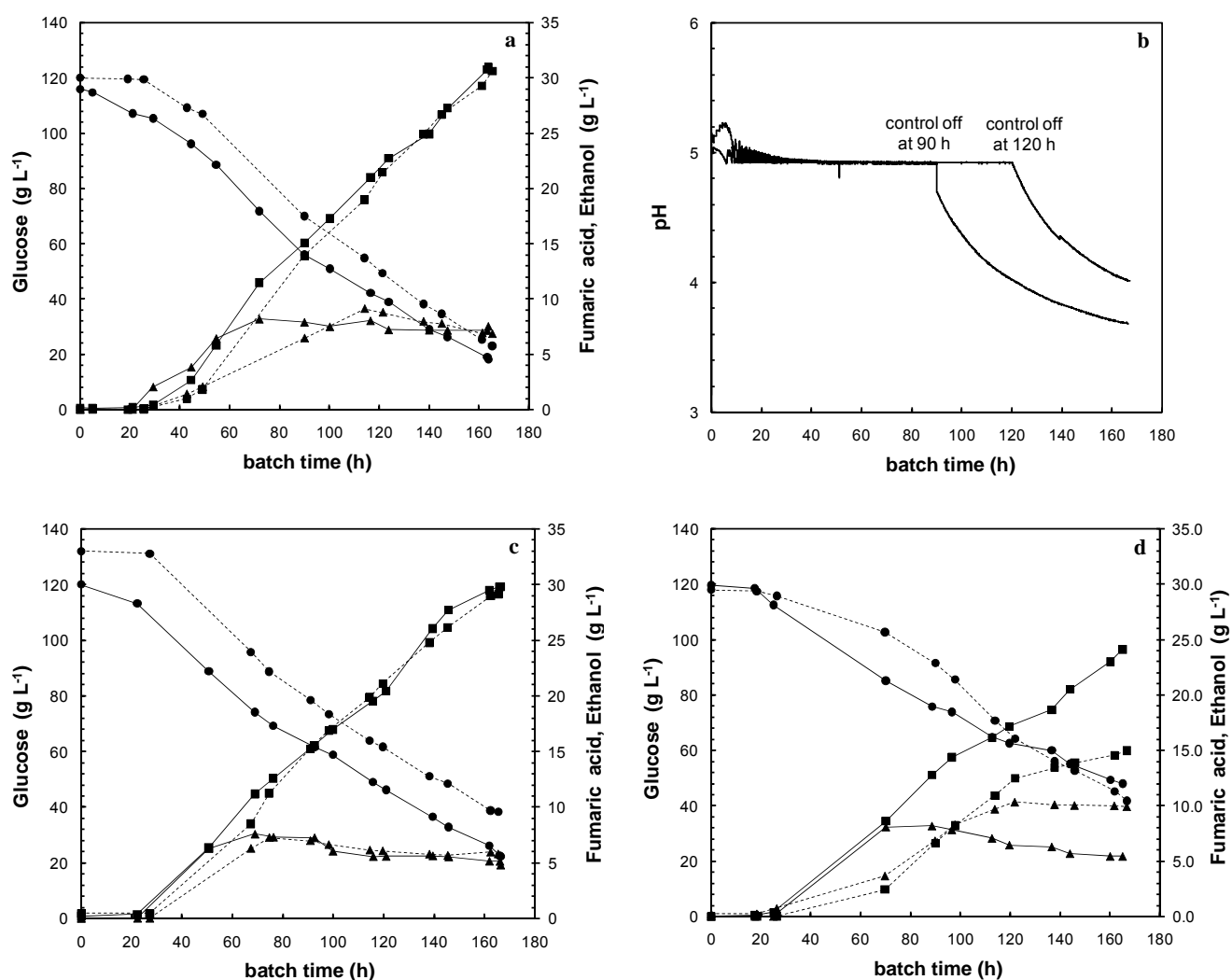

Figure 5: Fermentative fumaric acid production at, 35 ^{o}C, 600 rpm and ~10 % (v/v) of CO_2 in air. Concentration profiles: ● glucose, ▲ ethanol and ■ fumaric acid. a) Fermentation pH kept at 5.0; b) pH profiles of fermentations with pH control stopped at 120 h and 90 h; c) Fermentation pH control stopped at 120 h; d) Fermentation pH control stopped at 90 h. Full and dashed lines are duplicates.

Despite that the procedure used for the fermentation did not enable determination of the initial cell mass amount, it was expected that the lack of N-source should had minimised growth. However, the fungi was still growing on the stirrer of the fermentor during the production phase and it was not possible to precisely control the amount of *R. oryzae* pellets with which the fermentors were inoculated. Therefore, the performance of the fermentations is better compared by analysing the cell mass specific fumaric acid production rate (q_p). The q_p value is obtained by dividing the total amount of fumaric acid produced by the total cell mass and fermentation time. It was found that when the fermentation pH was controlled at lower values, q_p was lower and thus less fumaric acid was produced (see Table 3). This may be explained by higher ATP consumption by the fungi at lower pH to keep their internal pH at neutral values. To maximise the production of ATP the cell mass might need to convert more glucose fully into CO_2 instead of fumarate.

As can be seen in Figure 5, fumarate productivities of the different experiments start after 24 h. These observations suggest that it takes to the strain $\sim$ 24 h at pH 5.0 to adapt to the new media and switches from growing to production phase. Surprisingly, the overall productivities in fermentations where the pH control was stopped were not so different from productivities in the fermentations with continuing pH control at 5.0 (Table 3), meaning that before 90 h the fungi reached their maximum production rate and they are less sensitive to pH changes after that time. Furthermore, amounts of NaOH added to the fermentation are around 50 % lower (Table 3) when fermentation pH control was stopped at 90 h than when fermentation pH is kept at 5.0. This means that by switching off pH control a significant reduction of the added amount of neutralising agent was achieved whereas fumarate yields and productivities are not negatively affected.

3.4　Effect of the CO_2 on fumaric acid production by fermentation

The effect of CO_2 in the in-gas on fumaric acid production was studied in batch fermentations controlled at pH 3.5, 35 $^{\circ}$C under various CO_2 volume percentages of 0, 10, 20, 50 and 70. Table 4 presents the initial glucose concentration, fermentation titers, $Y_{p/s}$, q_p and amount cell dry mass of all fermentations. Table 4 indicates that during the fermentation the fumarate productivity goes down when the CO_2 volume percentage increases. This can be explained by the fact that by mixing the inlet air with increasing amounts of CO_2 the O_2 content in the in-gas decreases, which affects the fermentation performance. Indeed, ethanol concentrations were higher when the CO_2 volume percentage was increased from 10 to 20%, suggesting that the fermentations became O_2 limited.

Nevertheless, the ethanol concentration at CO_2 volume percentages of 50 and 70% was lower than at 20%, but at 50 and 70% the whole fermentation performance was poor.

Table 4: Experimental data from *R. oryzae* fermentations carried out at different CO_2 % (v/v) in the in-gas (pH = 3.5).

	Air	*10 % CO₂*	*20 % CO₂*	*50 % CO₂*	*70 % CO₂*
Initial glucose (g l⁻¹)	117.00 ± 8.99	111.96 ± 6.05	118.94 ± 6.47	119.74 ± 9.21	114.65 ± 8.82
Final cells dry mass (g)	2.69 ± 0.92	3.74 ± 0.90	3.10 ± 0.74	1.34 ± 0.46	1.16 ± 0.40
Final fumaric acid (g l⁻¹)	14.91 ± 4.26	19.84 ± 3.94	13.48 ± 2.72	4.74 ± 1.35	0.35 ± 0.10
Final ethanol (g l⁻¹)	3.69 ± 1.26	5.82 ± 1.40	9.09 ± 2.19	6.70 ± 2.29	3.00 ± 1.03
Final glycerol (g l⁻¹)	6.04 ± 3.05	6.60 ± 2.27	3.41 ± 1.21	1.19 ± 0.60	0.28 ± 0.14
q_p (g g⁻¹ h⁻¹)	0.04 ± 0.01	0.04 ± 0.01	0.03 ± 0.01	0.03 ± 0.01	0.00 ± 0.00
$Y_{p/s}$ (g g⁻¹)	0.18 ± 0.05	0.19 ± 0.04	0.15 ± 0.03	0.10 ± 0.03	0.02 ± 0.01
Total NaOH added (g)	12.50 ± 3.81	17.81 ± 3.69	13.00 ± 2.80	3.55 ± 1.08	5.83 ± 1.78

It was also observed that the productivity of the fermentation is not negatively affected when the inlet air is not blended with CO_2. Apparently, the CO_2 that is produced by the cells is sufficient to fulfil the CO_2 requirements for pyruvate carboxylation. There might be a CO_2 gradient in the pellets such that the concentration in the pellet centre is higher than in the bulk liquid. However, the highest yield and final titers were obtained in the fermentation where the CO_2 volume percentage in the in-gas was 10%, which suggests that CO_2 blending may still be beneficial for fumaric acid production.

Table 5: Fumaric acid titers obtained by fermentation with *R. oryzae*

Acid	*Final titer (g L⁻¹)*	*Final pH*	*Strain*	*Reference*
Fumaric	20	3.5	*Rhizopus oryzae*	This work
Fumaric	65	5.0	*Rhizopus oryzae*	Cao et al., 1996
Fumaric	36	5.5	*Rhizopus oryzae*	Zhou 1999

The best results obtained in this study with a final low pH (3.5) were compared to previous studies on fumaric acid fermentation using the same strain but at pH 5.0. The $Y_{p/s}$ values we obtained were around 50% lower than some values reported in literature (Cao et al., 1996; Du et al., 1997; Zhou et

al., 2002). Final fumaric acid titers were also lower than in previous work (see Table 5) but final pH values of those studies are higher therefore, to recover fumaric acid more waste salts are generated. However, final fumaric acid titers of fermentations performed in this work at pH 5.0 are in agreement with some data reported using the same strain and fermentation set up (Zhou 1999), which means that pH values affect final fumaric acid titers.

Table 6: Carboxylic acid titers obtained at low fermentation pH

Acid	Final titer (g L^{-1})	Final pH	Strain	Reference
Acetic	5	4.5	*Clostridium thermoaceticum*	Schwartz and Keller 1982
Citric	240	2.1	*Aspergillus niger*	Papagianni et al., 1999
Fumaric	20	3.5	*Rhizopus oryzae*	This work
Gluconic	60	1.4	*Aspergillus niger*	Singh et al., 2003
Gluconic	140	2.1	*Aspergillus niger*	Sankpal et al., 1999
Itaconic	75	2.0	*Aspergillus terreus*	Yahiro et al., 1997
Lactic	70	<2.5	*Saccharomyces cerevisiae*	Valli 2006
Lactic	109	3.0	*Kluyveromyces lactis*	Porro et al., 1999

Furthermore, according to final carboxylic acid titers, a number of experimental values have been reported in literature for low pH (Table 6). Comparing these, our fumaric acid titers are relatively low. Nevertheless, considering the low solubility of fumaric acid (7 g l^{-1} at 25°C) the possibilities of recovering the undissociated form of it from our fermentation broth might be higher than in the other fermentation cases.

4   Conclusions

Results obtained from shake flask experiments with *R. oryzae* revealed that cultivation parameters such as pH, shaking frequency and working volumes significantly affect the morphology of *R. oryzae*. The average pellet diameter decreased slightly with decreasing pH and clumps of mycelia were mostly formed at high initial pH values (pH 5.9 or higher). Because the differences in observed morphology between cultures grown in shake flasks of different volumes were much larger than the differences observed after cultivation in one working volume at different initial pH, it was expected

that the influence of the hydrodynamic conditions in the flask was larger than the initial pH. The average pellet diameter decreased with increasing shaking frequency and with increasing flask size.

From *R. oryzae* fermentations carried out at different pH it was found that the cultivation pH has a very strong effect on the fumaric productivity and by-product formation. Lowering the fermentation pH led to decreased fumaric acid production and increased production of by-products like glycerol and ethanol. However, applying a pH profile by terminating the pH control at 90 h in order to obtain a decreased pH at the end of the fermentation was successfully achieved and did not affect the fumaric acid productivity and substrate-product yield. When the pH control was stopped at 90 h the final pH of the fermentation was around 3.6, which might simplify product recovery. In addition, the total amount of NaOH required for pH control was significantly reduced with this strategy. Furthermore, the best feeding strategy of CO_2 in the in-gas was obtained when 10 % (v/v) of this gas was blended in the in-gas air mixture. More CO_2 negatively affected fumarate production, most likely due to O_2 limitation. Follow up work should address the integration of fumaric acid fermentation and product recovery.

References

Büchs J, Maier U, Milbradt C, Zoels B (2000) Power consumption in shaking flasks on rotary shaking machines: I. power consumption measurement in unbaffled flasks at low liquid viscosity. Biochem Biotech (68) 589.

Cao NJ, Du JX, Gong CS, Tsao GT (1996) Simultaneous production and recovery of fumaric acid from immobilized *Rhizopus oryzae* with a rotary biofilm contactor and an adsorption column. Appl Environ Microbiol (62) 2926.

Du JX, Cao NJ, Gong CS, Tsao GT, Yuan NJ (1997) Fumaric acid production in airlift loop reactor with porous sparger. Appl Biochem Biotech (63-65) 541.

Dynesen J, Nielsen J (2003) Surface hydrophobicity of *Aspergillus nidulans* conidiospores and its role in pellet formation. Biotechnol Prog (19) 1049.

Gangl IC, Weigand WA, Keller FA (1990) Economic comparison of calcium fumarate and sodium fumarate production by *Rhizopus arrhizus*. Appl Biochem Biotech (24 -25) 663.

Joglekar HG, Rahman I, Babu S, Kulkarni BD, Joshi A (2006) Comparative assessment of downstream processing options for lactic acid. Sep Purif Technol (52) 1.

Liu Y, Liao W, Chen S (2008) Study of pellet formation of filamentous fungi *Rhizopus oryzae* using a multiple logistic regression model. Biochem Biotech (99) 117.

Lohbeck K, Haferkorn H, Fuhrmann W, Fedtke N (1990) Maleic and fumaric acids. Ullmann's Encyclopedia of Industrial Chemistry, 5th ed., Vol. A16, VCH., 53-62. Weinheim, Germany

Mager WH and Siderius M (2002) Novel insights into the osmotic stress response of yeats. FEMS Yeast Res (2) 251.

Papagianni M, Mattey M, Kristiansen B (1999) The influence of glucose concentration on citric acid production and morphology of *Aspergillus niger* in batch and culture - the low affinity carrier is only formed during growth on high glucose concentrations. Enzyme Microb Technol (25) 710.

Porro D, Bianchi MM, Brambilla L, Menghini R, Bolzani D, Carrera V, Lievense J, Liu CL, Ranzi BM, Frontali L, Alberghina L (1999) Replacement of a metabolic pathway for large-scale production of lactic acid from engineered yeasts. Appl Environ Microbiol (65) 4211.

Roa Engel CA, Straathof AJJ, Zijlmans TW, van Gulik WM, van der Wielen LAM (2008) Fumaric acid production by fermentation. Appl Microbiol Biotechnol (78) 379.

Rhodes RA, Moyer AJ, Smith ML, Kelley SE (1959) Production of fumaric acid by *Rhizopus arrhizus*. Appl Microbiol (7) 74.

Sankpal NV, Joshi AP, Sutar II, Kulkarni BD (1999) Continuous production of gluconic acid by *Aspergillus niger* immobilized on a cellulosic support: study of low pH fermentative behaviour of *Aspergillus niger*. Proc Biochem (35) 317.

Schwartz RD and Keller FA (1982) Isolation of a strain of *Clostridium thermoaceticum* capable of growth and acetic acid production at pH 4.5. Appl Environ Microbiol (43) 117.

Singh OV, Jain RK, Singh RP (2003) Gluconic acid production under varying fermentation conditions by *Aspergillus niger*. J Chem Technol Biotechnol. 78 (2-3) 208.

Valli M, Sauer M, Branduardi P, Borth N, Porro D, Mattanovich D (2006) Improvement of lactic acid production in *Saccharomyces cerevisiae* by cell sorting for high intracellular pH. Appl Environ Microbiol (72) 5492.

Werpy T and Petersen G (2004) Topten value added chemicals from biomass feedstocks. U.S. Department of Energy. USA

Yahiro K, Shibata S, Jia SR, Park Y, Okabe M (1997) Efficient itaconic acid production from raw corn starch. J Fermen Bioeng (84) 375.

Zhou Y (1999) Fumaric acid fermentation by *Rhizopus oryzae* in submerged system. Thesis dissertation. Purdue University. La Fayette, Indiana, USA. pp149.

Zhou Y, Du JX, Tsao GT (2000) Mycelial pellet formation by *Rhizopus oryzae* ATCC 20344. Appl Biochem Biotech (84-86) 779.

Zhou Y, Du JX, Tsao GT (2002) Comparison of fumaric acid production by *Rhizopus oryzae* using different neutralizing agents. Bioproc Biosyst Eng (25) 179.

CHAPTER 4

Solubility of fumaric acid and its sodium salts in the presence of fermentation co-solutes

Fumaric acid is a carboxylic acid with a wide application in food industry and with a potential to be used as a raw material for some polymers. Currently, its fermentative production from renewable resources is receiving much attention. The aqueous solubility of fumaric acid is low, and crystallisation is used to recover fumaric acid from fermentation mixtures. To determine the window of operation for crystallisation from multicomponent fermentation mixtures, the aqueous solubilities of fumaric acid and its sodium salts were investigated as function of temperature and pH. Crystals were observed of fumaric acid, sodium hydrogenfumarate, and sodium fumarate, with solubilities and pH increasing in this order because of increasing polarity and acid dissociation. A mathematical model was developed to predict which crystal type(s) and amount(s) would be obtained at a certain temperature and pH. Additionally, it was shown that the effect of glucose (1.5 and 3.0 mmol mol^{-1}) on the solubility can be neglected but ethanol (1.0 mmol mol^{-1}) increases the solubility of fumaric acid and decreases the solubility of the sodium salts, because the aqueous solution becomes less polar upon ethanol addition but not upon glucose addition.

1 Introduction

Fumaric acid (*trans*-1,2-ethenedicarboxylic acid) is an important starting material for the production of food additives and has a great potential in the production of some polymers (Werpy and Petersen, 2004). The production of fumaric acid (H_2FA) by fermentation of carbohydrates has recently become an attractive alternative to the current process, which uses petroleum-derived maleic anhydride. The fermentation process not only would replace a petroleum based process, but also involve carbon dioxide fixation (Roa Engel et al., 2008), which would increase the sustainability of the fumaric acid production. As with other carboxylic acids produced by fermentation (e.g., lactic acid, citric acid) the highest cell-specific production rates are found around neutral pH values (Du et al., 1997). In the case of fumaric acid, to achieve the optimal pH (~5), sodium hydroxide (NaOH) was identified as a very effective neutralising agent (Zhou et al., 2000).

Crystallisation, upon acidification by sulphuric acid, is the most common method used to recover carboxylic acid fermentation products from fermentation broths (Buque-Taboada et al., 2006; Cuellar, 2008). However, this acidification leads to production of waste salts. In the case of fumaric acid, the acidification step leads to the production of sodium sulphate (Na_2SO_4) if NaOH is used as neutralising agent. Because of the low aqueous solubility of fumaric acid (~7 g/L at 25 ^{o}C), recovery from the fermentation broth by cooling crystallisation is a very interesting option (Buque-Taboada et al., 2006). However, the speciation of fumaric acid might be affected by the multicomponent fermentation broth composition and pH (Harjo et al., 2007). This can result in the formation of different fumarate salts upon crystallisation.

We aim to control the fumaric acid crystallisation in the pH range from 3.0 to 5.0. Therefore, in this chapter we investigate the solubility of fumaric acid and its salts as a function of temperature, pH and concentration of fermentation co-solutes (focusing on glucose, which is the fermentation raw material and ethanol, which is the main by-product). In addition, speciation of fumarate salts is addressed, to be able to predict which solid state will be obtained from fermentation broth at different pH and temperature conditions. The information required is obtained by using phase diagrams to identify crystal formation like in previous studies with other organic compounds (ter Horst et al., 2009). The used diagrams provide valuable information in the preparation of single crystals, in co-crystallisation optimisation, in process scale up, and as a tool to discover new co-crystals (ter Horst et al., 2009). At fixed initial mole fractions of fumaric acid and sodium fumarate(Na_2FA) but in different proportions, the saturation temperature T_S will be measured and

plotted versus the solvent-free mole fraction of fumaric acid: $y_{H2FA} = x_{H2FA}/(x_{H2FA} + x_{Na2FA})$. At the value of $y_{H2FA} = 1$, the solution only contains fumaric acid with a concentration x_{H2FA}.

2 Experimental section and methods

2.1 Chemicals

Fumaric acid (99 %), sodium fumarate (98 %), glucose (99 %) and ethanol (98 %) (Sigma-Aldrich products) were used without further purification. Distilled water was used in all preparations.

2.2 Saturation temperature determination

Saturation temperatures were determined using the Crystal16 equipment of Avantium Technologies (Amsterdam, The Netherlands). In the Crystal16, cloud points and clear points of sixteen 1 mL solution aliquots were measured in parallel based on automatic turbidity detection. The temperature at which the suspension became a clear solution upon heating at 0.5 °C/min was taken as the saturation temperature of the measured sample. After re-crystallisation at 5 °C the saturation temperature was measured again. Saturation temperatures were determined in this way for a number of pre-weighed samples containing fumaric acid, sodium fumarate, or a mixture of both in water, water/ethanol mixtures or water/ethanol/glucose mixtures. The samples containing fumaric acid, sodium fumarate and water were prepared with initial mole fractions of fumaric acid (x_{iH2FA}) of 2.33, 5.35 and 7.55 mmol mol solvent^{-1} and ending with sodium fumarate mole fractions (x_{iNa2FA}) of 24.15 mmol mol solvent^{-1}. The component pairs were dissolved at 80 °C before being placed in the Crystal16.

The different mixtures of fumaric acid and sodium fumarate in aqueous solutions were generated according to equations 1 and 2 (ter Horst et al., 2009).

$$\frac{x_{Na_2FA}}{x_{iNa_2FA}(T)} = 1 - \frac{x_{H_2FA}}{x_{iH_2FA}(T)} \qquad [1]$$

$$y_{H_2FA} = \frac{x_{H_2FA}}{x_{H_2FA} + x_{Na_2FA}} \qquad [2]$$

In Equation 1, the van't Hoff equation was used to calculate the initial mole fractions. Figure 1 shows the compositions of the mixtures prepared.
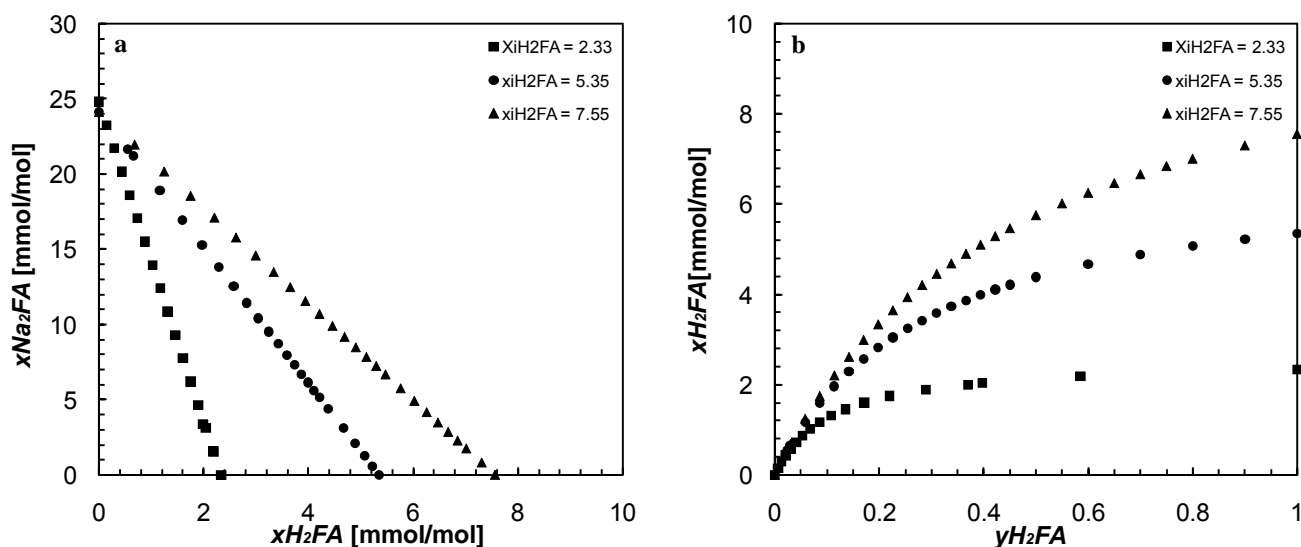

Figure 1: a) Mole fractions of fumaric acid (x_{H2FA}) and sodium fumarate (x_{Na2FA}) used to generate aqueous solutions in this study of these two compounds. b) Mole fraction of fumaric acid in the mixtures (x_{H2FA}) as a function of its solvent-free mole fraction (y_{H2FA}).

2.3 X-ray Powder Diffraction

X-ray powder diffraction (XRPD) patterns were recorded in a Bragg-Brentano geometry on a Bruker D5005 diffractometer equipped with an incident beam monochromator and a Braun PSD detector. Data collection was carried out at room temperature using monochromatic Cu Kα1 radiation (λ = 1.540562 Å) in the 2θ region between 5° and 90°.

2.4 Solubility as a function of pH

In a 100 mL jacketed glass reactor a certain excess amount of dry fumaric acid crystals was added to 50 mL of a 140 g L^{-1} solution of sodium fumarate in water. The resulting suspension was stirred magnetically for 24 h at constant temperature (thermostat bath Lauda RMG). The pH was measured using a Metrohm 691-pH meter. After the crystals had settled for 1 h, solution samples were taken using a pipette and immediately diluted with a known amount of water to avoid re-crystallisation. The total concentration of the fumaric acid species in the diluted sample was determined using HPLC analysis.

2.5 Sodium analysis

Inductively Coupled Plasma – Optical Emission Spectrometry (ICP-OES) was used to analyse sodium in the crystal samples. Perkin-Elmer Optima 3000dv equipment was used at 589.592 and 588.995 nm wavelength. The used concentrations were the average results of the measurements at the selected wavelengths.

2.6 High Performance Liquid Chromatography (HPLC)

Fumaric acid, glucose and ethanol concentrations were quantified by HPLC with a Bio-Rad Aminex HPX-87H ion-exclusion column (300 x 7.8 mm) with a refractive index detector (Waters 2414) and U.V. detector at 210 nm (Waters 2489). The column was eluted with dilute phosphoric acid (1.5 mmol L^{-1} in Milli-Q water) at a column temperature of 59 ^{o}C and a flow rate of 0.6 mL min^{-1}.

3 Results and discussion

Three solid states have been described that might occur in a system containing water, sodium ions and fumaric acid at relevant conditions: fumaric acid, disodium fumarate and the less known sodium hydrogenfumarate. The dissociation and solubility equilibria in aqueous solution of these species are presented in Figure 2.
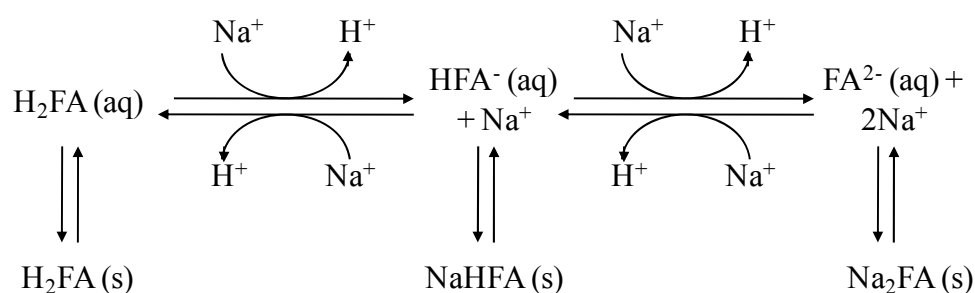

Figure 2: Fumarate equilibria in aqueous solution for Na^{+} as the counter-ion.

At low pH values fumaric acid (H$_2$FA) is the prevailing form and if the aqueous solution is saturated, fumaric acid can crystallise. On the other hand, at high pH sodium fumarate (Na$_2$FA) is

prevailing and at intermediate pH sodium hydrogenfumarate (NaHFA). In the following sections the pH and temperature ranges are indentified for the formation of these three fumarate compounds.

3.1 Phase diagram and fumarate speciation

Figure 3 depicts the saturation temperature (T_S) as a function of y_{H2FA}. When y_{H2FA} = 1, fumaric acid is the only solute and the points plotted there are the T_S values of mixtures with different amounts of fumaric acid. When a higher proportion of fumaric acid is added to the solution a higher temperature is required for dissolution in the range 0.4 < y_{H2FA} < 1. However, Figure 3 shows a local maximum when 0.05 < y_{H2FA} < 0.4. Therefore, another stable salt is formed in this region. When y_{H2FA} = 0 the solutions contain only sodium fumarate and water, but no saturation temperature was observed for the conditions studied.
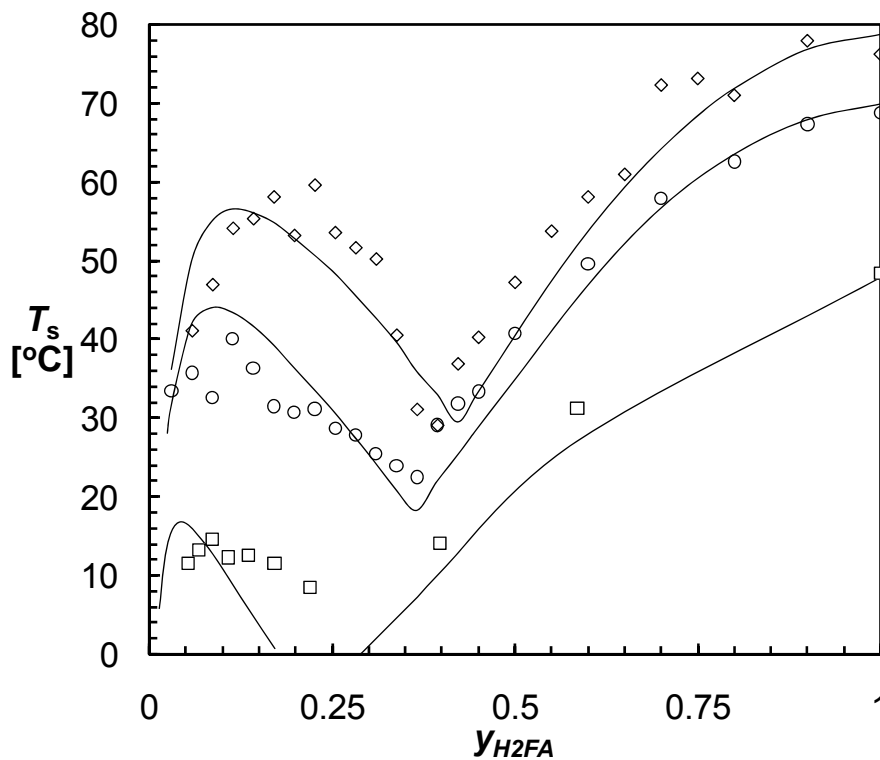

Figure 3: Saturation temperature as a function of the solvent excluded mole fraction y_{H2FA} of H_2FA in the presence of Na_2FA. □, initial x_{iH2FA} = 2.33 mmol mol^{-1}; ○, initial x_{iH2FA} = 5.35 mmol mol^{-1}; ◊, initial x_{iH2FA} = 7.55 mmol mol^{-1}. Lines are model lines.

The phase transition points of the two systems where x_{iH2FA} = 7.55 and x_{iH2FA} = 5.33 are at y_{H2FA} = 0.394 (29 $^{\circ}$C) and 0.366 (23 $^{\circ}$C), respectively. These points are located almost at the same y_{H2FA}

value, which means that the effect of the temperature is small in this range. The phase transition point for the system were x_{iH2FA} = 2.33 seems to be located at temperatures below 0 ^{o}C and it was not determined experimentally.

The stable additional phase that was observed in the phase diagram system in the region of the local maximum is expected to be sodium hydrogenfumarate (NaHFA). The X-Ray powder diffraction pattern of crystals at a y_{H2FA} value of ~0.2 was compared not only with the theoretical sodium hydrogenfumarate pattern but also with experimental patterns of fumaric acid and sodium fumarate (Figure 4).
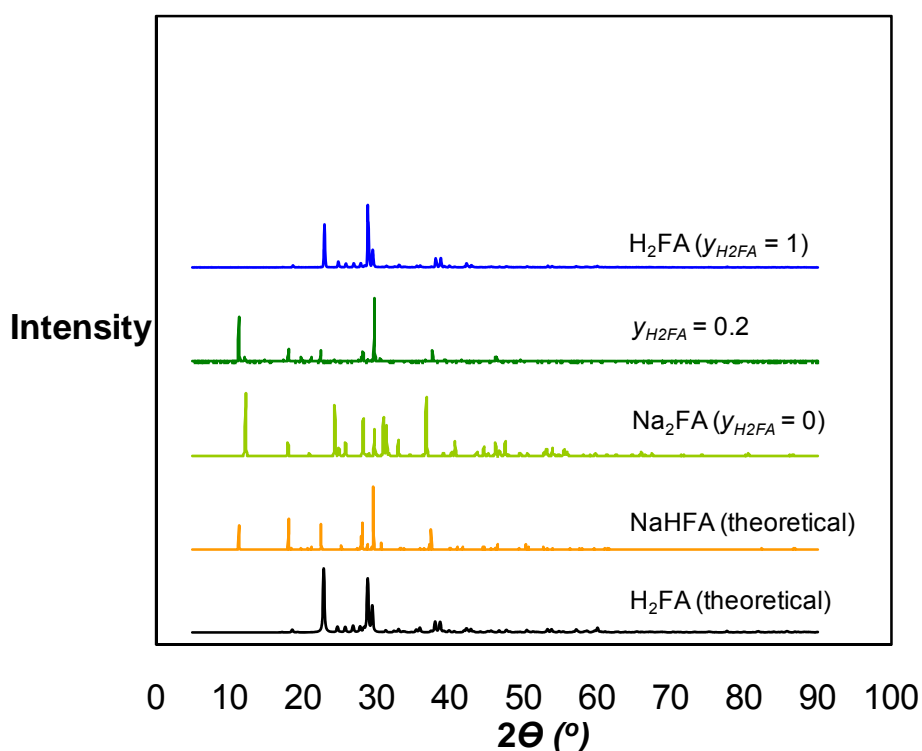
Figure 4: XRPD analysis of crystals mentioned in the text. Theoretical values were obtained using PowderCell 2.3 (Berlin, Germany) and adjusted with literature data (Welton and McCarthy, 1988; Brown, 1966).

The pattern of y_{H2FA} = 0.2 (x_{iH2FA} = 7.55 mmol mol^{-1}) indicate formation of sodium hydrogenfumarate crystals as it looks very similar to the theoretical one, especially the peaks present at 2Θ = 10° and 22°. Moreover, the hypothesis that the salts obtained are sodium hydrogenfumarate is also based on observations for carboxylic acids in similar systems (Harjo et al., 2007; Gupta et al., 1961).

Furthermore, suspensions with fumaric acid crystals were clear with flake-like structures, which floated around in the solution while the suspension with the sodium hydrogenfumarate crystals looked milk-like and no individual crystals could be seen. Sodium fumarate crystals also looked different, though. Optical microscopy shows the different morphologies (Figure 5).
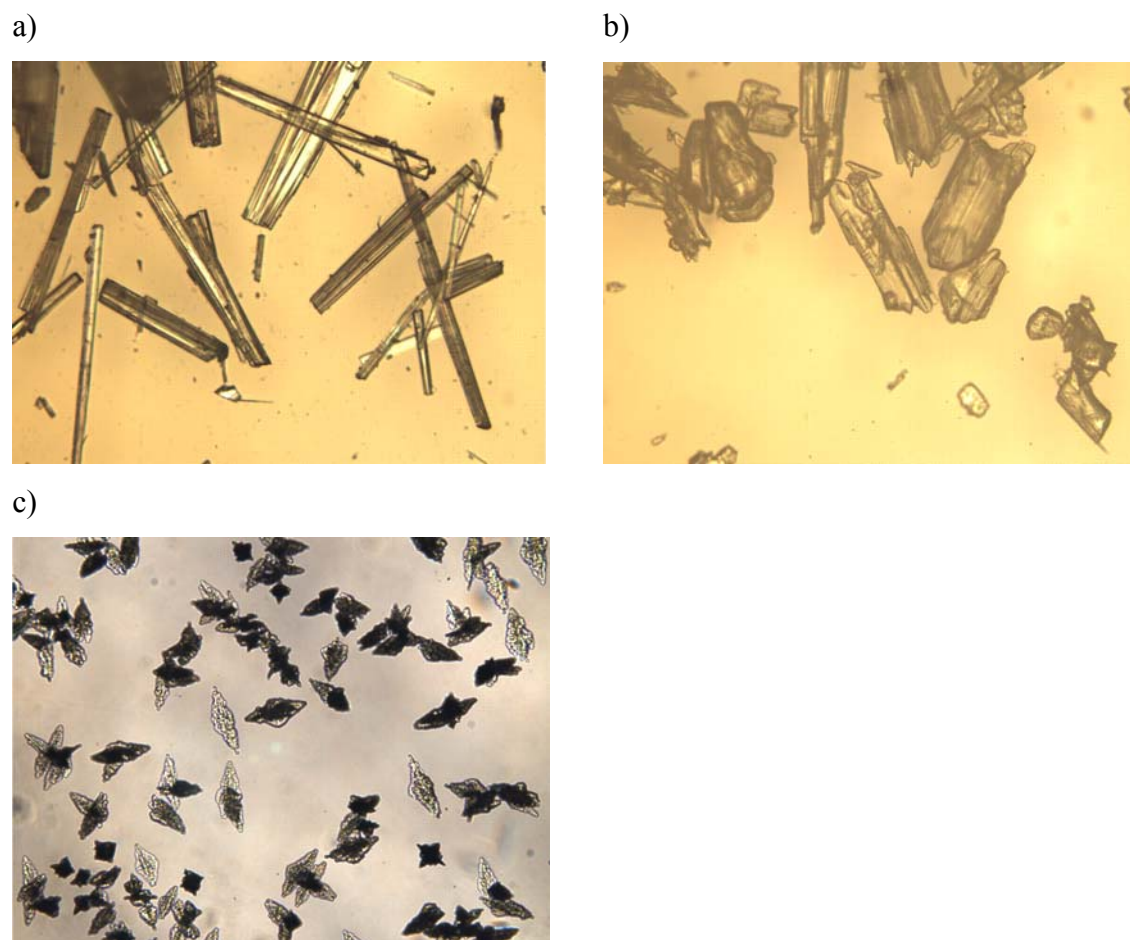
a)

b)

c)

Figure 5: Microscope pictures of a) sodium fumarate (x 10); b) fumaric acid (x 10); c) sodium hydrogenfumarate (x 5).

The ratio between sodium and fumarate of the crystals in Figure 5c was determined to be 1.09 ± 0.1 [Na]/[FA] by measuring both sodium and fumarate concentrations of a non saturated solution by flame Atomic Absorption Spectrometer. A ratio of 1 would be expected for sodium hydrogenfumarate, 0 for fumaric acid and 2 for sodium fumarate. According to these results the additional crystal type is indeed sodium hydrogenfumarate.

The experimental data presented in Figure 3 were validated using a thermodynamic model, which is based on the equilibria presented in Figure 2. AESolve (www.halotec.com), a simulator for

performing complex equilibrium calculations on aqueous electrolyte systems, was used to calculate the equilibrium compositions. The model simultaneously solved the equilibria shown in Figure 2 and the conservation balances for the ten species involved. The aqueous species were H_2O, H^+, OH^-, Na^+, H_2FA, HFA^-, and FA^{2-} and the solid species were H_2FA, $NaHFA$ and Na_2FA. Four independent conservation balances were used, for total sodium; total fumarate; $H_2O + OH^-$; and charge. Values of six thermodynamic equilibrium constants were required, and these are treated subsequently.

The first and second dissociation constant of fumaric acid ($K_{a,1}$ and $K_{a,2}$) as a function of temperature were taken from Das et al. (1980),

$$K_{a,1} = \frac{\gamma_{HFA^-} \cdot m_{HFA^-}^{aq} \cdot \gamma_{H^+} \cdot m_{H^+}^{aq}}{\gamma_{H_2FA} \cdot m_{H_2FA}^{aq}} \qquad [3]$$

$$K_{a,2} = \frac{\gamma_{FA^{2-}} \cdot m_{FA^{2-}}^{aq} \cdot \gamma_{H^+} \cdot m_{H^+}^{aq}}{\gamma_{HFA^-} \cdot m_{HFA^-}^{aq}} \qquad [4]$$

where m the molality (mol kg^{-1} solvent) and γ is the activity coefficient in the appropriate framework.

These correlations are based on experimental data in the range of 15-45 °C. Using correlations based on experimental data of Boily and Seward (2005) in the range 10-90 °C, led to worse predictions.

Activity coefficients for ions with charge z can be calculated using an extended Debye-Hückel (Smith, van Ness and Abbott, 2001) expression, which is valid for up to ionic strength $I = 0.5$ mol kg-solvent^{-1}:

$$-\log \gamma_i = \frac{A_{EDH} z^2 I^{0.5}}{1 + I^{0.5}} - bI \qquad [5]$$

The constants are taken as $A_{EDH} = 1.8249 \cdot 10^3 \cdot \rho_{water} \cdot (\varepsilon \cdot T)^{(-3/2)}$, $b = 0.2$ with I in mol kg^{-1}. Temperature correlations were used for the density ρ_{water} and the dielectric permittivity ε. For undissociated fumaric acid a simple relation was used to obtain the activity coefficient.

$$\log \gamma_i = 0.1 I \qquad [6]$$

The water dissociation into H^+ and OH^- is an equilibrium reaction not shown in Figure 2, but to be able to properly calculate the amounts of all species involved, a literature correlation for the water dissociation constant was used (Harrison et al., 1991).

The equilibrium constant for the conversion H_2FA (s) $\leftrightarrow H_2FA$ (aq) equals to

$$K_{d1} = \frac{a^{aq}_{H_2FA}}{a^{S}_{H_2FA}} = \frac{\gamma^{aq}_{H_2FA} \cdot m^{aq}_{H_2FA}}{1} \qquad [7]$$

For the solid phase, the standard state is the solid state, so $a = 1$ For the dissolved species, a hypothetical one-molal aqueous solution is used as the standard state, so $\gamma = 1$ at infinite dilution, while a correction for ionic strength can be used as given before. The measured solubility of fumaric acid is distorted by the dissociation reactions, which have their own equilibria. Data from Lange and Sinks (1930), Weiss and Downs (1923) and own data, from additional measurements, were used. These data were converted to mol kg^{-1} water. The fumaric acid will be partly dissociated, so the true solubility of the undissociated species, i.e. if it would dissolve but not dissociate, was found by correcting for the fraction undissociated species, using the aforementioned pK_a model. Due to the correction the ionic strength of the solution changes and hence the fraction undissociated species, but it was checked that this effect was negligible. Figure 6 shows the result, indicating that all data can be used for obtaining a good linear fit, so that K_{d1} is well predictable.

The solubility correlation found needs to be corrected by the aforementioned activity coefficient of fumaric acid to obtain the equilibrium constant for dissolution:

$$pK_{d1} = -0.01679 \cdot T + 6.32107 - 0.1 \cdot I \qquad [8]$$

This equation is valid for T in K and I in mol kg^{-1}.

For the reaction NaHFA (s) $\leftrightarrow Na^+$ (aq) $+ HFA^-$ (aq) the equilibrium constant is:

$$K_{d2} = \frac{a^{aq}_{Na^+} \cdot a^{aq}_{HFA^-}}{a^{S}_{NaHFA}} = \frac{\gamma^{aq}_{Na^+} \cdot m^{aq}_{Na^+} \cdot \gamma^{aq}_{HFA^-} \cdot m^{aq}_{HFA^-}}{1} \qquad [9]$$

From experimental data, the points from Figure 3 were taken where the system was supposed to be saturated by sodium hydrogenfumarate, i.e. the points at low fractions of fumaric acid. For these data, at various temperatures, K_{d2} was calculated using the aforementioned model equations. The results (Figure 7) show an increasing K-value with increasing temperature, which is usual for dissolution. The scatter is relatively large. This might be due to the relatively high ionic strengths in the experiments, which would lead to inaccurate calculations of the activity coefficients. The model equation obtained from Figure 7 is:

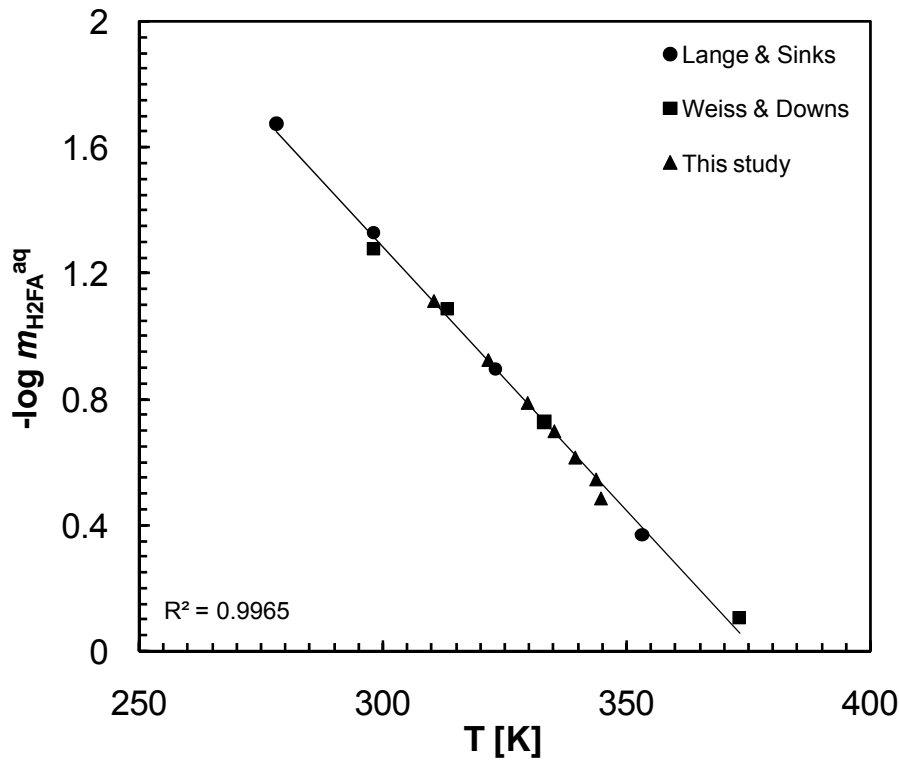$$pK_{d2} = \frac{1187.2}{T} - 3.2097$$ [10]

Figure 6: Temperature dependence of m_{H2FA}^{aq} in saturated aqueous solution. Markers are solubility measurements of fumaric acid corrected for calculated fractions undissociated fumaric acid species, the line is a fit.

For sodium fumarate, a solubility of 228 g/kg for 25°C (Weiss and Downs, 1923) was included in the model, but the exact value for this solubility did not have any influence on the results because sodium fumarate was completely dissolved in all cases evaluated.

The explained model describes the experimental data in Figure 3 quite well for the systems with x_{iH2FA} = 7.55 and x_{iH2FA} = 5.35. However, the model lines do not represent very well the experimental data in the range when $0 < y_{H2FA} < 0.3$ when x_{iH2FA} = 2.33 (Figure 3). Additionally, the model lines confirm that the solid phase transition points (the local minimum in the curves in Figure 3) occur at higher y_{H2FA} and T_S when x_{H2FA} increases. This phenomenon may be explained by the fact that $K_{a,1}$ increases with temperature whereas $K_{a,2}$ decreases, which leads to a higher proportion of sodium hydrogenfumarate compared to fumaric acid in aqueous solutions with increasing temperature (Boily and Seward, 2005). Then, relatively much fumaric acid needs to be added to reach saturation of both sodium hydrogenfumarate and fumaric acid, and this will occur at high values of y_{H2FA}.
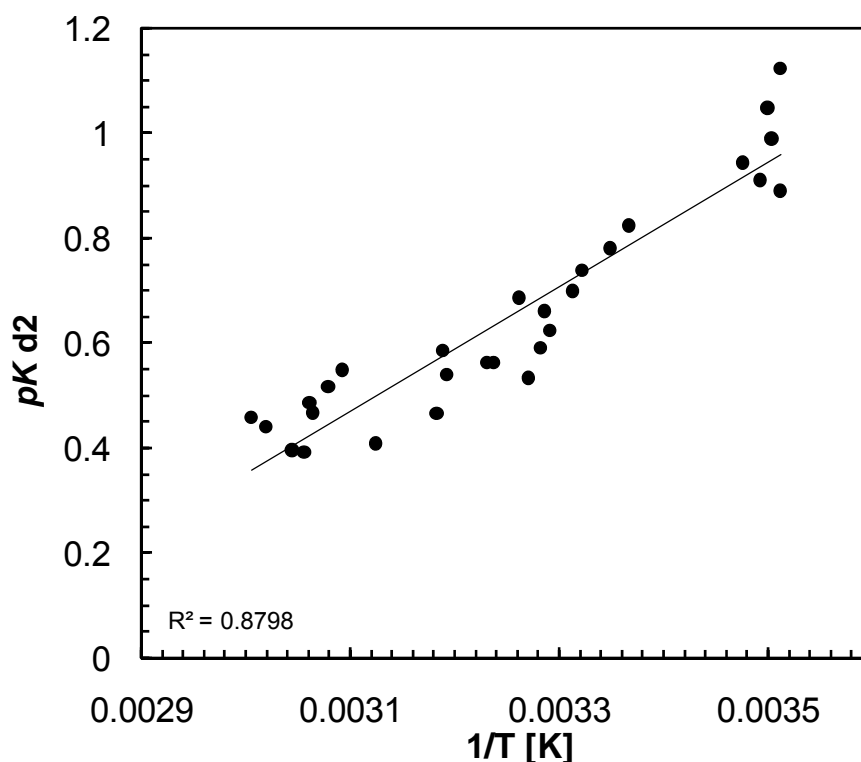
.

Figure 7: Temperature dependence of the negative logarithm of K_{d2}. Markers are values calculated from individual measurements of solubility of sodium hydrogenfumarate, the line is a fit.

Additionally, Weiss and Downs (1923) measured solubilities of sodium hydrogenfumarate. However, they did not check the identity of the crystals they obtained. According to our model, they obtained fumaric acid at 25 and 40 °C but sodium hydrogenfumarate at 60 and 100 °C. Our Crystal16 experiments reduce the risk that the solubility is determined of a different crystal type than expected.

3.2 Apparent solubility of total fumarate as function of pH and temperature

Using the model, the apparent (measured) total fumarate solubility can be calculated for the equilibria in Figure 2 as function of temperature and pH. This solubility is often required in practical applications. To validate the model, calculated and experimental values are compared. Figure 8 shows the effect of different pH and temperature values on the solubility of fumarate. As expected, the solubility of fumarate increases with pH and temperature (Lange and Sinks, 1930).
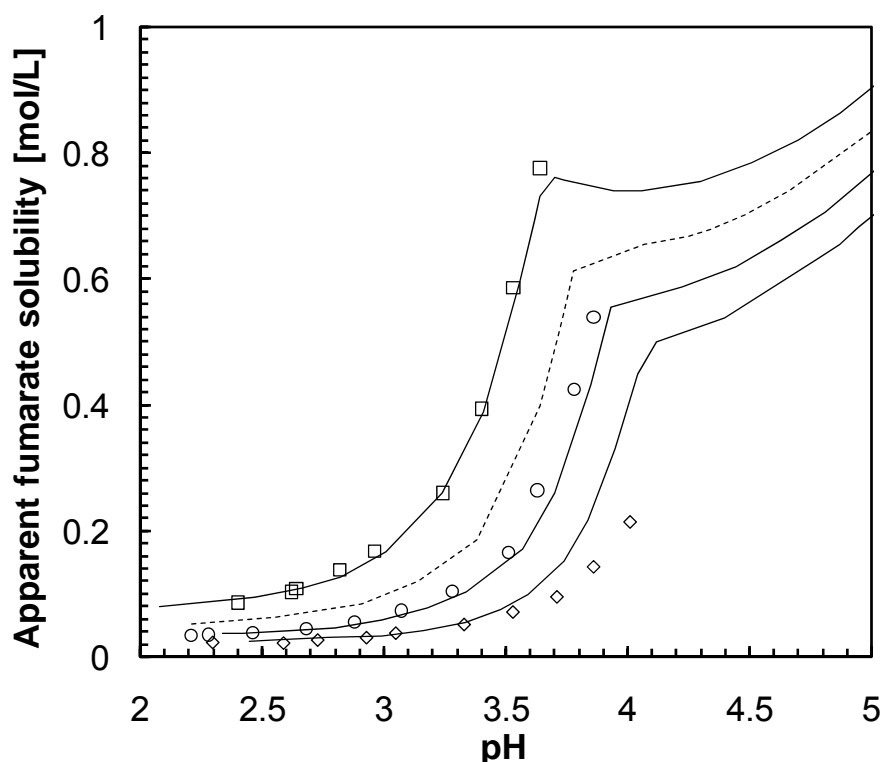

Figure 8: Solubility of total fumarate as a function of pH at different temperatures. □ experimental points at 35 °C; ○ experimental points at 15 °C; ◊ experimental points at 5 °C. Lines are model lines. The dashed line is a model line at standard conditions (25 °C).

In Figure 8 the model predicts quite well the experimental data, especially at 35 and 15 °C. However, at 5 °C the model does not predict so well experimental data at pH values of 3.5 and above. This could be due to inaccuracy of the pK_a calculations at low temperature. Moreover, Figure 8 shows the discontinuity in the solubility curves because sodium hydrogenfumarate is determining the apparent solubility at higher pH, for example for 35 °C at pH > 3.6. Still, the tendency of the curve is to increase with pH and temperature. In addition, during the performance of the solubility experiments in the range of pH 3.8-4.2 (dependent on temperature) the pH did not increase any

further when more sodium fumarate was added to a saturated solution of fumaric acid. The model explains that the reason of this phenomenon was the formation of sodium hydrogenfumarate crystals.
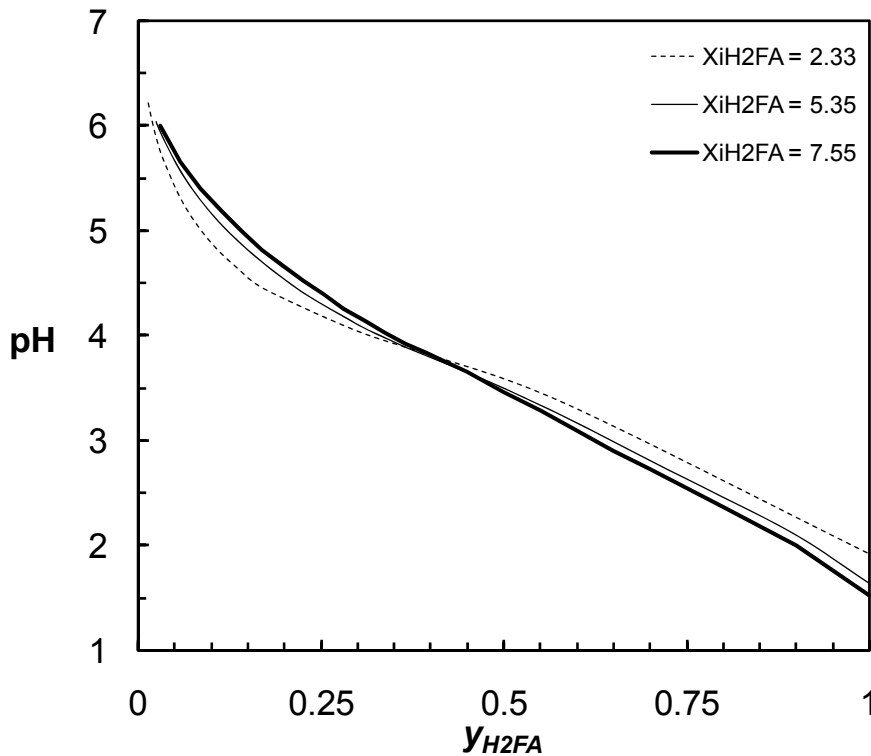

Figure 9: Calculated pH of aqueous mixtures of fumaric acid and sodium fumarate.

Furthermore, reported fumarate fermentations using *R. oryzae* have been performed in a pH range from 4.5 to 6.5 (Roa Engel et al., 2008). We wondered which pH would be required to be able to obtain fumaric acid crystals upon cooling. Figure 9 shows the calculated pH as a function of y_{H2FA} for the conditions of Figure 3. Figure 9 together with Figure 3 illustrate that to get fumaric acid crystallisation the pH for fumaric acid fermentation should be below 3.7. The lines of the three mixtures are crossing at y_{H2FA} = 0.35. This could be occurring by the fact that at higher x_{iH2FA} values more extreme pH values can be achieved because there is more acid or base added to the solutions. In addition, above pH 3.7, the fumarate in the fermentation can be present as sodium hydrogenfumarate and then when cooling crystallisation is applied to recover the fumaric acid, sodium hydrogenfumarate can crystallise as well. However, cooling from 35 ^{o}C to 5 ^{o}C moves the transition point from fumaric acid to sodium hydrogenfumarate around pH 4, giving a higher range for fumaric acid production. Despite this, the solubility curve of fumaric acid at 5 ^{o}C shows that after pH 3.5 the solubility increases rapidly with the pH setting pH 3.5 as the limit to crystallise the acid.

Therefore, if one tries to integrate fumaric acid fermentation with its recovery by cooling crystallisation, the whole system should operate at a pH not higher than 3.5.

3.3 Influence of co-solutes on the sodium-fumarate system

The saturation temperatures were also determined in the presence of dissolved glucose and ethanol since these are common compounds present in the production of fumaric acid by fermentation. The mole fractions were for glucose x_{iGlu} = 1.5 and 3 mmol mol^{-1} and for ethanol x_{iEtOH} = 1 mmol mol^{-1}. The effect of glucose and ethanol on the solubility of the fumarate salts is shown in Figure 10. The model lines and the experimental points from Figure 3 have been added to Figures 10a, b and c to facilitate the comparison.

Figure 10a illustrates the phase diagram of the mixture of sodium fumarate where x_{iH2FA} = 7.55 mmol mol^{-1} plus the changes in the phase diagram when 1.5, 3.0 mmol mol^{-1} of glucose and 1.0 mmol mol^{-1} of ethanol were part of the mixture. The same systems are shown in Figures 10b and 10c for x_{iH2FA} = 5.35 and 2.33 mmol mol^{-1}, respectively. When only glucose up to 3.0 mmol mol^{-1} is added to the sodium-fumarate systems the solubility of these mixtures is hardly affected. Ethanol, however, affects the solubility in different ways.

Figure 10 shows that when ethanol is present the saturation temperature left of the minimum increases so the solubility of sodium hydrogenfumarate decreases by adding ethanol. Because ethanol is a less polar solvent than water, it is expected that solubility of fumarate salts decreases when ethanol is present in the mixtures. On the other hand, right of the discontinuity the presence of ethanol decreases the saturation temperature, corresponding to an increase in the solubility of fumaric acid. This is occurring because fumaric acid is a hydrophobic compound, which will dissolve better when the solution become less polar upon addition of ethanol (fumaric acid solubility in ethanol: 58 g L^{-1} in 95% ethanol at 30 $^{\circ}$C (Merck Index, 2009)). This effect of ethanol is stronger at lower temperature. The same behaviour has been reported for another organic compound, threonine. Threonine solubility increased with T and decreased upon addition of 20% ethanol, but the effect of ethanol was stronger at lower T than at higher T (Ferreira et al., 2004).

Finally, no new solid states seem to appear when glucose and ethanol are present in the fumarate solution.
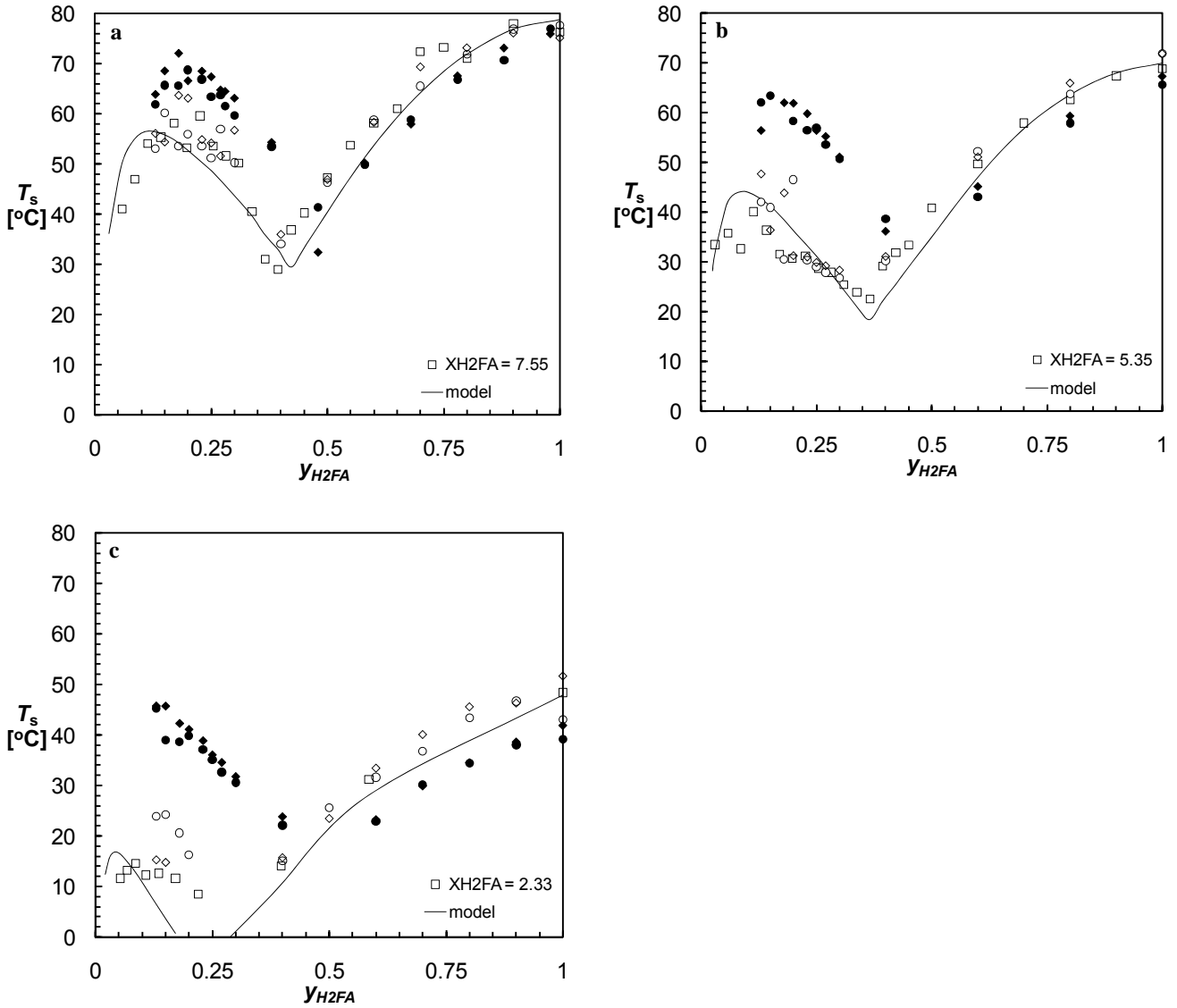
Figure 10: The influence of fermentation co-solutes on saturation temperatures of mixtures of H_2FA and Na_2FA. a) $x_{iH2FA} = 7.55$ mmol mol^{-1}; b) $x_{iH2FA} = 5.35$ mmol mol^{-1}; c) $x_{iH2FA} = 2.33$ mmol mol^{-1}. ○ sodium-fumarate solution + $x_{iGlu} = 1.5$ mmol mol^{-1}; ◇ sodium-fumarate solution + $x_{iGlu} = 3.0$ mmol mol^{-1}; ● sodium-fumarate solution + $x_{iGlu} = 1.5$ mmol mol^{-1} + $x_{iEtOH} = 1.0$ mmol mol^{-1}; ♦ sodium-fumarate solution + $x_{iGlu} = 3.0$ mmol mol^{-1} + $x_{iEtOH} = 1.0$ mmol mol^{-1}. The lines are model lines from Figure 3.

4 Conclusions

The solubility of the aqueous sodium-fumarate system increases with temperature and especially with pH. This solubility behaviour can be described reasonably well by a mathematical model that is based on dissociation and dissolution equilibria. The solubility is determined by sodium hydrogenfumarate in the region of $y_{H2FA} < 0.4$ and by fumaric acid in the region of $y_{H2FA} > 0.4$. Solutions of sodium hydrogenfumarate ($y_{H2FA} = 0.5$) may, upon cooling, yield fumaric acid crystals.

Glucose up to 3.0 mmol mol^{-1} did not significantly influence the solubility of fumarate species but, 1.0 mmol mol^{-1} of ethanol decreased the solubility of sodium hydrogenfumarate and increased the solubility of fumarate. Moreover, the presence of ethanol increases the stability region for sodium hydrogenfumarate crystals, and the minimum value of y_{H2FA} leading to fumaric acid crystals was shifted to about 0.5 for the conditions employed.

Acknowledgements

Nomenclature:

a: activity

I: ionic strength

i: initial value

K_a: dissociation equilibrium constant

K_d: dissolution equilibrium constant

m: molality

T: temperature

x: mole fraction

y: solvent free mole fraction

Greek:

γ: activity coefficient

Subscripts:

aq: for aqueous phase

EtOH: ethanol

Glu: glucose

H_2FA: fumaric acid

Na_2FA: sodium fumarate

NaHFA: sodium hydrogenfumarate

S: for solid phase

References

Boily JF, Seward TM (2005) Dissociation of fumaric acid: spectrophotometric investigation in aqueous solutions from 10 to 90 ∘C and theoretical considerations. J Sol Chem (34) 1167.

Brown CJ (1966) The crystal structure of fumaric acid. Acta Cryst (21) 1.

Buque-Taboada EM, Straathof AJJ, Heijnen JJ van der Wielen LAM (2006) In situ product recovery (ISPR) by crystallization: basic principles, design, and potential applications in whole-cell biocatalysis. Appl Microbiol Biotechnol (71) 1.

Cuellar Soares MC (2008) Towards the integration of fermentation and crystallization. A study on the production of L-phenylalanine. PhD Thesis. TU Delft, Delft, The Netherlands. pp163.

Das RC, Dash UN, Panda KN (1980) Thermodynamics of dissociation of DL-malic, maleic and fumaric acids in water and water + dioxan mixtures. J Chem Soc Faraday Trans I (76) 2152.

Du JX, Cao NJ, Gong CS, Tsao GT, Yuan NJ (1997) Fumaric acid production in airlift loop reactor with porous sparger. Appl Biochem Biotech (63-65) 541.

Ferreira LA, Macedo EA, Pinho SP (2004) Solubility of amino acids and diglycine in aqueous–alkanol solutions. Chem Eng Sci (59) 3117.

Gupta MP, Barnes WH (1961) The potassium salts of fumaric acid: preparation. Can J Chem (39) 1739.

Harjo B, Ng KM (2007) Development of Amino Acid Crystallization Processes: L-Glutamic Acid. Ind Eng Chem Res (46) 2814.

Harrison RM, de Mora SJ, Rapsomanikis S, Johnson WR (1991) Introductory Chemistry for the Environmental Sciences, CUP.

ter Horst JH, Deij MA, Cains PW (2009) Discovering new co-crystals. Cryst Growth Des (9) 1531.

Lange BA, Sinks MH (1930) The solubility, specific gravity and index of refraction of aqueous solutions of fumaric, maleic and malic acids. J Ame Chem Soc (52) 2602.

Merck Index (2009) John Wiley & Sons, Whitehouse Station, N.J., U.S.A.

Roa Engel CA, Straathof AJJ, Zijlmans TW, van Gulik WM, van der Wielen LAM (2008) Fumaric acid production by fermentation. Appl Microbiol Biotechnol (78) 379.

Smith JM, van Ness HC, Abbott MM (2001) Chemical engineering thermodynamics. Mc. Graw Hill. Sixth Ed. ISBN 0072402962.

Weiss JM, Downs CR (1923) The salts of maleic, fumaric and inactive malic acids. J Am Chem Soc (45) 2341.

Weiss JM, Downs CR (1923) The physical properties of maleic, fumaric and malic acid. J Am Chem Soc (45) 1003.

Welton J, McCarthy G (1988) North Dakota State University, Fargo, North Dakota, USA, ICDD Grant-in-Aid.

Werpy T, Petersen G (2004) Topten value added chemicals from biomass feedstocks. U.S. Department of Energy, USA.

Zhou Y, Du JX, Tsao GT (2000) Mycelial pellet formation by Rhizopus oryzae ATCC 20344. Appl. Biochem Biotech (84-86) 779.

CHAPTER 5

Integration of fermentation and crystallisation in the production of fumaric acid

Fumaric acid is used in industrial polymerisation processes. Currently, fumaric acid is mainly produced by chemical processes using fossil carbon feedstocks. Fermentation processes using renewable resources might potentially be more economical, thus leading to wider application of fumaric acid. One of the main problems of fumaric acid production by fermentation is the formation of fumarate salts instead of undissociated fumaric acid at the conventional final pH in the range of 4.5–6.5. A new process for a repeated-batch aerobic production of fumaric acid by *Rhizopus oryzae* at pH 3.5 – 5.0 is presented and evaluated experimentally at lab scale. Cell free liquid from a stirred tank fermentation is sent to a cooling crystallisation and mother liquor is recycled to the fermentor. The direct integration of fermentation and crystallisation steps avoids the shifting of pH between the different production steps and hence simplifies the downstream processing, at the expense of the fermentation performance. The integrated process shows a reduction in the number of recovery operation units, which is beneficial for the process economy. The consumption of neutralising agents was reduced by ~37%. Preferably, this process should be performed with a microbial strain that would be able to withstand pH 3 or lower.

1 Introduction

Production of fumaric acid by fermentation has the potential to substitute petrochemical routes (Roa Engel et al., 2008; Werpy and Petersen 2004). The fermentation process may reduce our dependency on oil and has the additional advantage that it consumes CO_2 as supplementary feedstock. *Rhizopus oryzae* ATCC 20234 has been reported as a strain capable of producing fumaric acid at pH 5.0 obtaining high product yields (Cao et al., 1996; Du et al., 1997; Zhou et al., 2002). One of the main problems of the conventional fermentation process is that it is carried out at a pH in the range of 4.5–6.5, leading to fumarate salts instead of undissociated fumaric acid (Roa Engel et al., 2008). Stoichiometric amounts of bases such as NaOH and $CaCO_3$ are added during fermentation to control the pH. To recover fumaric acid, the supernatant has to be acidified, for example with stoichiometric amounts of sulfuric acid, so that undissociated fumaric acid can precipitate. Figure 1 shows the fumaric acid species as function of pH according to $pK_{a,1} = 3.03$ and $pK_{a,2} = 4.44$ (Lohbeck et al., 2005).
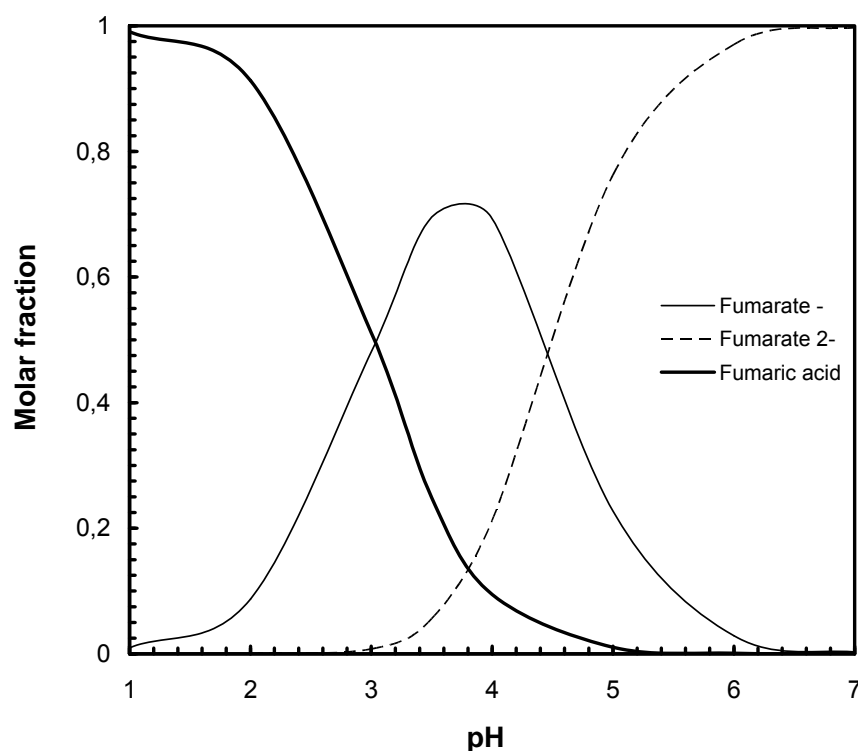

Figure 1: Speciation diagram of fumaric acid.

Stoichiometric amounts of waste salts such as sodium or calcium sulfate are formed in this manner in the same mole proportion as the main product (Figure 2). The process costs might be drastically reduced if acid/base consumption and waste salt formation could be prevented.
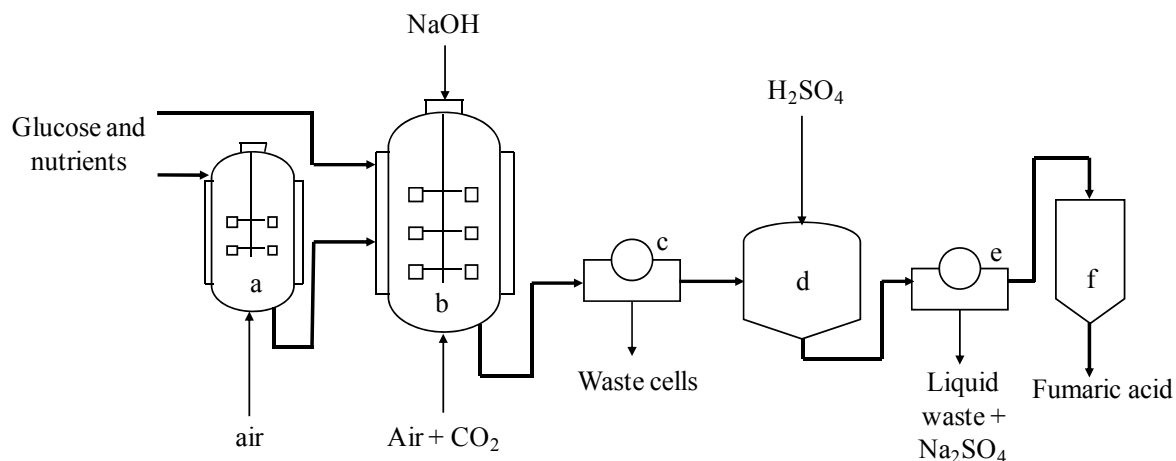
Figure 2. Conventional process scheme for fumaric acid production via fermentation. a) Seed fermentor; b) Production fermentor; c) Filter; d) Acidification tank; e) Filter; f) Rotary dryer. (adapted from Roa Engel et al., 2008).

Different studies have been performed to reduce or even avoid the precipitation step, e.g. by using ion exchange techniques to recover the fumarate after the fermentation (Cao et al., 1996; Zhou, 1999; Xu et al., 2006). Nevertheless, the recovery by ion exchange requires regeneration of the ion exchange column and hence also results in the production of waste salts. Liquid-liquid extraction, electrodialysis, and membrane separation, which have been studied for the recovery of fermentative produced carboxylic acids, might also be applied to the fumaric acid production (Huh et al., 2006; Moresi et al., 2002; Joglekar et al., 2006). However, simple and inexpensive techniques are required for the production of fumaric acid to be economically competitive (Berglund et al., 1991). Due to the low solubility of fumaric acid (7 g/kg at 25 $^{\circ}$C; 89 g/kg at 100 $^{\circ}$C (Stephen, 1965)), crystallisation techniques have a high potential to recover the undissociated acid directly from the fermentation supernatant, if the fermentation is performed at low pH. Some studies on recovery of other fermentative products by direct crystallisation have been shown that this may be an effective and economically feasible method, which avoids the use of neutralising agents (Buque-Taboada et al., 2005; Patnaik et al., 2007; Roa Engel et al., 2009).

In Chapter 3 of this thesis, a concentration of ~20 g L^{-1} of fumaric acid was obtained at pH 3.6 by using *R. oryzae* pellets (~ 1.5 mm) in batch cultivation with CO_2 supplementation in a stirred tank fermentor. We will integrate this fermentation with cooling crystallisation to obtain fumaric acid. We have found that there is no need to change the pH between the fermentation and the fumaric acid crystallisation. Upon cooling and seeding, fumaric acid can directly crystallise from fermentation broth after cell removal. This can potentially lead to a drastic decrease of the consumption of

89

neutralising base during the fermentation and of acidifying agent during the product recovery. Moreover, the formation of waste salts can be minimised and the number and size of recovery operations can be decreased as well. An optimised procedure including preliminary evaluation will be presented.

2 Materials and Methods

2.1 Microorganism and growth conditions

R. oryzae ATCC 20344 was obtained from the American Type Culture Collection (Rockville, Md.). The culture was grown at 37 ^{o}C on YMP agar plates, containing 0.3% yeast extract (Bacto, NJ, USA), 0.3% malt extract (Scharlau, Barcelona, Spain), 0.3% peptone (Bacto, NJ, USA), 2% glycerol (99.5% Merck, The Netherlands) and 2% agar (Bacto, NJ, USA) in distilled water, to produce spores. After four days of sporulation the spores were harvested from the plates with a glycerol (10% v/v) and Tween 80 (0.05% v/v) solution. The obtained spore suspension contained approximately 10^6 spores per mL (of the glycerol-Tween solution) and was collected in vials of 2 mL and stored at -80 ^{o}C.

2.2 Pre-culture conditions

1 L shake flasks containing 200 mL of growth medium were inoculated with two vials (2 mL each) of spore suspension. The composition of the growth medium was (per 1000 mL) 10 g of glucose, 2.0 g of urea, 0.6 g of KH_2PO_4, 0.25 g of $MgSO_4 \cdot 7H_2O$, and 0.088 g of $ZnSO_4 \cdot 7H_2O$. The pH of the medium was, if necessary, adjusted by adding HCl (10% v/v). The medium, without the glucose, was heat sterilised (20 min at 121 ^{o}C). The glucose solution was sterilised separately (20 min at 110 ^{o}C). Pre-cultures were carried out at 35°C and 200 rpm in a gyratory incubator-shaker for 2 days. The shake flaks were covered with cotton. After cultivation, the obtained mycelium pellets were washed for one hour with 1 L of new fresh media free of glucose and urea. The pellets were transferred immediately after the washing into a fermentor containing the production medium (see below).

2.3 Fermentation conditions for fumaric acid production

The production medium to which the produced pellets were transferred aseptically was nitrogen free. The salt composition of the production medium was the same as of the inoculation medium. The initial glucose concentrations for the different experiments are listed in Table 1. Batch fermentations were performed at 35 °C in 2 L fermentors (Applikon, Schiedam, The Netherlands), with a working volume of 1.4 L. NaOH (25 % w/w) was used to control the pH at the desired values. The fermentation medium was stirred at 600 rpm to keep homogeneity with an aeration (air + 10% v/v CO_2) rate of 1.0 L L^{-1} min^{-1} for ~290 h. Samples were taken periodically, thus slightly decreasing the fermentation volume, and the oxygen and carbon dioxide contents in the off-gas from the fermentor were monitored using a NGA200 gas analyser (Rosemount Analytics, USA). Also the composition of the gas entering the vessel was analysed. The culture pH was continuously monitored and data archived using MFCS/WIN data acquisition software (Sartorius AG, Germany). Similarly, the additions of NaOH were also monitored on-line.

2.4 Crystallisation conditions

Cooling crystallisation experiments were performed in a temperature controlled vessel unit (Applikon, Schiedam, The Netherlands) of 1.5 L connected to a stirrer with a three blade mixer operated at a speed of 200 rpm. The temperature of the cooling crystallisation was controlled at either 5 or 0 °C. After transferring the supernatant of the fermentation to the crystalliser the crystallisation was initiated by adding ~0.2 g seed crystals obtained from previous experiments. During the crystallisation the pH was monitored, but not controlled.

2.5 Metastability zone width determination

Cooling crystallisation was performed with solutions of fumaric acid in water, in water containing the main fermentation substrate and product (30 g L^{-1} glucose and 10 g L^{-1} ethanol) and in cell free fermentation medium (see composition in the Results and Discussion section). The pH of the fermentation medium was adjusted to 3.5 by adding concentrated HCl. The experiments were performed in a crystalliser as described in the previous section. An in-situ laser immersion probe was used to collect on-line infrared spectra. The spectrum indicates the turbidity of suspensions. The crystalliser was externally covered to avoid light entering it and disturbing the measurement of the

turbidity. The solutions were kept at 75 °C for 30 min to ensure that all crystals had been dissolved. Subsequently, the solutions were cooled at a rate of 0.17 °C min^{-1} until the solution became turbid, at which the primary nucleation occurred. This point was considered to be the metastable temperature. Later on the solution was heated and when the solutions became clear again that point was considered to be the solubility temperature. The solutions were diluted by 100 mL. Glucose and ethanol were supplemented preventing a change of the initial concentrations. After new metastability and solubility temperatures had been reached, samples were taken and analysed by the HPLC method described below.

2.6   Integration Set up

Fermentation of *R. oryzae* was carried out in batch mode for ~290 h. The initial fermentation pH was adjusted to 5.0 with NaOH (25 % w/w). After 80 h, the pH control was switched off. After 165 h, 0.7 L of the supernatant free of *R. oryzae* pellets was pumped in one hour with a Cole Parmer pump 7544-12, 100 rpm (U.S.A. Chicago) from the fermentor to the crystalliser (see step 1 in Figure 3).

The crystalliser was already set at the desired cooling temperature and 0.2 g of fumaric acid seed crystals obtained from previous experiments were added. The crystallisation was carried out for 24 h and then the stirrer was stopped to allow the crystals to settle on the bottom of the vessel.

When 0.7 L of supernatant had been taken from the fermentor, 140 mL of glucose solution of 50% w/w was added to the fermentor (see step 2 in Figure 3). The stirrer and air/CO_2 flow were connected again and the fermentation was continued. The crystalliser mother liquor was separated from the crystals and pumped back to the fermentor to recirculate glucose that was not consumed and fumarate that was not crystallised (see step 3 in Figure 3). Collected crystals were washed with ice water, filtered and dried (see step 4 in Figure 3). The whole described cycle was repeated when the total fermentation time was around 290 h, up to the mother liquor recycling step.
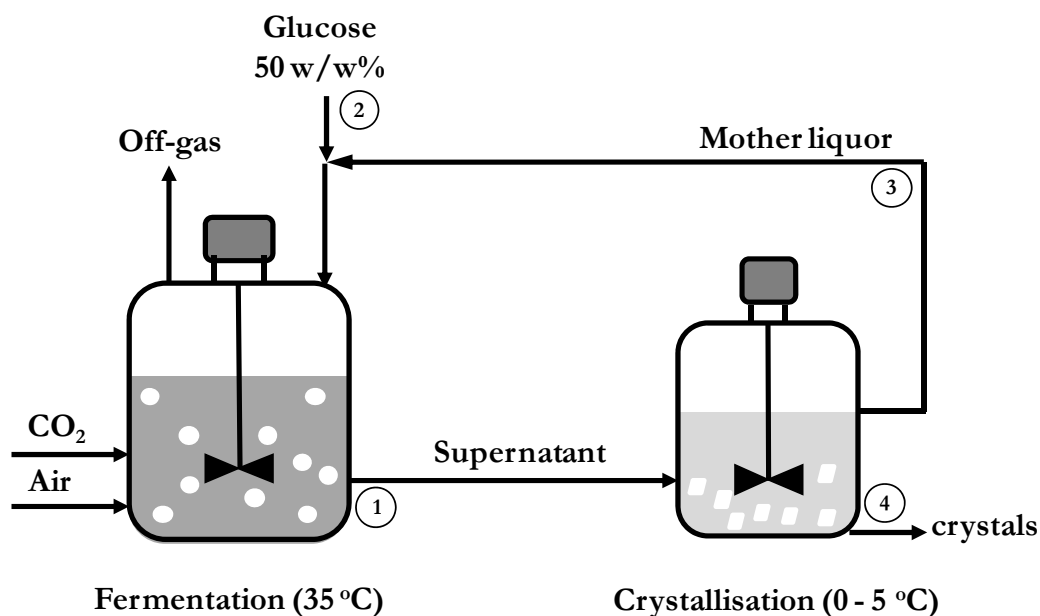
Figure 3: Schematic experimental set up for the production of fumaric acid by fermentation and its recovery by direct cooling crystallisation. The numbers in circles are referred to in the text.

2.7 Analytical methods

Fumaric acid, glucose, ethanol and glycerol concentrations were determined by HPLC with a Bio-Rad Aminex HPX-87H ion-exclusion column (300 x 7.8 mm), a refractive index detector (Waters 2414), and a U.V. detector at 210 nm (Waters 2489). The column was eluted with dilute phosphoric acid (1.5 mmol L^{-1} in Milli-Q water) at a column temperature of 59 ^{o}C and a flow rate of 0.6 mL min^{-1}. The final cell mass was filtered on pre-weighed Whatman, GF/C, diameter 47 mm filter paper. The solid fraction was washed completely with de-ionised water, dried at 70 ^{o}C for 24 h, and weighed to yield the final dry weight. Produced crystals were washed with ice water and filtered with a pre-weighed Pall filter Supor-450, 47 mm diameter and 0.45 μm pore size. Crystals were dried at 1 bar for 24 h and weighed. Their identity was checked by X-ray diffraction analysis and compared with Sigma-Aldrich fumaric acid crystals and theoretical patterns obtained using PowderCell 2.3 (Berlin, Germany) and adjusted with literature data (Welton et al., 1988; Brown 1966).

3   Results and Discussion

3.1   Fermentation of R. oryzae

Figures 4a and 4b show the fermentation profiles of duplicate batch experiments to produce fumaric acid by fermentation of *R. oryzae*, whereas Figure 4c shows an experiment with higher amounts of cell mass. In these experiments the initial pH was adjusted to 5.0 and controlled at this value until 80 h; then pH control was shut off. At the end of the first cycle (around 165 h) the pH had dropped to ~ 3.6 because fumaric acid was produced and no extra neutralising agent had been added (see Table 1). It can be seen from Figures 4a to 4c that the concentration of fumaric acid increases with time during the first cycle until the production slows down around 150 h. Probably the high concentrations of fumaric acid and the associated low pH of the broth inhibit fumaric acid production by *R. oryzae*. Therefore, the fermentations were interrupted at ~165 h and part of the supernatant was transferred to the crystalliser to proceed with product recovery. Due to quick settling of the pellets in the fermentor, the supernatant was transferred without pellets.

The fermentation profiles in Figures 4a to 4d show that most of the fumaric acid transferred to the crystalliser after ~165 h was returned with the mother liquor at ~185 h, indicating that only a minor proportion of fumaric acid is removed by the crystallisation.

Addition of the glucose solution and mother liquor to the fermentor initialised the second fermentation cycle (see Figure 4d). The fumaric acid concentration started increasing again, but not as fast as in the beginning of the first cycle (see Figures 4a-c). This can once more be explained by inhibition, because the initial pH value of the second cycle was around 3.9 and the fumaric acid concentration was still high. To avoid product inhibition during the second cycle, more fumaric acid should be removed by the crystallisation or the fungi would have to be modified in order to tolerate lower pH values at higher fumaric acid concentrations. Moreover, Figures 4a-c illustrate that during the first cycle the ethanol concentration was increasing, especially after ~50 h. Ethanol is being produced as a by-product by *R. oryzae* under oxygen limited conditions (Cao et al., 1996). This occurs if *R. oryzae* grows in the form of large pellets or clumps due to limited oxygen diffusion into the clumps. Unfortunately, we could not avoid growth of the fungi on the stirrer in our fermentation experiments. Because clump formation on the stirrer did occur, we suspect that oxygen limited conditions inside the clumps has been the cause of ethanol production by the fungus. Nonetheless, ethanol can be consumed again by *R. oryzae* (Chapter 3), especially, when glucose is exhausted.

Figures 4a and 4b show that the amount of ethanol during the second cycle of the low density fermentations slightly decreases, and ethanol disappears completely during the second cycle of the high cell density experiment (Figure 4c). This can be caused ethanol evaporation during the fermentation. (see Chapter 3).
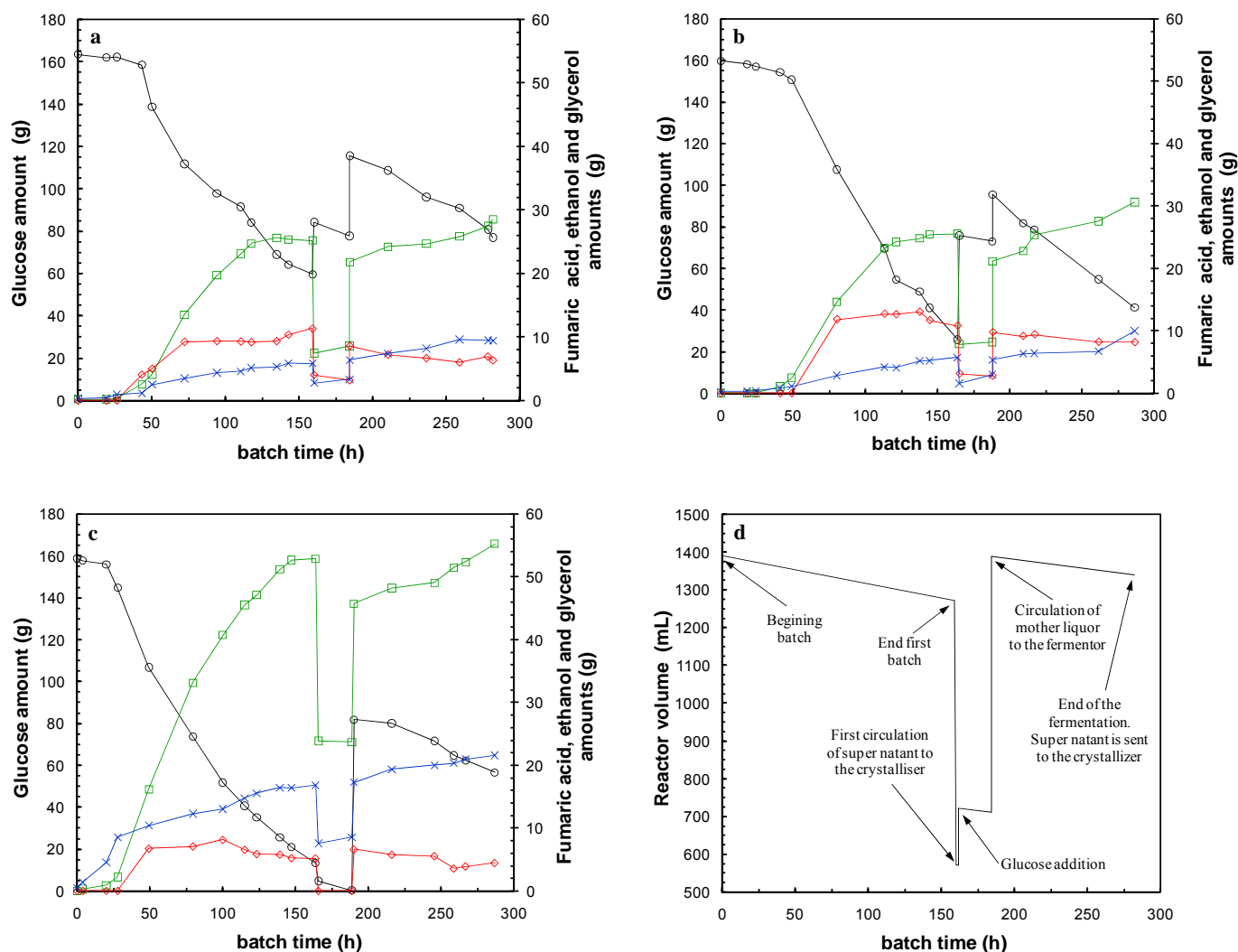

Figure 4: a, b and c) Mass profiles of experiments 1, 2 and 3 respectively, in the fermentor during integration with product removal by cooling crystallisation in experiments 1, 2 and 3, respectively. ○ Glucose; □ Fumaric acid ◊ Ethanol; x Glycerol mass amounts. Conditions are indicated in Tables 1 and 2. d) Example of volume profile during fumaric acid fermentation integrated with product removal by crystallisation. Profile of glucose addition applies for experiments 1 and 2. Glucose addition for experiment 3 was done together with mother liquor recirculation due to set up problems during the experiment.

The glycerol amount increased in a more or less linear fashion, indicating that the rate of production rate remains at a stable value. This could be due to the fact that during the fermentation the fungi have been exposed for a long period to a high glucose concentration. Therefore, glycerol

95

might be produced as a stress response, to cope with the osmotic pressure that high glucose concentrations cause in the media (Mager and Siderius 2002).

Figure 4c illustrates that fumaric acid production is doubled when the cell concentration is doubled compared to experiment 1 and 2. It is important to mention that during this high cell density fermentation experiment, clump formation on the stirrer was less severe, which might cause a lower ethanol production because less cells were exposed to oxygen limited conditions. As the production of fumaric acid was higher than in Figure 4a and b the consumption of glucose during the first cycle was faster. This probably causes that at the end of first fermentation cycle, ethanol was consumed as an alternative carbon source as was mentioned before.

Table 1: Experimental data from *R. oryzae* fermentations.

Experiment	1	2	3 (double cell density)
pH at 165 h	3.56	3.63	3.82
pH at 288 h	3.40	3.34	3.74
Initial glucose (g L^{-1})	117.5	115.0	114.1
Final cells dry mass (g)	3.01	4.46	7.30
Final fumaric acid (g L^{-1})	21.3	22.3	40.4
Final ethanol (g L^{-1})	4.70	5.90	0.00
Final glycerol (g L^{-1})	7.05	7.29	15.78
q_P at 165 h (g g^{-1} h^{-1})	0.053	0.035	0.044
$Y_{p/s}$ at 165 h (g g^{-1})	24.3	19.1	36.4
Total NaOH added (g)	15.58	12.65	31.23

Table 1 presents the overall results of the three integration experiments. It can be seen that for experiment 3, the yield of product on substrate (Y_{sp}) was almost doubled compared to experiments 1 and 2. This is surprising, because the cell mass specific productivities (q_P) for the three experiments are in a narrow range, so more fumaric acid is produced when the cell density increases, but the other processes that consume glucose did not increase proportionally. Additionally, the total amount of neutralising agent (NaOH) added during the first 80 h to keep the pH at 5.0 is also higher when more fumaric acid is produced, which is expected. Furthermore, the subsequent drop of pH was less for experiment 3 but it was not clear why (see Table 1).

Figure 4 indicates that removal of fumaric acid during its production by fermentation can enhance the productivity of the fermentation process. However, to make the production of fumaric acid a feasible process more fumaric acid should be removed by the crystallisation and the titers of the acid will have to be higher.

3.2   Window of operation

In order to identify the window of operation for fumaric acid crystallisation after its production from fermentation with *R. oryzae*, solubility and supersaturation curves were determined for aqueous fumaric acid including solutions containing other compounds (glucose and ethanol) present in the fermentation media and furthermore, for real fermentation broth. Figure 5 shows the supersaturation and solubility curves of fumaric acid in the three different solutions at pH 3.5, which is representative of the final fermentation pH.
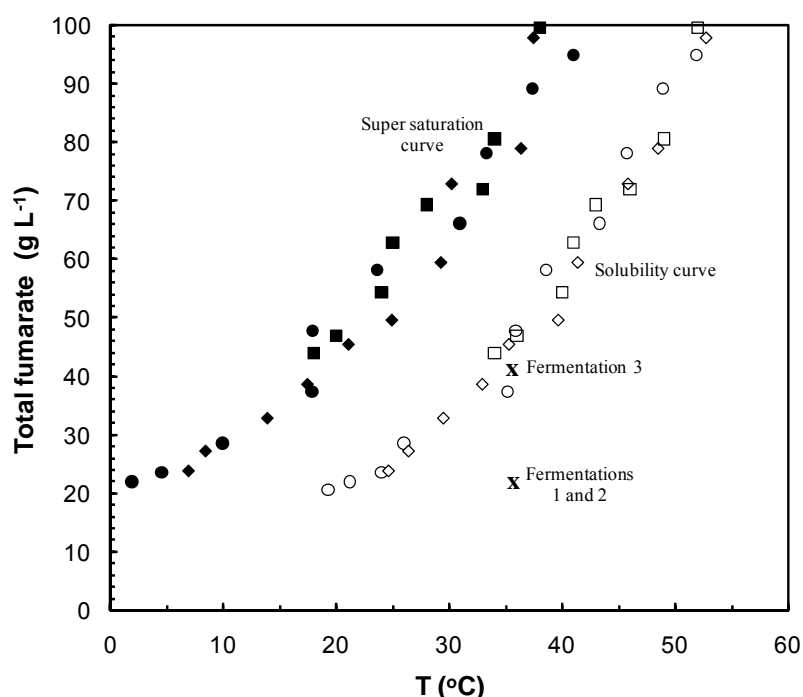
Figure 5: Results indicating the metastable zone, i.e. the region between open and closed markers. ● Metastable points in water; ♦ Metastable points in synthetic media (30 g L^{-1} glucose and 10 g L^{-1} ethanol); ■ Metastable points in fermentation broth (40.9 g L^{-1} glucose, 5.02 g L^{-1} ethanol and 6.63 g L^{-1} glycerol); ○ Solubility points in water; ◊ Solubility points in synthetic media; □ Solubility points in fermentation broth. **x** Final fermentation conditions close to pH 3.5. All other solutions are at pH 3.5.

Figure 5 shows that at pH 3.5 the fumaric acid solubility and supersaturation curves are not affected by the tested ethanol and glucose concentrations. Glycerol is also present in the fermentation media, but it is assumed that its influence will not be different from that of glucose. The curves, which form the metastable zone of fumaric acid in these solutions, are also hardly different in the presence of real fermentation media, at least for the tested compositions.

For experiments 1 and 2, fumaric acid fermentation titers at pH 3.5 are ~20 g L^{-1} and this concentration is plotted in Figure 5, which illustrates that to reach saturation and crystallise fumaric acid from the fermentation media this solution has to be cooled or concentrated, unless the fermentation titers increase. Decreasing the pH by addition of mineral acid would also provoke fumaric acid crystallisation like mentioned in the Introduction, but this would imply waste salts generation. For concentrating the solution, equipment for evaporation, nanofiltration or reverse osmosis is required, adding complexity to the system (Cuellar et al, 2009). Therefore, cooling crystallisation is selected as a removal technique.

3.3 Recovery of fumaric acid

Two processes are involved in recovery of fumaric acid. First, pellets were removed from the fermentation broth, by stopping the stirring at the end of each batch phase. They sink within ~5 min to the fermentor bottom. Supernatant was transferred to the crystallisation unit for the second recovery step.

Cooling supernatant of fermentations of experiments 1 and 2 to 5 ^{o}C moved the composition into the metastability zone according to Figure 5. Therefore, seed crystals were used, which grew out. For fermentation 3, cooling to 0 ^{o}C should give supersaturated solutions, and after adding seed crystals (to avoid nucleation) crystallisation indeed occurred. Table 2 shows the overall results of the crystallisations.

It can be seen from Table 2 that the conditions of experiment 1 and 2 were comparable, whereas for experiment 3 the initial fumaric acid concentration was higher and the cooling temperature was lower. This increases the amount of fumaric acid recovered. Additionally, as is expected, more undissociated acid is recovered when the pH value is lower. This is illustrated from the amount of crystals recovered after the second batch of each experiment because the pH was lower at the end of

the second batch compared to the first one. This also implies that more fumaric acid was present in the solution and hence more can be recovered.

Table 2: Experimental data from cooling crystallisations to recover fumaric acid.

Integrated with fermentation experiment	1	2	3
1ˢᵗ crystallisation			
Working volume (L)	0.70	0.70	0.61
Cooling temperature (^{o}C)	5	5	0
Initial fumaric acid concentration (g L^{-1})	19.84	19.56	40.41
Calculated NaOH concentration (g L^{-1})	6.80	7.03	16.90
Initial pH	3.56	3.63	3.82
Final pH	3.74	3.73	4.15
Calculated final pH	3.74	3.75	4.01
Fumaric acid crystals obtained (g)	1.49	1.39	2.34
Calculated fumaric acid crystals concentration (g L^{-1})	1.76	1.03	4.76
Calculated fumaric acid crystals obtained (g)	1.23	0.72	2.90
2ⁿᵈ crystallisation			
Working volume (L)	0.90	0.80	1.10
Cooling temperature (^{o}C)	5	5	0
Initial fumaric acid concentration (g L^{-1})	21.30	22.28	40.42
Calculated NaOH concentration (g L^{-1})	6.50	6.60	16.15
Initial pH	3.40	3.36	3.74
Final pH	3.72	3.79	4.13
Calculated final pH	3.73	3.73	4.00
Fumaric acid crystals obtained (g)	4.11	3.32	5.99
Calculated fumaric acid crystals concentration (g L^{-1})	3.82	4.60	6.12
Calculated fumaric acid crystals obtained (g)	3.44	3.68	6.73
Total fumaric acid obtained (g)	**5.6**	**4.71**	**8.33**
Total calculated fumaric acid obtained (g)	**4.67**	**4.40**	**9.64**

It was assumed that the extent of crystallisation was determined by the solubility of fumaric acid (Patnaik et al, 2007). To quantitatively explain the amount of crystals obtained after every fermentation batch, a fumaric acid solubility model (Chapter 4) was used. This model incorporates the dissociations of fumaric acid, and the solubilities of fumaric acid, sodium hydrogenfumarate and sodium fumarate, all as function of temperature and ionic strength. Up to pH ~4.0 fumaric acid determines the solubility, whereas at higher pH sodium hydrogenfumarate may be obtained (see discontinuities in model lines in Figure 6). The results of the model calculations are presented in Table 2, together with the experimental data obtained for the crystallisations performed after each

fermentation. The calculated final pH values agree well with the experimental ones obtained for the crystallisations at 5 °C, but for 0 °C the correspondence was less. The same tendency was observed for the amount of crystals obtained from the simulations for 5 °C and 0 °C. This can be explained by a lower accuracy of the model at lower temperatures. It lacked experimental pK_a values for temperatures below 10 °C as input data (Chapter 4). Nevertheless, as the model predicts the experimental trends quite reasonably it seems that the amounts of crystals obtained in the crystallisations performed after the fermentation approximate the maximum amounts that can be recovered by this method according to the solubilities. This implies that the model can be used for predictions at other conditions.
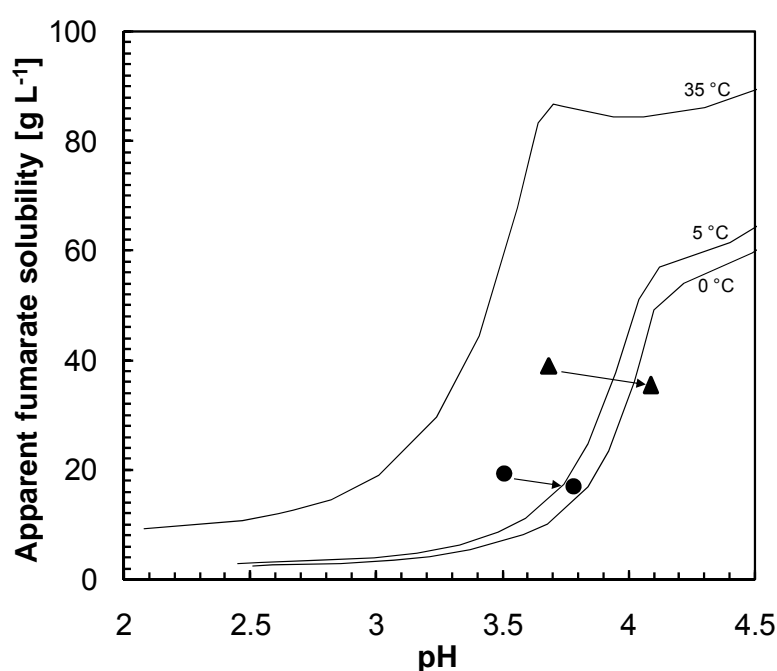

Figure 6: Solubility of total fumarate as a function of pH at different temperatures. Lines represent model predictions. ● Average course of crystallisation of experiments 1 and 2; ▲ Average course of crystallisation of fermentation experiment 3. Only final values in the crystallisation experiments (at the end of arrows) are at saturation.

It can be seen from Figure 5 and 6 that the fermentation titers are 3-4 times higher than the solubilities at 0 or 5 °C, for the same pH. However, only 5 – 20 % of the dissolved fumaric acid was recovered by cooling to 0 or 5 °C, because the crystallisation increases the pH by 0.3-0.5 unit as shown in Figure 5, and hence solubility 2-4 fold. Because, the extent of recovery of the undissociated fumaric acid by crystallisation is also limited by the pH of the solution (Figure 1), and this extent can be improved if the fermentation can be carried out at lower pH values (between 2 and 3). The difference between cooling to 0 or to 5 °C seems to be modest with respect to recovery, when the solutions are below pH 3. Additionally, as has been reported previously (Chapter 4) the

influence of fermentation co-solutes on fumarate solubility in the pH range from 2 to 4 is almost negligible.

The overall results indicate that attempts to increase the fumaric acid production rate, e.g. by increasing the cell mass specific productivity and/or the cell mass concentration in the fermentor, are not sufficient to increase the feasibility of the integrated process. Also efficient product removal is essential to maintain a high productivity. Achieving a higher extent of fumaric acid recovery in the crystalliser would increase the pH of the mother liquor, decreasing in that way product inhibition in the fermentor. Nonetheless, the product removal achieved in these experiments was simple and clearly improved fumaric acid production. Additionally, X-Ray powder diffraction confirmed that all crystals obtained from the integration of fermentation and crystallisation were fumaric acid and not one of its sodium salts.

3.4   Perspectives for industrial production

Figure 7 shows a schematic overview of the proposed integrated process for producing fumaric acid.
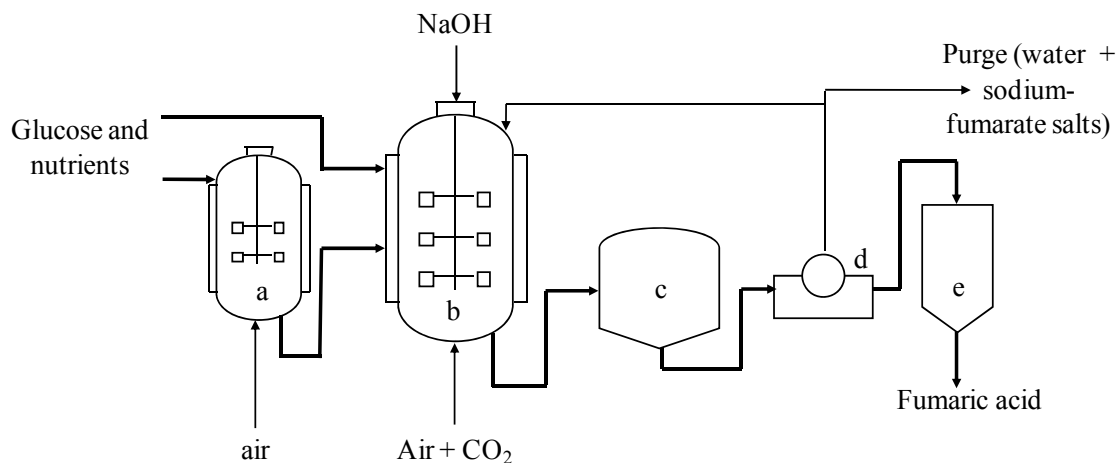

Figure 7: Proposed process for fumaric acid production via fermentation. a) Seed fermentor; b) Production fermentor; c) cooling crystalliser; d) Filter; e) dryer.

To obtain a preliminary evaluation of the proposed process for different operation scenarios, the solubility model (Chapter 4) was used for recovery predictions when the fermentation was carried out at different pH values. Conditions and titers of the integration experiment 3 were used to start the simulations. It was decided to vary the fermentation pH, because this determines how much neutralising agent is required and how much waste salts might be generated to recover fumaric acid from the broth. Table 3 summarises the results obtained with the modelling.

Table 3: Simulation data for producing fumaric acid on lab scale at different pH values.

Process	A	B	C
1st crystallisation			
Working volume (L)	0.61	0.61	0.61
Temperature (^{o}C)	35	0	0
Initial fumaric acid concentration (g L^{-1})	40.41	40.41	40.41
Calculated NaOH added (g)	15.86	10.31	2.44
Calculated H$_2$SO$_4$ added (g)	19.52	0.00	0.00
Calculated Na$_2$SO$_4$ produced (g)	19.12	0.00	0.00
Initial pH	5.02	3.82	3.00
Calculated final pH after crystallisation	1.99	4.01	3.70
Calculated fumaric acid crystals concentration (g L^{-1})	30.74	4.76	28.88
Calculated fumaric acid crystals obtained (g)	18.75	2.90	17.62
2nd crystallisation			
Working volume (L)	1.10	1.10	1.10
Cooling temperature (^{o}C)	35	0	0
Initial fumaric acid concentration (g L^{-1})	40.42	40.42	40.42
Calculated NaOH added (g)	28.60	17.77	4.40
Calculated H$_2$SO$_4$ added (g)	35.20	0.00	0.00
Calculated Na$_2$SO$_4$ produced (g)	34.47	0.00	0.00
Initial pH	5.03	3.74	3.00
Calculated final pH after crystallisation	1.99	4.00	3.70
Calculated fumaric acid crystals concentration (g L^{-1})	30.76	6.12	28.89
Calculated fumaric acid crystals obtained (g)	33.84	6.73	31.78
Total calculated NaOH consumed (g)	**44.46**	**28.07**	**6.84**
Total calculated H$_2$SO$_4$ consumed (g)	**54.72**	**0.00**	**0.00**
Total calculated Na$_2$SO$_4$ produced (g)	**53.59**	**0.00**	**0.00**
Total calculated fumaric acid produced (g)	**52.59**	**9.64**	**49.40**

According to this preliminary study, the proposed process (Table 3, column *B*) might reduce the consumption of neutralising agent by ~ 37% compared to the conventional process shown in Figure 2, where the fermentation is carried out at pH 5.0 (Table 3, column *A*). Furthermore, while consumption of NaOH is reduced, production of waste salt, in this case sodium sulfate, is reduced as well. The process where the fermentation pH was kept at 5.0 produces equal amounts of sodium sulfate and fumaric acid. The total amount of fumaric acid crystals produced in process *A*, however, is 4-5 times higher than in process *B*. Therefore, to be able to compete with the conventional process at pH 5.0 it is necessary for the proposed process to go to lower pH values for the fermentation step

as is shown in the results of process *C* in Table 3. Considering previous results (Roa Engel et al., 2009), this cannot be achieved with the current strain.

The fermentation of process *C* runs at pH 3.0, and will thus be less productive. However, for the sake of argument we consider the hypothetical situation that the productivity is the same for the three processes. The amount of fumaric acid recovered by cooling crystallisation in process *C* is close to the amount recovered by shifting pH with sulfuric acid in process *A*. These results clearly show the main bottleneck in our integrated process and the further improvements that are required to make our process competitive. Nevertheless, as productivity increases when fumaric acid is being removed, it would be interesting to consider an integrated process with continuous product removal and compare the theoretical productivity of such a process with the results obtained so far experimentally. Additional issues to be taken into account for further economic analysis are energy requirement for cooling and for cycling the liquids between fermentation and crystallisation.

4   Conclusions

A novel approach was demonstrated for producing fumaric acid by fermentation at low pH with integrated cooling crystallisation. Product recovery directly from the fermentation broth is possible, which reduces product inhibition. Adapting the fermentation conditions to facilitate recovery is a strategy that was proven to be viable for the process that was developed. Although the process proposed is very simple and reduces waste salts production yields have to be improved to make the production of fumaric acid with the proposed process economically feasible. The integrated process might also be applied to other systems where conditions close to saturation are achieved in the fermentation.

Acknowledgements

References

Berglund KA, Elankovan P, Glassner DA (1991) Carboxylic acid recovery and crystallization process. U.S. Patent 5,034,105.

Brown CJ (1966) The crystal structure of fumaric acid. Acta Cryst (21) 1.

Buque-Taboada EM, Straathof AJJ, Heijnen JJ, van der Wielen LAM (2006) In situ product recovery (ISPR) by crystallization: basic principles, design, and potential applications in whole-cell biocatalysis. Appl Microbiol Biotechnol (71) 1.

Cao NJ, Du JX, Gong CS, Tsao GT (1996) Simultaneous production and recovery of fumaric acid from immobilized *Rhizopus oryzae* with a rotary biofilm contactor and an adsorption column. Appl Environ Microbiol (62) 2926.

Cuellar MC, Herreilers SN, Straathof AJJ, Heijnen JJ, van der Wielen LAM (2009) Limits of operation for the integration of water removal by membranes and crystallization of L-phenylalanine. Ind Eng Chem Res (48) 1566.

Du JX, Cao NJ, Gong CS, Tsao GT, Yuan NJ (1997) Fumaric acid production in airlift loop reactor with porous sparger. Appl Biochem Biotech (63-65) 541.

Huh YS, Jun YS, Hong YK, Song H, Lee SY, Hong WH (2006) Effective purification of succinic acid from fermentation broth produced by Mannheimia succiniciproducens. Process Biochem (41) 1461.

Joglekar HG, Rahman I, Babu S, Kulkarni BD, Joshi A (2006) Comparative assessment of downstream processing options for lactic acid. Sep Purific Technol (52) 1.

Lohbeck K, Haferkorn H, Fuhrmann W, Fedtke N (2005) Maleic and Fumaric Acids. Ullmann's Encyclopedia of Industrial Chemistry, 5th ed., Vol. A16, VCH., 53-62. Weinheim, Germany

Mager WH, Siderius M (2002) Novel insights into the osmotic stress response of yeats. FEMS Yeast Res (2) 251.

Moresi M, Ceccantoni B, Presti SL (2002) Modelling of ammonium fumarate recovery from model solutions by nanofiltration and reverse osmosis. J Mem Sci (209) 405.

Patnaik R, Zolandz RR, Green DA, Kraynie DF (2008) L-Tyrosine Production by Recombinant Escherichia coli: Fermentation Optimization and Recovery. Biotechnol Bioeng (99) 741.

Roa Engel CA, Straathof AJJ, Zijlmans TW, van Gulik WM, van der Wielen, LAM (2008) Fumaric acid production by fermentation. Appl Microbiol Biotechnol (78) 379.

Roa Engel CA, Straathof AJJ, van Gulik WM, van de Sandt EJAX, van der Does T, van der Wielen LAM (2009) Conceptual Process Design of Integrated Fermentation, Deacylation, and Crystallization in the Production of β-Lactam Antibiotics. Ind Eng Chem Res (48) 4352.

Stephen WI (1965) Solubility and pH calculations. Anal Chim Acta (33) 227.

Welton J, McCarthy G (1988) North Dakota State University, Fargo, North Dakota, USA, ICDD Grant-in-Aid.

Werpy T, Petersen G (2004) Topten value added chemicals from biomass feedstocks. U.S. Department of Energy, USA.

Xu C, Long C, Li A, Liu F, Yang W, Zhang Q (2006) Adsorption Characteristics of Fumaric Acid onto Weakly Basic Hypercrosslinked Polystyrene Ion-exchangers. Adsorption Sci Technol (24) 65.

Zhou Y (1999) Fumaric acid fermentation by *Rhizopus oryzae* in submerged system. PhD thesis. Purdue University. Lafayette, Indiana, USA. pp 149.

SECTION 2

7-aminodeacetoxycephalosporanic acid

CHAPTER 6

Conceptual process design of Integrated fermentation, deacylation and crystallisation in the production of β-lactam antibiotics

Integration of fermentation and downstream steps is required to improve the sustainability of industrial biotechnology processes. In this context, a new integrated process for β-lactam nuclei production is proposed, which and has been theoretically investigated and conceptually designed. This process is an integration of fermentation and enzymatic deacylation of adipyl-7-aminodeacetoxycephalosporanic acid (adADCA) in one reactor producing 7-aminodeacetoxycephalosporanic acid (ADCA) directly from glucose. Although the deacylation equilibrium is unfavourable at the fermentation pH, it is pulled to completion because ADCA starts to crystallise and the liberated side-chain, adipic acid (AA), is consumed by the fermentation. Therefore the integrated process requires much less AA than the non-integrated process. In addition, the new process will lead to a reduction in number of downstream processing units, should avoid the use of acids and bases for pH shifts and might lead to a reduction in waste salts production. A conceptual process was designed including an economic and technical analysis. The design goal was to produce 2000 ton/year of ADCA of 99% purity. Rigorous simulations were performed to evaluate different process options. Amongst the economic advantages of the new integrated process are 13.4% lower capital investments and 7.8% lower manufacturing costs. An analogous process for 6-aminopenicillanic acid (APA) is not feasible due to chemical degradation of this product.

1   Introduction

Following Alexander Fleming's discovery of the antibacterial activity of the fungus *Penicillium notatum* in 1928, more than a decade passed before Florey & Chain finally isolated penicillin G (Pen G) in 1940. Unfortunately, an increasing number of bacterial strains became resistant to Pen G, which was phased out of clinical use in the late 1960s. Since then, a large range of alternative β-lactam antibiotics has been developed, which are very effective against bacterial diseases. These consist of penicillins and cephalosporins, for which the β-lactam nuclei 6-aminopenicillanic acid (APA) and 7-aminodeacetoxycephalosporanic acid (ADCA) are the major starting materials (Bruggink 2001). The production of these nuclei is described schematically in Figure 1.
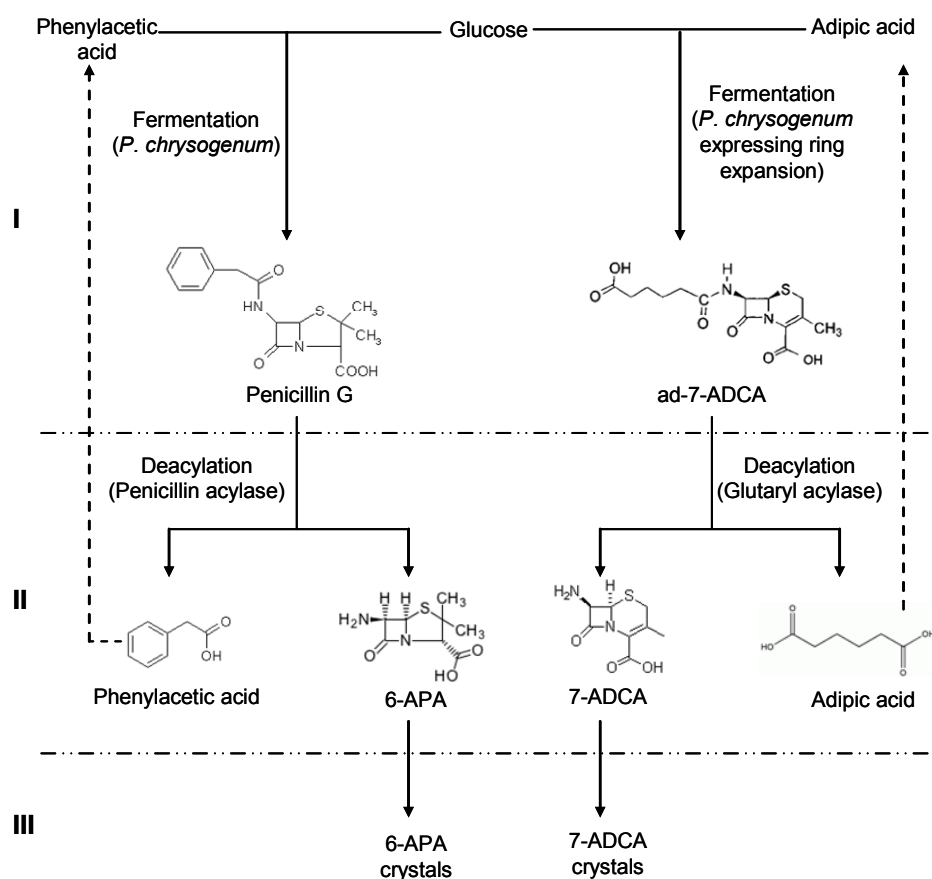
Figure 1: Schematic overview of the reactions occurring in the production of APA and ADCA from glucose (I: fermentation stage; II: deacylation stage; III: crystallisation stage).

APA is obtained by Pen G conversion, Pen G being produced via fermentation using *Penicillium chrysogenum*. Pen G recovery involves various downstream processing steps. First, Pen G is extracted from the fermentation broth by using organic solvents. Subsequently, Pen G is either back-

extracted to an aqueous phase, and then crystallised, or directly crystallised from the organic phase by adding solid potassium acetate or sodium acetate (Diender et al., 2002). Pen G crystals are used for the production of APA by enzymatic deacylation. Phenylacetic acid (PAA) is a co-product of this reaction. After this step, APA is crystallised from the aqueous solution. The main sections of the process, fermentation, deacylation and APA crystallisation, operate at pH 6.2, 8.0 and 4.0 respectively. Large amounts of acids and bases are therefore required in order to shift the pH, leading to waste salts formation. This problem increases the production costs and has a negative impact on the environment. PAA, the co-product of the deacylation reaction, is also the side chain precursor (SCP) for the Pen G fermentation. PAA, produced during deacylation, is optionally purified and recirculated to the fermentation unit. This recycle stream increases the number of downstream process units.

The traditional production process of ADCA also involves a fermentation step to produce penicillin (Pen G), followed by chemical oxidation and chemical ring expansion. An enzymatic cleavage of the side chain, similar to that of the penicillin to APA, yields ADCA. The chemical ring expansion is costly and causes a significant environmental burden. An enzyme named deacetoxycephalosporin C synthase but often referred to as expandase and capable of catalysing the β-lactam ring expansion has been extensively characterised (Kohsaka et al., 1976; Cho et al., 1998; Adrio et al., 1999). As *Penicillium chrysogenum* is a very efficient β-lactam producer, expandase activity has been successfully expressed in this organism in order to produce adipyl-7-aminodeacetoxycephalosporanic acid (adADCA) by introducing a gene from *Streptomyces clavuligerus* (Cantwell et al., 1992; Crawford et al., 1995) upon the SCP adipic acid (AA). Subsequently adADCA is enzymatically deacylated into ADCA and AA. This procedure has been implemented in the industrial production process. This new ADCA production process has complications similar to the APA process, such as the pH shifting between the main units of the process. Therefore, new process concepts are desired to decrease the number of unit operations and the waste salts production of the present processes.

The main objective of this study is to develop a novel process concept for production of β-lactam nuclei, with a focus on APA and ADCA. Therefore, we will integrate fermentation and deacylation with product removal by crystallisation. Integration of fermentation and crystallisation has been reviewed recently for other fermentations (Buque-Taboada et al., 2006). We will avoid the involvement of organic solvents, which were used in previous studies aiming to integrate downstream processing with fermentation.

A hierarchical conceptual process design method (Douglas 1988; Seider, Seader and Lewin 1999) will be applied to identify the best process alternative to produce APA and ADCA. The design phases of the conceptual process design are (Swinkels et al., 2004):

1. Problem definition (Basis of Design)

2. Knowledge acquisition

3. Synthesising alternatives at different design levels: product choice, process structure, unit operations and equipment, process control.

4. Analysis of behaviour (including mass and energy balances)

5. Evaluation of performance (including economy)

After defining a base case and a basis of design, process integration alternatives for APA and ADCA production will be presented. Secondly, mathematical models that are used as a tool to analyse the behaviour of each unit operation for the selected options will be described. Schematic flow diagrams will be employed to show the results obtained from the models and finally an economic evaluation will be presented to complete the feasibility comparison among the different options proposed. No experimental verification of the results is included.

2   Base Case definition and basis of design

To compare different process options for APA and ADCA production, a Base Case was developed, taking into account common units operation and process parameters in the production of these two β-lactam nuclei. This Base Case is a non-integrated process of the three main units that are involved in the production of APA and ADCA: fermentation, deacylation and crystallisation (Figure 2). The optimal pH value for these units where conversion yields reach their maximum are: fermentation at 6.2; deacylation at 8; crystallisation at 4.

In the first stage of the Base Case, glucose is fed to a fermentor and Pen G or adADCA is produced, for the APA and ADCA processes, respectively. Then, this intermediate compound is passed through a deacylation unit, leading to the production of the β-lactam nucleus (APA or ADCA) and acid (PAA or AA). After this conversion, crystallisation serves as the separation and purification technique, producing β-lactam nuclei crystals from the solution that contains water and the acid (PAA or AA). The acid serves as the SCP for the fermentation. The Base Case is a simplification of the reality where the fermentation products Pen G and adADCA are separated from

the broth by solvent extraction and adsorption techniques respectively (Diender et al., 2002; van de Sandt 2005). Moreover, the Base Case concept originated from the process concept proposed for ADCA production (Schroën et al., 2002) and is operating in batch mode. For the fermentation model fed-batch mode was chosen because is beneficial in order to increase product concentration, which facilitates product recovery (Heijnen et al., 1992).

The designed capacity for producing the β-lactam nuclei is 2000 ton/year. This capacity constitutes 10% of the worldwide β-lactam nuclei production, which is 20,000 ton/year. The operating time for the production process is assumed to be 330 days per year. This is comparable to the on-stream time of most bulk chemical manufacturing plants. This is due to the mandatory provision for servicing of the plant, or for any plant malfunction, during either of which the plant must be shut down. A plant life of 10 years is assumed for economic analysis and it is expected that the total plant investment is recouped before this period.

The system boundaries for the evaluated β-lactam nuclei production processes, including the Base Case, are presented in Figure 2. In order to simplify the system, it is assumed that raw materials, solid waste and wastewater are treated outside the process. However, as one of the objectives of the new process configuration is the reduction of waste salts, the disposal price of this waste is taking into account for the final economic evaluation.
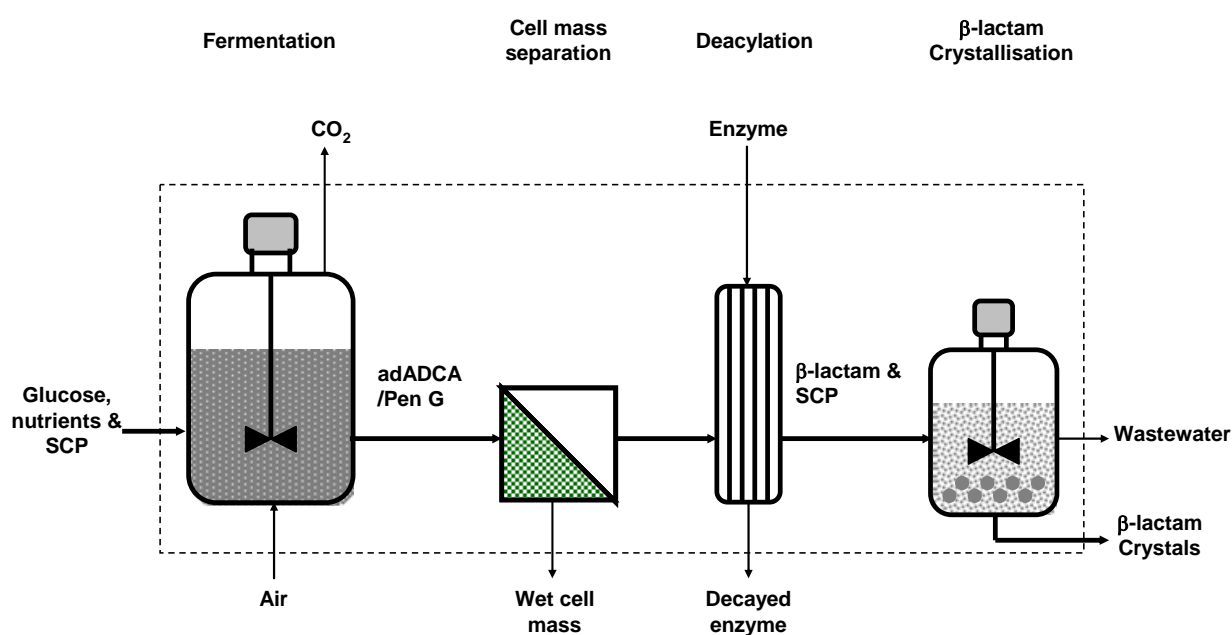

Figure 2: Base Case for β-lactam nuclei production using glucose as feedstock (SCP: side chain precursor). The dashed line shows the system boundaries.

Newly integrated options will be developed taking the Base Case as the starting point. The new options will be compared technically and economically with each other and with the Base Case. To develop different integrated options for the production of APA or ADCA, one of the main factors that must be analysed in detail is the pH shifting between the process steps. It has been mentioned that fermentation, deacylation and crystallisation perform at their best at the pH value of 6.2, 8.0 and 4.0, respectively. However, if integration should be achieved without the addition of stoichiometric amounts of acids or bases, avoiding the production of its associated waste salts, the pH has to be constant for the whole process. In order to choose one process pH value, the influence of pH on the performance of every unit has to be analysed. This will be discussed at the end of the next section.

3 Model development for evaluation of process options

Because of the different possible combinations of integrated processes for the production of β-lactam nuclei, a tool is required for the evaluation of this kind of configurations. This tool should have the following characteristics: flexible enough to analyse additional aspects and changing conditions; give a principal insight of the performance of every option and easily interpretable in order to allow an intuitive understanding of the results.

For this purpose mathematical models were constructed to calculate the yields and productivities of the different process options for production of APA and ADCA. In these models the production by means of fed-batch fermentation, as well as the deacylation and crystallisation of APA and ADCA were incorporated. In such models the pH is an important parameter, because the performance of the individual unit operations, fermentation, deacylation and crystallisation are all highly pH dependent. A constant temperature of 25 ^{o}C for fermentation and deacylation and atmospheric pressure (1 bar) for the whole process were assumed. Parameters and equations for APA and ADCA production models are described in the following sections. The reported parameters used in the model have been experimentally validated and the corresponding references are included.

3.1 Product degradation

3.1.1 APA production process

The first product in the APA production process, Pen G, is more stable in the pH range between 5 and 8 than out of this range for subsequent isolation. Increase in temperature as well as working out

of the range of 5 – 8 for pH increased the decomposition of penicillin G. This is due to the formation of penicilloic acid via opening of the β-lactam ring (Kheirolomoom et al., 1999).

An APA degradation study in the pH and temperature ranges of 5.8 - 6.6 and 35 - 90 $^{\circ}$C, respectively, showed that APA follows spontaneous first order degradation, which is faster at lower pH values (Dennen 1967). This conclusion was in agreement with the results obtained at 25 $^{\circ}$C in the pH range of 3.5 – 5 (Ferreira et al., 2004). The degradation constants for pH values from 5 to 8 and 25 $^{\circ}$C were extrapolated from these data. Subsequently, only the pH range 4 – 8 will be considered for the evaluation of β-lactam production because β-lactams are unstable outside this range.

Besides the aforementioned degradation, carboxylation of the amino group of APA takes place in the presence of CO_2. This is followed by the expansion of the β-lactam ring into an imidazolidone ring leading to 8-hydroxy-penicillic acid (HPA). HPA cannot re-enter the penicillin biosynthetic pathway and is therefore an undesirable by-product. The rate of carboxylation of APA has been described by the following equation (Henriksen et al., 1997).

$$\Gamma_{HPA} = k^* \cdot C_{CO_2} \cdot C_{APA} \qquad\qquad [1]$$

A k^* value of 12 L mol^{-1} h^{-1} was used for the conditions at 25°C and pH 6.5 (Henriksen et al., 1997). The total degradation rate is the sum of the two aforementioned rates.

3.1.2 ADCA production process

The fermentation product of ADCA process, adADCA, has a degradation rate that follows first-order kinetics with a value of the rate constant of 5.3x10^{-4} h^{-1} at 25 $^{\circ}$C and pH 6.5 (Robin et al., 2003). This value is in agreement with other literature (Schroën et al., 2002) and will be used for the model calculations.

In the case of ADCA chemical degradation plays an important role in a continuous stirred tank reactor (CSTR). At high temperatures and high substrate concentrations, chemical degradation is very pronounced because of the longer residence times that are required in CSTR (Schroën et al., 2002). However, continuous operations at 27 $^{\circ}$C and low substrate concentrations can reduce ADCA degradation to less than 1%. The system under investigation operates at 25 $^{\circ}$C and low substrate concentration, hence degradation of ADCA is negligible.

3.2 Fermentation

The production of APA occurs in a two steps process, whereby first Pen G is produced by fed-batch fermentation, using an industrial strain of *P. chrysogenum* and subsequently Pen G is deacylated to APA. In case of ADCA production, adADCA is directly produced in a fed-batch fermentation process using a transformed *P. chrysogenum* strain expressing the expandase gene from *Streptomyces clavuligerus*. The modelling of the fed-batch fermentations was based on black-box kinetic equations and mass balances for the relevant compounds, in a similar way as has been described by Heijnen et al. (1979).

The stoichiometry and kinetics of growth and penicillin production in *P. chrysogenum* have been studied and validated by different authors in the past decades (Heijnen et al., 1979; Bajpai et al., 1980; Christensen et al., 1995; Jørgensen et al., 1995; van Gulik et al., 2001). The detailed research done by van Gulik et al. in 2001 served as the main source of kinetic information for the Pen G fermentation model used in this study. In the case of adADCA, not all kinetic parameters are reported for the transformed strain of *P. chrysogenum* that is used in this process. Therefore, some of the kinetic parameters were obtained from reported experiments performed with the transformed strain. (Henriksen et al., 1997; van Gulik et al., 2001) Table 1 summarises the kinetic and stoichiometric parameters we have applied in the Pen G and adADCA fermentation models.

Table 1: Kinetic and stoichiometric parameters used in the Pen G and adADCA fermentation models (25 ^{o}C, pH 6.2).

Kinetic parameter	Pen G	adADCA
Y_{sx_max} (C-mol mol^{-1})	3.978 (van Gulik et al., 2001)	3.2 (Robin et al., 2001)
μ_{max} (h^{-1})	0.11 (Bajpai et al., 1980)	0.19 (Robin et al., 2001)
μ (h^{-1})	0.03 (van Gulik et al., 2001)	0.05 (Robin et al., 2001)
Y_{sp_max} (mol mol^{-1})	0.18 (van Gulik et al., 2001)	0.11[a,] (van Gulik et al., 2001)
m_s (mol C-mol^{-1} h^{-1})	0.0014 (van Gulik et al., 2001)	0.0014 (van Gulik et al., 2001)
K_s (mmol L^{-1})	0.7 (Bajpai et al., 1980)	0.7 (Bajpai et al., 1980)

a) 60% of 0.18. See section 3.2 for further explanation.

In the case of adADCA the fermentation yield of product on substrate has not been determined for the transformed *P. chrysogenum* strain. Therefore, 60% of the published yield of Pen G on substrate was used for the adADCA fermentation model. This assumption was based on the fact that the published maximum productivity of the adADCA fermentation process (Robin et al., 2003) is 60% of the maximum productivity of the Pen G fermentation (van Gulik et al., 2001). Also the maintenance coefficient and the K_s for glucose are not known for the transformed strain and have been assumed the same as for the non-transformed, Pen G producing strain.

The specific growth rate values in Table 1 are valid during the exponential feed phase. Those specific growth rates were chosen according to the maximal production rate reported for Pen G and adADCA production (Robin et al., 2003; van Gulik et al., 2000). If the feed is kept constant this will lead to a decrease of the specific growth rate. Therefore, the calculation of the specific growth rate was done taking into account the substrate uptake rate.

The substrate uptake rate was assumed to be a function of the extracellular substrate concentration according to saturation kinetics:

$$-q_s = q_{max} \cdot \frac{C_S}{K_S + C_S} \qquad [2]$$

The division of the substrate between growth, product formation and maintenance was described by the Herbert-Pirt equation for substrate consumption:

$$-q_s = \frac{\mu}{Y_{SX}^{\;max}} + \frac{q_p}{Y_{SP}^{\;max}} + m_S \qquad [3]$$

Combining Equations 2 and 3 yields the following expression for the specific growth rate as a function of the substrate concentration:

$$\mu = Y_{SX}^{\;max} \cdot \left(\frac{q_S^{\;max} \cdot C_S}{K_S + C_S} - \frac{q_P}{Y_{SP}^{\;max}} - m_s \right) \qquad [4]$$

In equations 3 and 4, q_p is the product formation rate. The production rate equations for Pen G and adADCA were obtained from the experimental data published (Robin et al., 2003; van Gulik et al., 2000).

$$q_{PenG} = 3.8729\mu^3 - 0.6843\mu^2 + 0.0339\mu \qquad [5]$$

$$q_{adADCA} = 6 \cdot 10^{-5}\mu^2 + 2 \cdot 10^{-4}\mu + 4 \cdot 10^{-4} \qquad [6]$$

The equation for q_{PenG} is valid for specific growth rate (μ) values between 0 and 0.075 h^{-1} and q_{adADCA} for values between 0.03 and 0.05 h^{-1}. The current industrial production rates for Pen G and adADCA production are probably much higher but they have not been reported.

The increase of the feed rate during the exponential phase of the fed-batch cultivation was calculated according to:

$$\Phi_{feed,in} = \frac{q_s \cdot M_{broth,0} C_{X,0}}{C_{S,in} - C_S} \cdot \exp(\mu t) \qquad [7]$$

The resulting fermentation model consists of five ordinary differential equations, describing the changes of the total mass of broth (8), substrate concentration (9), biomass concentration (10), β-lactam concentration (11) and SCP concentration (12).

$$\frac{dM_{broth}}{dt} = \Phi_{feed,in} + \Phi_{O_2} + \Phi_{CO_2} \qquad [8]$$

$$\frac{dC_S}{dt} = q_S \cdot C_X + \frac{\Phi_{feed,in} C_{S,in}}{M_{broth}} - \frac{C_S}{M_{broth}} \cdot \frac{dM_{broth}}{dt} \qquad [9]$$

$$\frac{dC_X}{dt} = \mu \cdot C_X - \frac{C_X}{M_{broth}} \cdot \frac{dM_{broth}}{dt} \qquad [10]$$

$$\frac{dC_{product}}{dt} = q_{product} \cdot C_X - k_d \cdot C_{product} - \frac{C_{product}}{M_{broth}} \cdot \frac{dM_{broth}}{dt} \qquad [11]$$

$$\frac{dC_{SCP}}{dt} = q_{SCP} \cdot C_X - \frac{C_{SCP}}{M_{broth}} \cdot \frac{dM_{broth}}{dt} \qquad [12]$$

The flows of oxygen and carbon dioxide in the broth which are in equation 8 can be calculated with the equations described in Appendix 1. The oxygen consumption, SCP consumption and carbon dioxide production rates were obtained from the mass and degree of reduction balances, which are also present in Appendix 1.

3.3 Deacylation

The Pen G deacylation is catalysed by penicillin acylase and the adADCA deacylation by glutaryl acylase. In these systems the theoretical yield is controlled by the chemical equilibrium. The apparent equilibrium constant K_{app} is expressed in molar concentration terms assuming that the system behaves thermodynamically ideal (all activity coefficients equal unity). It is important to mention that for non-ideal solutions, increasing ionic strength causes a decrease in activity coefficient, it enhances the extent of dissociation of weak electrolytes and thereby increases the extent of deacylation by typically $0 - 10\%$ (van der Wielen et al., 1997).

$$K_{app,\beta-lactam} = \frac{C_{SCP}{}^{tot} \cdot C_{\beta-lactam}{}^{tot}}{C_{\beta-lactam\_nucleus}{}^{tot}} \qquad [13]$$

The apparent equilibrium constant uses the total dissolved concentration of the different charged species of a compound involved in the reaction and is therefore pH dependent. This constant can be expressed in terms of pH and the theoretical equilibrium constant (K_{th}).

$$K_{app,PenG} = \left(1 + \frac{10^{-pH}}{10^{-pK2,APA}}\right)\left(1 + \frac{10^{-pKPAA}}{10^{-pH}}\right)K_{th,PenG} \qquad [14]$$

$$K_{app,adADCA} = \frac{\left(1 + \frac{10^{-pK1,AA}}{10^{-pH}} + \frac{10^{-pK2,AA} \cdot 10^{-pK1,AA}}{10^{-pH}}\right) \cdot \left(1 + \frac{10^{-pK1,ADCA}}{10^{-pH}} + \frac{10^{-pH}}{10^{-pK2,ADCA}}\right)}{\left(1 + \frac{10^{-pK1,adADCA}}{10^{-pH}} + \frac{10^{-pK2,adADCA}}{10^{-pH}}\right)} \cdot K_{th,adADCA} \qquad [15]$$

Using equations 14 and 15 the apparent equilibrium constants of the Pen G and adADCA deacylation reactions can be calculated. The pKs needed in these equations are given in Table 2.

For the thermodynamic equilibrium constant (K_{th}), the following equation is applied (Švedas et al., 1980).

119

$$K_{th} = \exp\left(\frac{-\Delta G^0{}_c}{RT}\right) \qquad\qquad [16]$$

$\Delta G^o{}_c$ is the (pH-independent) standard Gibbs energy change. As this value is known for Pen G and adADCA (Table 3), the K_{app} values are also known as a function of temperature and pH (Schroën et al., 2000).
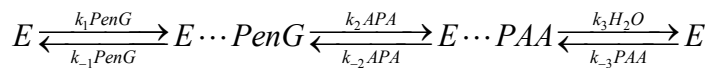
Table 2. Dissociation constant values (25 ^{o}C)

Compound	pK$_1$	pK$_2$	Reference
PAA	4.2	-	Diender et al., 1998
APA	2.6	4.6	Berezin et al., 1976
Pen G	2.6	-	Tewari et al., 1988
AA	4.4	5.3	Weast 1971
ADCA	2.95	4.87	Yamana et al., 1974;
			Yamana et al., 1976
adADCA	2.95	5.3	Schroën et al., 2000

Table 3. Standard Gibbs energy change values for deacylation

Compound	$\Delta G^o{}_c$ (kJ mol^{-1})	Reference
Pen G	20.13	Švedas et al., 1980
adADCA	19.8	Schroën et al., 2000

The kinetic model presented by Spieß in 1999 is used in the current research for the Pen G deacylation system. This model is based on a ping-pong mechanism in which the water concentration is constant.

$$E \underset{k_{-1}PenG}{\overset{k_1 PenG}{\rightleftarrows}} E\cdots PenG \underset{k_{-2}APA}{\overset{k_2 APA}{\rightleftarrows}} E\cdots PAA \underset{k_{-3}PAA}{\overset{k_3 H_2O}{\rightleftarrows}} E$$
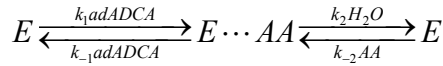
This leads to the following rate equation (Spieß et al., 1999).

$$\Gamma_{PenG} = -\frac{\dfrac{k_{cat}}{K_{m,PenG}} \cdot C_{E(0)} \cdot \left(C_{PenG} - \dfrac{C_{APA} \cdot C_{PAA}}{K_{app,PenG}} \right)}{1 + \dfrac{C_{PenG}}{K_{m,PenG}} + \dfrac{C_{APA}}{K_{m,APA}} + \dfrac{C_{PAA}}{K_{m,PAA}} + \dfrac{C_{PenG} \cdot C_{PAA}}{K_{m,PenG} \cdot K_{m,PAA}} + \dfrac{C_{APA} \cdot C_{PAA}}{K_{m,APA} \cdot K_{m,PAA}}} \qquad [17]$$

C_{Eo} is the initial concentration of the enzyme. The kinetic constants at 37 ^{o}C were expressed as a function of pH (Spieß et al., 1999). We assume the same values at 25°C, which is the temperature of our model system.

A comparable mechanism for adADCA deacylation by glutaryl acylase, but merged the first two steps was assumed (Schroën et al., 2000).

$$E \underset{k_{-1} adADCA}{\overset{k_1 adADCA}{\rightleftharpoons}} E \cdots AA \underset{k_{-2} AA}{\overset{k_2 H_2O}{\rightleftharpoons}} E$$

This leads to the following equation.

$$\Gamma_{adADCA} = -\frac{k_1 \cdot C_{E(0)} \left(C_{adADCA} - C_{ADCA} \cdot C_{AA} \cdot \dfrac{1}{K_{app,adADCA}} \right)}{1 + \dfrac{k_{-1}}{k'_2} \cdot C_{adADCA} + \dfrac{k_1}{k'_2} \cdot C_{ADCA} + \dfrac{k_{-2}}{k'_2} \cdot C_{AA}} \qquad [18]$$

Where:

$$K_{app,adADCA} = \frac{k_1 \cdot k'_2}{k_{-1} \cdot k_{-2}} \qquad [19]$$

The pH independent kinetic constant values are presented in Table 4 and the pH-dependent kinetic constant, k'_2, can be calculated with equation 19.

Table 4: Calculated kinetic constant values.

Constant	Estimated value (L/h)
k_1[a]	42.0
k_{-1}[a]	66.0
k_2[b]	51.6

a) from experiments carried out at pH's 7.5 to 8.0 and 20 ^{o}C (Schroën et al., 2002).

b) from experiments carried out at pH's 7.0 to 9.5 and 20 ^{o}C (Schroën et al., 2000).

The kinetic models for Pen G and adADCA deacylation are completed with equation 20.

$$\Gamma_{\beta-lactam\_nucleus} = -\Gamma_{\beta-lactam} = -\Gamma_{SCP} \qquad\qquad [20]$$

The deacylation equilibrium conversion yields were experimentally measured and validated with the mathematical models described above for APA as well for ADCA (Schroën et al., 2000; Spieß et al., 1999). The results showed high yield values at high pH (see Figure 3).
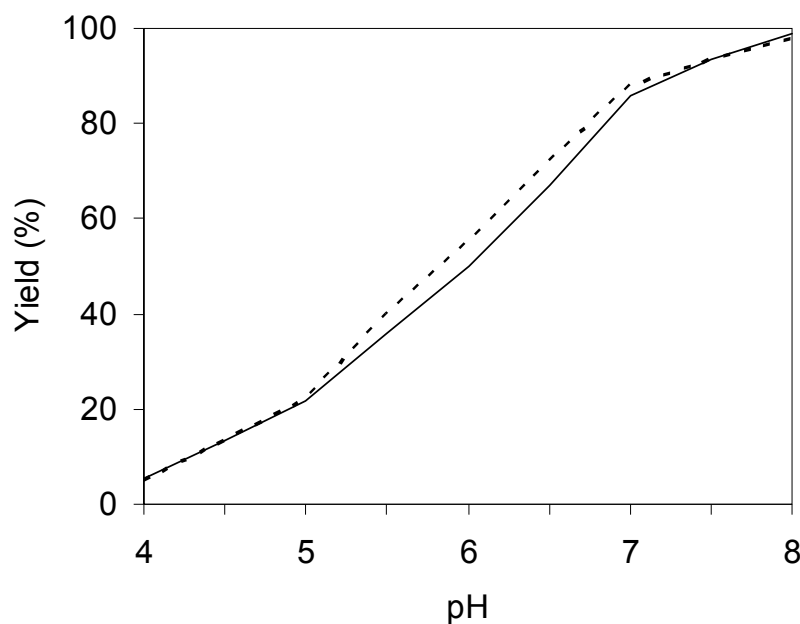

Figure 3: Deacylation equilibrium yield for APA (full line) and ADCA (dashed line) production as a function of pH at 25 ºC. (Initial concentrations: 66 mM of Pen G and 20 mM of adADCA).

Results illustrated in Figure 3 are also used for choosing the optimal pH condition for the integrated options. This issue will be discussed at the end of this section.

3.4   Crystallisation

An evaporative crystallisation system (while keeping the pH constant) for the case of APA production and a cooling system for ADCA production were selected according to the method of Kramer (et al., 1999). The cooling crystallisation system for ADCA is working at 15 ºC and the temperature was selected according to the reported increase of ADCA solubility with temperature in pure water (Jingkang et al., 2003). Both crystallisation models are developed as solubility dependent systems, which makes them pH and temperature dependent at the same time.

A solubility equation for β-lactam nuclei (21) as a function of pH, was given by previous literature (Nys et al., 1977).

$$S_{\beta-lactam} = S_o \left(\frac{10^{-pK1} \cdot 10^{-pH}}{\left(10^{-pH}\right)^2 + 10^{-pK1} \cdot 10^{-pH} + 10^{-pK1} \cdot 10^{-pK2}} \right) \qquad [21]$$

In this equation, S_o is the intrinsic solubility value of the β-lactam nucleus (Table 5).

Table 5: Intrinsic solubility values ($15^{o}C$)

β-lactam	S_o (mol/L)	Source
APA	0.012	Berezin et al., 1976
ADCA	$9.07 \cdot 10^{-4}$	Extrapolated (Nys et al., 1977)

The intrinsic solubility value of ADCA was determined at 20 and $25^{o}C$ (Jingkang et al., 2003). As the desired cooling temperature for the ADCA crystallisation model is 15 ^{o}C, the intrinsic solubility value at that temperature was found by data extrapolation.

Solubility curves for APA and ADCA as a function of pH were generated from the previous data (see Figure 4).
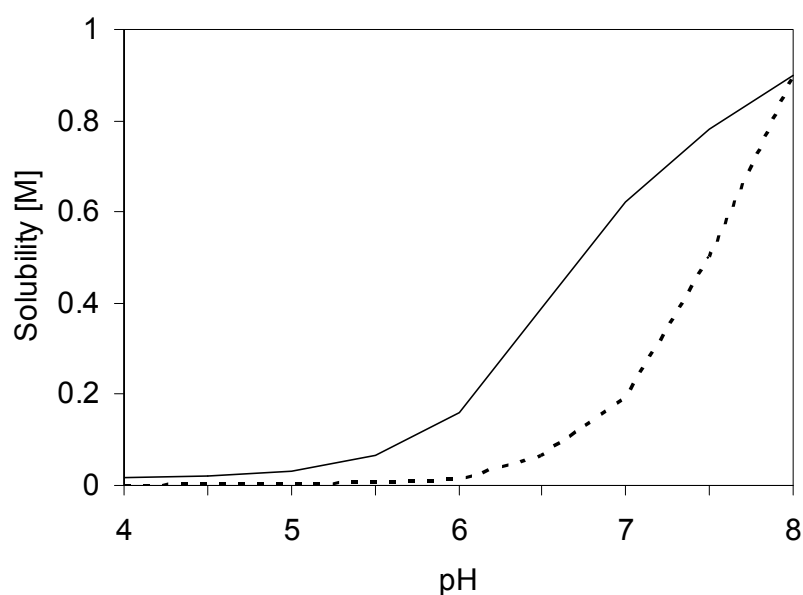

Figure 4: Solubility value for APA (full line) and ADCA (dashed line) as a function of pH at 25 ^{o}C.

Figure 4 shows that, above pH 6, the solubilities increase rapidly and this phenomenon will decrease the crystal yield. Also the crystallisation rate slows down due to the lower supersaturation. The solubility values presented in Figure 4 are crucial for choosing the operating pH for the integrated options. The supersaturation ratio (*s*) and crystal growth rate (*G*) for both crystallisation models are given in equations 22 and 23.

$$s = \frac{C_{\beta-lactam}}{S_{\beta-lactam}} \qquad\qquad [22]$$

$$G = k_g \cdot (s-1)^n \qquad\qquad [23]$$

The corresponding parameters are taken from the literature and are presented in Table 6. Like in the literature, we assume seeded crystallisation and we neglect nucleation kinetics. Mass balance equations for the crystallisation process were derived following Kramer et al. (1999).

Table 6: Crystallisation kinetics parameter values at pH 5 and 25 ^{o}C.

β-lactam	*Growth rate constant k_g (m s^{-1})*	*Growth rate order n*	*Reference*
APA	$4.26 \cdot 10^{-9}$	2	Ferreira et al., 2006
ADCA	$1.89 \cdot 10^{-11}$	1.07	Jingkang et al., 2003

3.5   Determination of pH value for the model system

As was mentioned before, it is important for the development of a new production processes for APA or ADCA to set one operational pH value because this will avoid the addition of salts or bases that are necessary for pH shifting between process units. In addition, a constant pH can facilitate units integration in the process due to the fact that two or more operations may be performed simultaneously in one vessel.

In order to find a preferred pH value for the production of APA and ADCA, the performance of the main units for those processes (fermentation, deacylation and crystallisation) was analysed as a function of pH. It is known that the expression of penicillin biosynthesis in *P. chrysogenum* is strongly pH dependent (Penalva et al., 1998). Therefore the pH of the fermentation broth should be kept close to the optimum value for maximum productivity which lies for most strains between 6.0

and 6.5. In the case of the deacylation system, Figure 3 shows that above pH 6, the equilibrium conversion yield is higher than 50% for APA as well for ADCA production, so pH 6 can still be a reasonable condition for the operation of this unit if one of the products is removed in situ. In situ product removal can pull the deacylation reaction to the side of product formation and in that way the reaction yield can be improved as well. Finally, Figure 4 illustrates that solubility values for APA and ADCA are increasing dramatically above pH 6 making crystallisation much more difficult above this pH value. Moreover, nucleation can take longer at high pH values and this will lead to larger crystallisation equipment.

Based on the previous analysis, the pH selected for the integrated options for the production of APA and ADCA is 6. It is assumed that the fermentation parameters at pH 6.2 (Table 1) are valid at pH 6 as well.

4   Process options

4.1   Case 1: No units integration at the same pH

The process configuration scheme for Case 1 is the same as proposed for the Base Case (Figure 2). The difference is that for Case 1 all the units are working at the same pH and hence acids and bases are not required to shift the pH values from one unit to another.

4.2   Case 2: Integration of fermentation and deacylation units

In this case (Figure 5), the fermentation and deacylation units are integrated. This can be done because the precursor for the fermentation is the acid produced as a co-product for the deacylation reaction (Figure 1).

It is assumed that the cell mass separation unit only retains cell mass and the β-lactam crystals that can be formed in the fermentation-deacylation unit will pass completely to the crystallisation unit. The consumption of the SCP by the fermentation might pull the deacylation equilibrium forward, improving in this way the deacylation conversion. After the two integrated steps, crystallisation is applied to recover the β-lactam nuclei.
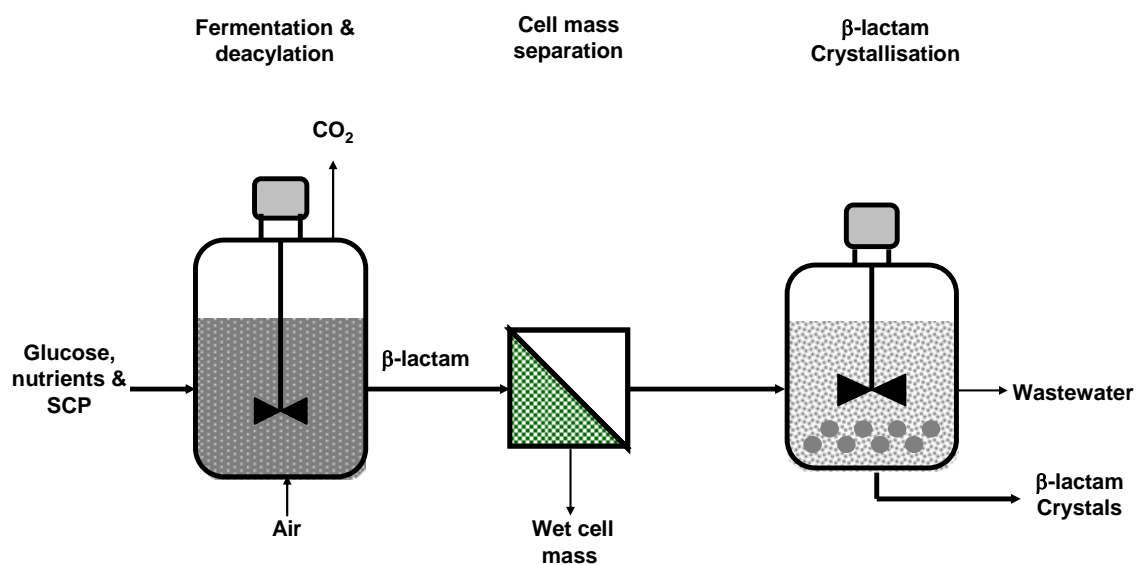
Figure 5: Process scheme for Case 2: Integration of fermentation and deacylation units.

4.3   Case 3: Integration of deacylation and crystallisation units.

Deacylation and crystallisation units are integrated in Case 3 (Figure 6). This integration is favourable when the equilibrium of the deacylation is shifted to the SCP side by promoting the crystallisation of β-lactam nuclei in the deacylation-crystallisation unit.
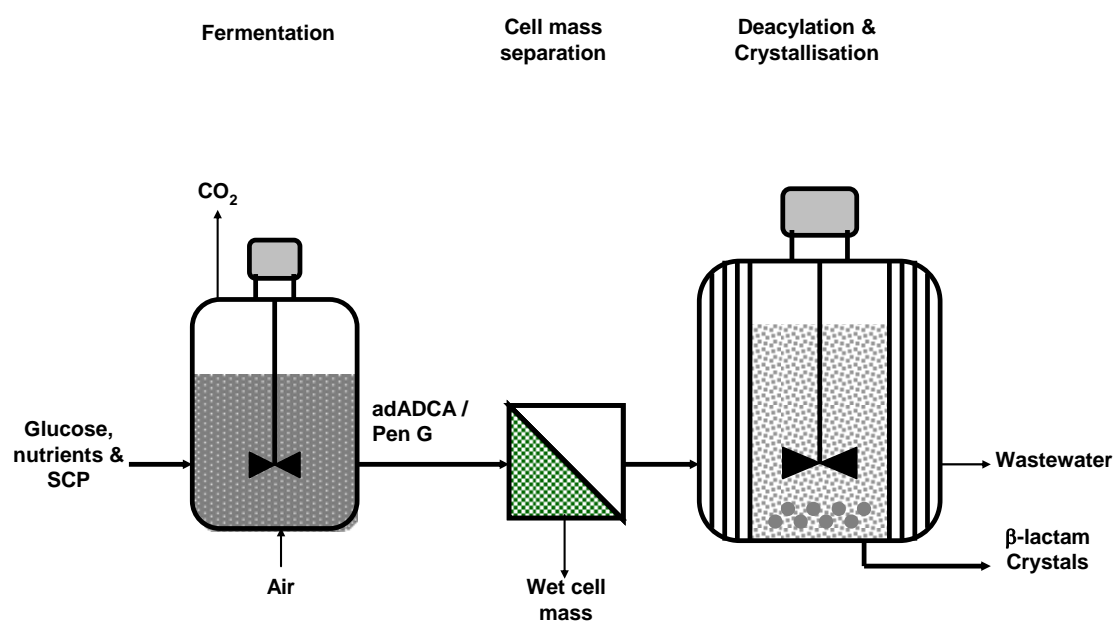

Figure 6: Process scheme for Case 3: Integration of deacylation and crystallisation units.

4.4   Case 4: Integration of fermentation, deacylation and crystallisation units.

The last integration option is the combination of fermentation, deacylation and crystallisation in one unit operation (Figure 7).

In this system, crystallisation of β-lactam nuclei is promoted by producing high concentrations of this compound in the reactor. The performance of the cell mass filtration unit is assumed to be the same as in the Case 2. In this case the potential advantages of the cases 2 and 3 (enzymatic equilibrium pulled forward by crystallisation and fermentation) are combined.
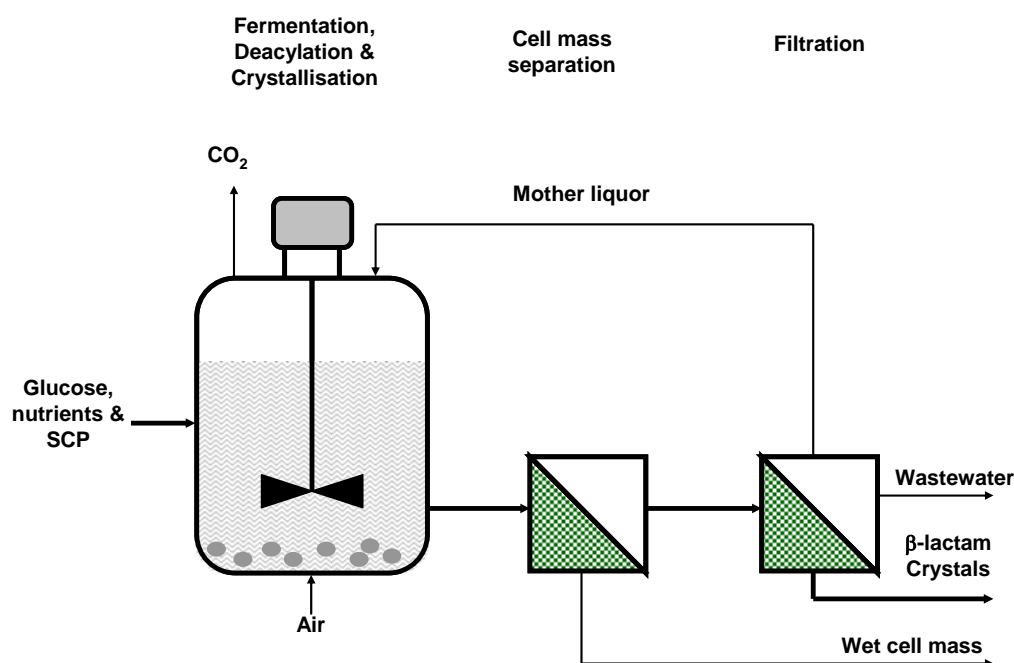

Figure 7: Process scheme for Case 4: Integration of fermentation, deacylation and crystallisation units.

5   Results and discussion

Model and economic analysis results are presented in this section. Modelling conditions and data assumed for APA and ADCA production are given in Table 7.

In the case of ADCA, for the fermentation unit, the inflow rate is fixed at a constant value after 40 hours in order to prevent oxygen limitation that is occurring after that time, according to the model

results. Moreover, a constant mass flow rate extends the production period and makes the fermentation process more productive. For the APA production, oxygen limitation problems are not present during the fermentation time. The difference in oxygen limitation values between the ADCA and the APA process is mainly due to the fact that growth rates used for the fermentation unit are different as was mentioned in section 3.2.

It is also important to mention that the cell mass separation unit performance was modelled assuming that no product losses are taking place and that the cell mass will contain 70% of its total weight as water. The assumption of no product loss in the cell mass separator is not realistic; however, as this is assumed for all options, it is fair enough for comparison purposes. Moreover, for simplicity of further technique and economic calculations the cell mass separator is assumed to be a filter.

Table 7: Fed-batch cultivation conditions of *P. chrysogenum* and modified *P. chrysogenum* for Pen G and adADCA production (pH 6, 25 °C).

Unit	Parameters	value
Fermentation	$M_{(0)}$ (kg)	300,000
	Aeration rate (m^3 of air/m^3 of reactor/min)	3
	$C_{x(0)}$ (C-mol/kg)	0.15
	$C_{s,in}$ (mol/kg)	2.5
	$C_{SCP(0)}$ (mol/kg) [a]	0.054
	Fermentation time (h)	90
Deacylation	$CE_{(0)}$ (%w/w)	0.01

a) This value applies only for the Base Case, Case 1 and Case 3.

5.1   Model results for APA production

Evaluation of different integrated options showed that there is not an economically and technically feasible integrated alternative for APA production (data not shown), due to the fact that none of the cases has better yields than the Base Case.

Amongst Case 1 – 4, Case 2 has the better production yield values, but still not better than the Base Case. Case 2 and 4 suffer from APA degradation by carboxylation to HPA. Figure 8 shows that the final HPA concentration is around 10% of the total final concentration of APA. As CO_2 is always

present as a by-product during the fermentation, no option was found to reduce the amount of HPA that is formed in this process. Cases 1 and 3 do not have carboxylation problems. However, production yields are not better than for Cases 2 and 4 because the pH value of 6 affects the performance of the deacylation and crystallisation units quite severely.

5.2   Model results for ADCA production

A preliminary evaluation of the fed-batch system for the integration of fermentation and deacylation units, which is the first step of Case 2, was done for ADCA production in order to check if degradation would occur like for APA (Figure 8). Fed-batch systems for ADCA and APA were simulated using the same models equations. The model parameters were also similar with the exception of the optimal growth rate (μ), production rate (q_p), substrate-product yield (Y_{sp}) and substrate-biomass yield (Y_{sx}), which were different for Pen G and adADCA fermentations (see Table 1).
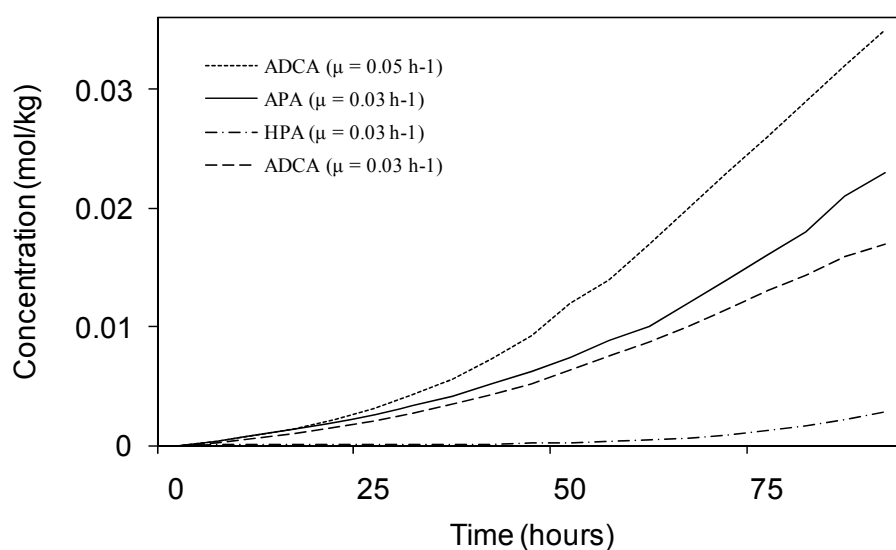

Figure 8: Modelling results of fermentation and deacylation for producing APA with HPA as a side product at $\mu = 0.03$ h^{-1} and for ADCA ($\mu = 0.05$ h^{-1} dotted line; $\mu = 0.03$ h^{-1} dashed line) in fed-batch systems (Conditions described in Table 1).

According to this preliminary evaluation, the product concentration in this fed-batch is higher for ADCA than for APA when the fermentation is run at different specific growth rate. The success of production of ADCA under these conditions is mainly due to the absence of a carboxylation reaction for ADCA. On the other hand, when ADCA is produced under fermentation conditions at the same

specific growth rate used for APA production, the production of ADCA is lower than for APA (see Figure 8, dashed line). This is due to the fact that ADCA maximum production rate is reached when the specific growth rate is around 0.05 h^{-1}. Therefore, for ADCA production the specific growth rate has to be kept at this value, which is the optimal growth rate. Moreover, besides the influence of the growth rate in the production of the β-lactam compound, the production rate equation for each antibiotic is also different. Therefore, the performance of the fermentation process not only depends of the influence of growth rate value in the production rate but also in the capacity of *P. chrysogenum* to convert glucose into the β-lactam antibiotic. Finally, as ADCA is not carboxylated, several integrated process options proposed in section 4 are attractive for ADCA production. The four options are evaluated using the model described in section 3.

After evaluating all the options for ADCA production, it can be seen in Table 8 that the Base Case and Case 2 are the ones with higher product on substrate yield according to the model results. Although the Base Case has a higher yield than Case 2, the yield difference between them is very small, making Case 2 an interesting option as well.

Table 8: Process options evaluation for ADCA production

Option	Y_{sp} (kg ADCA/kg glucose)
Base case [a]	0.024
Case 1 [b]	0.017
Case 2 [b]	0.023
Case 3 [b]	0.017
Case 4 [b]	0.014

a) Optimum pH value for each unit (Fermentation 6.2; hydrolysis 8; crystallisation 4)
b) All units operations at pH 6.

The major reason for the good performance of Case 2 is that as AA is consumed by *P. chrysogenum* the deacylation reaction equilibrium shifts to the side of ADCA. This phenomenon, which can happen only when fermentation and deacylation are occurring in the same unit operation, leads to an increment in the yield of the overall process. Despite that Case 4 also profits from this phenomenon, the amount of crystals produced is low because the solubility at pH 6 affects the crystal yield.

Figures 9 and 10 provide mass balance results for the Base Case and Case 2 (for one batch). These figures reveal that the Base Case has one more unit operation and consumes 93% more AA than

Case 2. In addition, the Base Case produces waste salts due to the pH shifting between units, which is a situation that does not occur in Case 2 (data not included in figures 9 and 10). Besides, if in Case 2 the crystallisation works at its optimal pH value (pH = 4), where the solubility is low, instead of at pH = 6, the crystallisation performance would improve. Therefore a modified Case 2, called Case 2-B, with crystallisation working at pH 4, was modelled and compared to the Base Case and the initial Case 2, now called Case 2-A. The new pH condition in the Case 2-B promotes crystal growth, making the residence time lower and hence fewer units are required (see Table 9). Waste salts will be also produced in Case 2, but they will nonetheless be smaller than in the Base Case (50% less).
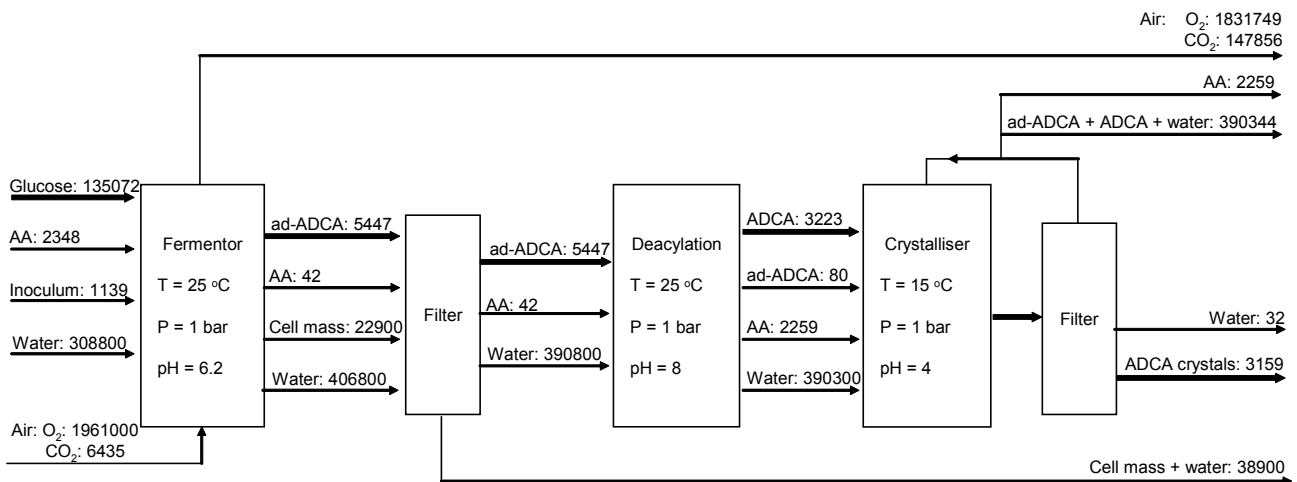
Figure 9: Block Scheme diagram for the Base Case (kg/batch; batch time: 90 hours).
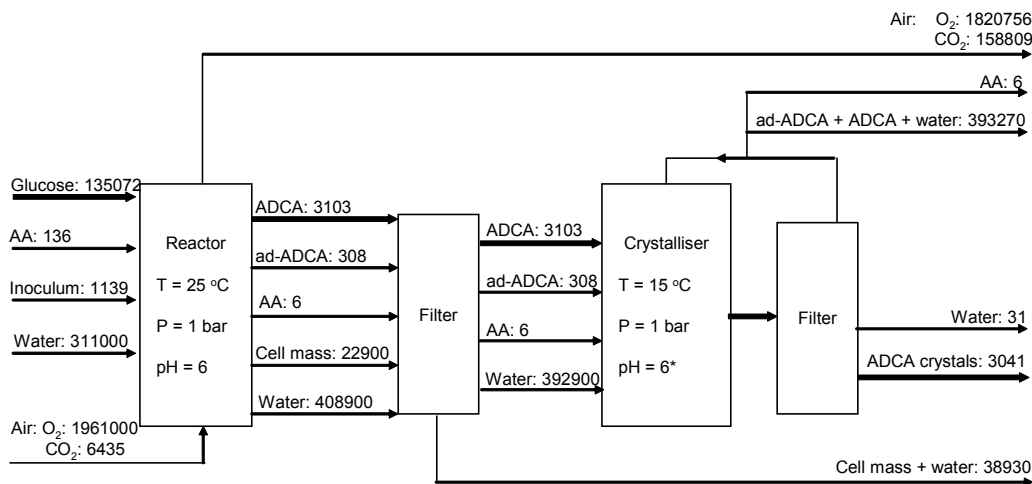
Figure 10: Block Scheme diagram for Case 2-A & 2-B (kg/batch; batch time: 90 hours). *pH value of 6 applies for Case 2-A and pH value of 4 for Case 2-B.

Table 9 summarises the main specifications and dimensions of the main equipment used for each case.

The main disadvantage of Case 2-A and 2-B with respect to the Base Case is the fact that ADCA crystals are formed in the fermentor for these first two cases and those crystals can interfere with the cell mass separation unit. This issue was not taken into account for the model calculations. So, it was assumed that cell mass can easily be separated from the crystal suspension, but additional studies will be required to support this assumption.

Table 9: Equipment specification for Base Case, Case 2-A and Case 2-B.

Case	Specification	Fermentor	Deacylation reactor	Crystalliser
Base Case	Volume (m^3)	500	450	370
	Number	7	1	1
	Residence time (h)	90	10	9
Case 2-A	Volume (m^3)	500	Coupled with	370
	Number	7	fermentation	16
	Residence time (h)	90		212
Case 2-B	Volume (m^3)	500	Coupled with	370
	Number	7	fermentation	1
	Residence time (h)	90		9

Case 2-A. Crystallisation operating at pH 6.
Case 2-B. Crystallisation operating at pH 4.

The main disadvantage of Case 2-A and 2-B with respect to the Base Case is the fact that ADCA crystals are formed in the fermentor for these first two cases and those crystals can interfere with the cell mass separation unit. This issue was not taken into account for the model calculations. So, it was assumed that cell mass can easily be separated from the crystal suspension, but additional studies will be required to support this assumption.

5.3 Economic evaluation

To complete the feasibility comparison between the different process options for ADCA production, an economic analysis was performed. This took into account the cost of the main units of the process (reactors, crystallisers and filters), main raw material for ADCA production (glucose,

acid, base, nutrients and enzyme) and utilities costs for the operation of the main units (energy and cooling water).

The cost of the main equipment was calculated according to Peters & Timmerhaus (2003) and www.matche.com correlations. The correlations of Peter & Tmmerhaus (2003) were extrapolated to sizes outside the correlation limits. However, the prices obtained with these correlations were compared to the correlations derived from the prices list found in www.matche.com, which has a higher size range (see Appendix 2). The correlation exponents of the two sources were very similar, which indicates that the extrapolation done from Peter & Timmerhaus (2003) is quite realistic. Raw material prices are presented in Appendix 2. The ADCA selling price was assumed to be 30 euro/kg. For the calculation of the utilities costs, an energy price of 60 euro/MWh and a cooling water price of 2.5 euro/ton were assumed. Appendix 2 shows utilities amounts and cost for the three cases. Furthermore, to evaluate the impact of waste salts production in every case a waste salt disposal price of 40 euro/ton was assumed and included in the raw material costs.

The fixed capital investment (FCI) was calculated with an assumed percentage of the total main units cost (Peter & Tmmerhaus 2003). The details of the FCI calculation are presented in Table 10.

Table 10: Fixed Capital Investment for ADCA process options

Item	Cost (euro[a])		
	Base Case	Case 2-A	Case 2-B
Total direct plant cost [b]	14,672,119	21,983,081	12,699,677
Total indirect plant cost [c]	9,413,528	14,104,189	8,148,023
Fixed capital investment (FCI)	**24,085,647**	**36,087,270**	**20,847,700**
Working capital (20% FCI)	4,817,129	7,217,454	4,169,540
Start up (8% FCI)	1,926,851	2,886,982	1,667,816
Total Capital Investment	*30,829,628*	*46,191,706*	*26,685,056*

a) Euro rate 2nd quarter 2006.

b) Includes: purchased equipment (PE), installation equipment (20% PE), instrumentation (25% PE), piping (20% PE), electrical (5% PE), buildings (8% PE), yard improvements (20% PE) and services facilities (28% PE).

c) Includes: engineering and supervision (32% PE), construction expenses (20% PE), legal expenses (4% PE), contractors fee (19% PE) and contingency (70% PE).

Table 10 shows that the purchased equipment is considerably higher for Case 2-A than for the other two options, because more crystallisers are involved (Table 9). The equipment cost difference

between the Base Case and Case 2-B is caused by the fact that the Base Case requires a deacylation unit and Case 2-B does not.

The Total Manufacturing Cost (TMC) was calculated with an assumed percentage of the product cost (Peter & Tmmerhaus 2003). The product cost includes raw materials, utilities, labour cost and supervision. The amount of raw material and utilities requirements for each option was calculated according to the mass balances presented in Figures 9 and 10. A detailed description of the calculation of the manufacturing cost is presented in Appendix 2.

As was mentioned before, the calculation of the TMC is highly dependent on the cost of raw materials and utilities. Table A.4 shows that Case 2-A is the one with higher utilities cost and Table A.1 shows that the Base Case is the one with higher raw material cost. Consequently, those two cases are the ones with higher TMC cost (Table A.5). In Case 2-A, utilities costs are higher because this case is the one with more crystallisation units, causing this case to consume more energy and cooling water. In the Base Case, the raw material costs are higher due to the fact that in this case the AA that is released by the deacylation cannot be used by the fermentation and thus consumes new AA for every batch.
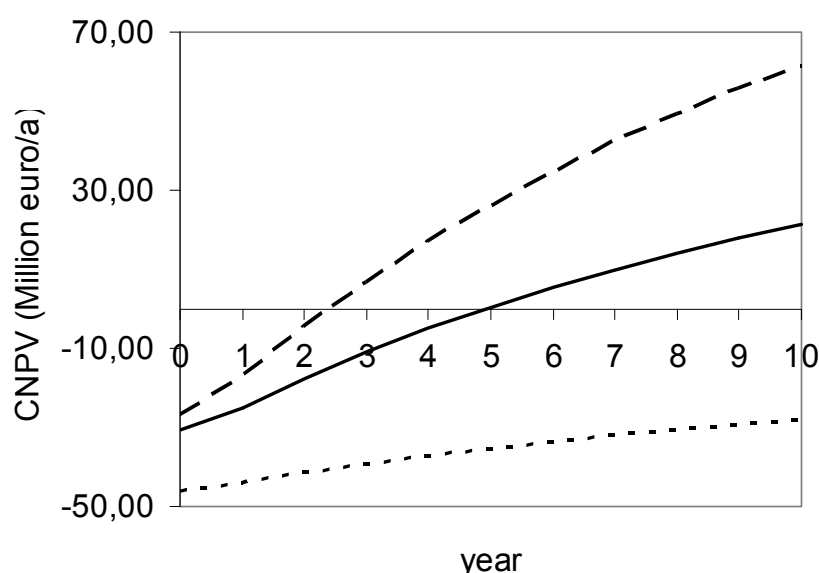

Figure 11: Comparison of cumulative net present value (CNPV) for Base Case (full line), Case 2-A (dotted line) & Case 2-B (dashed line).

Economic indicators used in this study to compare the performance of the different options under evaluation are pay-out time, discounted cash flow rate of return (DCFROR) and cumulative net

present value (CNPV). Calculated results for the economic evaluation are presented in Table 11 and graphically represented in Figure 11.

As can be seen in Figure 11, the CNPV is higher for Case 2-B than for the other two options. This is due to the fact the TMC and the total capital investment values are lower for Case 2-B. It is clear from Table 11 that Case 2-B is the one with a better economic performance among the three options with a DCFROR of 49.5 % and a pay-back time of 2.4 years. Thus Case 2-B is the best configuration for ADCA production and is interesting for experimental studies.

Table 11: Economic criteria

Criteria	Base Case	Case 2-A	Case 2-B
Pay-back time (years)	5	-	2.4
DCFROR (%)	23.7	-	49.5

Depreciation is yearly 10 % of the total capital investment; tax rate is 30 %; interest rate is 10 %.
Taxation is also included during the investment period.

Furthermore, the influence of the glucose price, equipment cost and ADCA selling price has been analysed for the chosen option. The selling price is the economic factor which has most influence on the economic feasibility of the process, according to the DCFROR (Figure 12) and the pay-back time (similar course, data not shown).
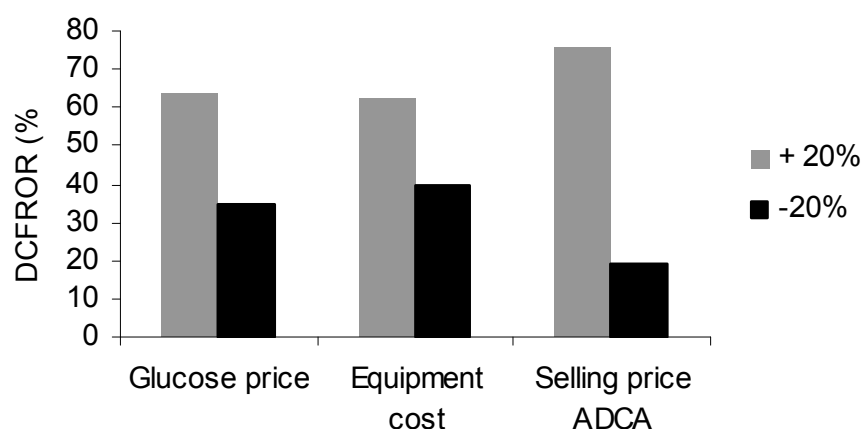

Figure 12: Sensitivity analysis for the DCFROR in Case 2-B

Finally, increasing or decreasing important process variables like the fermentation production rate by 20% will affect the feasibility of the process as well. The production rate will affect not only the

consumption of raw materials but also the equipment sizes due to the fact that the process efficiency is depending of this rate.

6   Conclusions

A conceptual process design approach has been successfully applied to find an interesting new integrated process concept for β-lactam antibiotics production. The suggested process integrates fermentation and deacylation at pH 6 with product removal by crystallisation. For ADCA the integrated process showed better performance than for APA, despite that for ADCA fermentation step lower yields and productivities were considered.
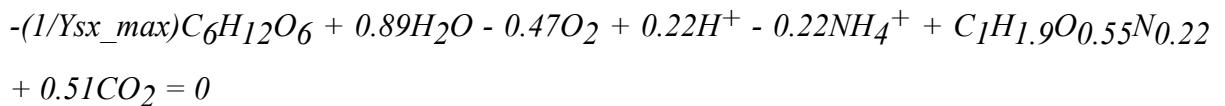
Industrial processes for ADCA and APA production nowadays use strains with higher productivities and yields. However, data for these strains have not been reported. It will be interesting for the near future to evaluate the proposed process for the current industrial strains.

Appendix 1

Stoichiometric equations for the fermentation model
- Growth equations:
- *Penicillium chrysogenum*

$$-(1/Ysx\_max)C_6H_{12}O_6 + 0.89H_2O - 0.47O_2 + 0.22H^+ - 0.22NH_4^+ + C_1H_{1.9}O_{0.55}N_{0.22} + 0.51CO_2 = 0$$

- Genetically modified *Penicillium chrysogenum*

$$-(1/Ysx\_max)C_6H_{12}O_6 + 1.255H_2O - 0.84O_2 + 0.22H^+ - 0.22NH_4^+ + C_1H_{1.9}O_{0.55}N_{0.22} + 0.875CO_2 = 0$$

- Product equations:
- Pen G

$$-(1/Ysp\_max)C_6H_{12}O_6 - 1C_8H_7O_2^- + 31.33H_2O - 2NH_4^+ - SO_4^{2-} + 2H^+ + C_{16}H_{17}O_4N_2S^- + 25.33CO_2 - 23.33O_2 = 0$$

- adADCA

$$(1/Ysp\_max)C_6H_{12}O_6 - 1C_6H_9O_4^- + 54.55H_2O - 2NH_4^+ - SO_4^{2-} + C_{14}H_{17}O_6N_2S^- + 46.55CO_2 - 45.55O_2 = 0$$
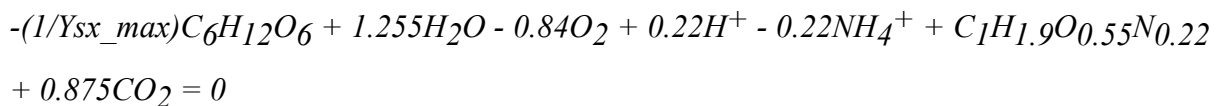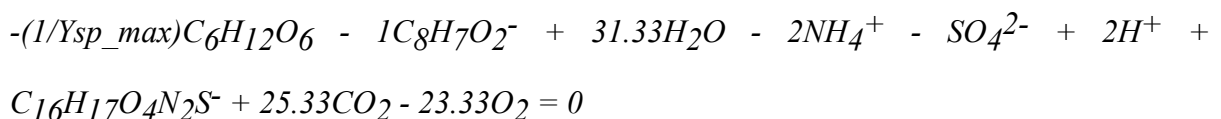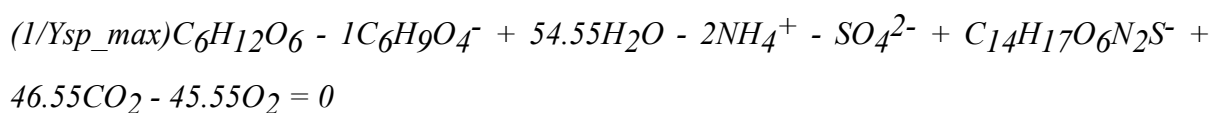
- Maintenance equation

$-1C_6H_{12}O_6 - 6O_2 + 6H_2O + 6CO_2 = 0$

Consumption and production rates

- Pen G fermentation process:

$q_{O_2} = -0.47\mu - 23.33q_{PenG} - 6m_s$

$q_{NH_4^+} = -0.22\mu - 2q_{PenG}$

$q_{SO_4^{-2}} = -q_{PenG}$

$q_{CO_2} = 0.51\mu + 25.33q_{PenG} + 6m_s$

$q_{H_2O} = 0.89\mu + 31.33q_{PenG} + 6m_s$

$q_{H^+} = 0.22\mu - q_{PenG}$

$q_{PAA} = -q_{PenG}$

- adADCA fermentation process:

$q_{O_2} = -0.84\mu - 45.55q_{adADCA} - 6m_s$

$q_{NH_4^+} = -0.22\mu - 2q_{adADCA}$

$q_{SO_4^{-2}} = -q_{adADCA}$

$q_{CO_2} = 0.87\mu + 46.55q_{adADCA} + 6m_s$

$q_{H_2O} = 1.25\mu + 54.55q_{adADCA} + 6m_s$

$q_{H^+} = 0.22\mu$

$q_{AA} = -q_{adADCA}$

- Oxygen and carbon dioxide flows in the broth:

$\Phi_{O_2} = 0.032 \cdot \Gamma_{O_2}$

$\Phi_{CO_2} = 0.044 \cdot \Gamma_{CO_2}$

$\Gamma_{O_2} = \frac{1}{4}\left(\gamma_S \cdot q_s \cdot C_X + \gamma_{SCP} \cdot q_{SCP} \cdot C_X - \gamma_X \cdot \mu \cdot C_X - \gamma_{product} \cdot q_{product} \cdot C_X\right)$

$\Gamma_{CO_2} = \left(6 \cdot q_s \cdot C_X + \alpha \cdot q_{SCP} \cdot C_X - \mu \cdot C_X - \beta \cdot q_{product} \cdot C_X\right)$

Where α and β are the numbers of the carbons in the SCP and product, respectively.

Appendix 2

- Equipment size calculation:

The following equation which is a correlation derived from a log-log plot of the equipment size vs. capacity, was used to calculate the equipment prices.[43] Cost references were taken from www.matche.com.

$$Cost(equip.a) = Cost(equip.b) \cdot \left(\frac{capac.equip.a}{capac.equp.b} \right)^{exp}$$

The exponents according to each equipment are summarised in the following table.

Table A.1: Exponents for equipment cost vs. capacity

Equipment	Range	Exponent	Reference
Fermentor	$2 - 40 \ m^3$	0.50	www.matche.com
Reactor	$0.2 - 3 \ m^3$	0.54	Peters and Timmerhaus, 2003
Crystalliser	$14 - 200 \ m^3$	0.37	Peters and Timmerhaus, 2003
Filter	$1 - 74 \ m^2$	0.40	www.matche.com

- Economic calculation data

Table A.2: Raw material prices

Raw material	Price (euro/kg)
Glucose	0.30 [a]
Adipic acid	1.5 [b]
Enzyme	1000 [c]
Base (NaOH)	0.058 [b]
Acid (H_2SO_4)	0.060 [b]

a) http://www.ers.usda.gov/briefing/sugar/data., for 2nd quarter of 2006
b) http://www.chemicalmarketreporter.com, 17-23 April 2006
c) The enzyme is assumed to be replaced twice per year

Table A.3: Glucose and AA description for the Base case, Case 2-A and Case 2-B

Case	Glucose		AA	
	Ton/a	euro/a	Ton/a	euro/a
Base Case	77,531	23,259,300	1,509	1,765,530
Case 2-A	77,531	23,259,300	88	102,960
Case 2-B	77,531	23,259,300	88	102,960

Table A.4: Utilities description for the Base case, Case 2-A and Case 2-B

Case	Energy		Cooling water	
	MWh/a	euro/a	Ton/a	euro/a
Base Case	1,037	62,220	370,000	925,000
Case 2-A	22,808	1,368,480	4,000,000	10,000,000
Case 2-B	1,300	78,000	300,000	750,000

Table A.5: Total Manufacturing Cost

Direct production cost	Calculation	Cost (euro/a)		
		Base Case	Case 2-A	Case 2-B
Operating labour	Calculation [a]	528,000	858,000	462,000
Direct supervisory & clerical labour	Calculation [b]	79,200	128,700	69,300
Maintenance and repairs	1% PC [c]	281,270	370,174	261,216
Operating supplies	10% PC	2,812,701	3,701,744	2,612,156
Laboratory charges	10% PC	2,812,701	3,701,744	2,612,156
Patents and royalties	2% PC	562,540	740,349	522,431
Raw materials	Table A.3	26,532,593	24,662,260	24,762,260
Utilities	Table A.4	987,220	11,368,480	828,000
Fixed charges	17% PC [d]	3,974,132	5,954,400	3,439,871
Plant overhead	Calculation [e]	621,929	949,812	554,761
Total production cost (TPC)		36,192,287	52,435,663	36,124,150
General expenses	10% TPC	3,919,229	5,243,566	3,612,415
Total manufacturing cost		43,111,515	57,679,229	39,736,565

a) Calculated base on one technician is required per equipment. Penalva et al. 1998

b) 15 % of the operating labour

c) PC (product cost) = Labour cost + supervision/clerical + plant overhead + raw materials + utilities

d) Includes: local taxes (1% PC), insurance (1% PC), depreciation (10% PC) and interest (5 % PC)

e) 70 % of operation labour + supervision and clerical + maintenance and repairs

Acknowledgments

Nomenclature:

C: concentration

E: Enzyme mass fraction

G: crystal growth rate

ΔG^o_c: standard Gibbs energy change

K: equilibrium constant

k: kinetic constant

k_d: degradation rate constant

k_g: growth rate constant

K_m: Michaelis-Menten constant

K_s: Monod constant

M: broth weight

m_s: maintenance coefficient

q: cell mass specific production rate

R: universal gas constant

s: supersaturation ratio

S: solubility

S_o: intrinsic

T: temperature

Y_{sx}: yield of biomass on substrate

Y_{sp}: yield of product on substrate

Greek:

γ: degree of reduction

Γ: broth mass specific production rate

μ: growth rate

Φ: flow rate

Subscripts:

(0): value at the time 0

AA: adipic acid

ADCA: 7-aminodeacetoxycephalosporanic acid

APA: 6-aminopenicillanic acid

adADCA: adipyl-7-aminodeacetoxycephalosporanic acid

app: apparent

cat: catalyst

HPA: 8-hydroxy-penicillic acid

In: inflow value

max: maximum

PAA: Phenylacetic acid

Pen G: Penicillin G

SCP: Side chain precursor

s: Substrate (Glucose)

th: theoretical

tot: total

x: Biomass

References

Adrio JL, Cho H, Piret JM, Demain AL (1999) Inactivation of deacetoxycephalosporin C synthase in extracts of *Streptomyces clavuligerus* during bioconversion of penicillin G to deacetoxycephalosporin G. Enzyme Microb Technol (25) 497.

Bajpai RK and Reuβ M (1980) A mechanistic model for Penicillin production. J Chem Tech Biotechnol (30) 332.

Berezin IV, Klyosov AA, Margolin AL, Nys PS, Savitskaya EM, Švedas VK (1976) Study of Penicillin amidases from *E. coli*, pH dependent equilibrium constants of benzylpenicillin fermentative hydrolysis. Antibiotild (21) 511.

Bruggink A (2001) Synthesis of β-lactam antibiotics. *Chemistry, biocatalysis and process integration*. Kluwer Academic Publishers. Dordrecht, The Netherlands.

Buque-Taboada EM, Straathof AJJ, Heijnen JJ, van der Wielen LAM (2006) In situ product recovery (ISPR) by crystallization: basic principles, design, and potential applications in whole-cell biocatalysis. Appl Microbiol Biotechnol (71) 1.

Cantwell C, Beckmann R, Whiteman P, Queener SW, Abraham EP (1992) Isolation of deacetoxycephalosporin C from fermentation broths of *Penicillium chrysogenum* transformants: construction of a new fungal biosynthetic pathway. Proc R Soc Lond B Biol Sci (248) 283.

Cho H, Adrio JL, Luengo JM, Wolfe S, Ocran S, Hintermann G, Piret JM, Demain AL (1998) Elucidation of conditions allowing conversion of penicillin G and other penicillins to deacetoxycephalosporins by resting cells and extracts of *Streptomyces clavuligerus* NP1. Appl Biol Sci (95) 11544.

Crawford L, Stephan AM, McAda PC, Rambosek A, Conder MJ, Vinci VA, Reeves CR (1995) Production of cephalosporin intermediates by feeding adipic acid to recombinant *Penicillium chrysogenum* strains expressing ring expansion activity. Bio/Technology (13) 58.

Christensen LH, Henriksen CM, Nielsen J, Villadsen J, Egel-Mitani M (1995) Continuous cultivation of *Penicillium chrysogenum*. Growth on glucose and penicillin production. J Biotechnol (42) 95.

Dennen DW (1967) Degradation kinetics of 6-Aminopenicillanic acid. J Pharm Sci (56) 1273.

Diender MB, Straathof AJJ, van der Wielen LAM, Ras C, Heijnen JJ (1998) Feasibility of the thermodynamically controlled synthesis of Amoxicillin. J Mol Catal B: Enzym (5) 249.

Diender M, Straathof AJJ, van der Does T, Ras C, Heijnen JJ (2002) Equilibrium modelling of extractive enzymatic hydrolysis of penicillin G with concomitant 6-aminopenicillanic acid precipitation. Biotechnol Bioeng (78) 395.

Douglas JM (1988) *Conceptual design of chemical processes*. International edition. McGraw-Hill Book Company, New York.

Ferreira JS, Straathof AJJ, Franco TT, van der Wielen LAM (2004) Activity and stability of immobilized penicillin amidase at low pH values. J Mol Catal B- Enzim (27) 29.

Ferreira JS, Straathof AJJ, Li XN, Ottens M, Franco TT, van der Wielen LAM (2006) Solution crystallization kinetics of 6-aminopenicillanic acid. Ind Eng Chem Res (45) 6740.

van Gulik WM, de Laat WTAM, Vinke JL, Heijnen JJ (2000) Application of metabolic flux analysis for the identification of metabolic bottlenecks in the biosynthesis of penicillin-G. Biotechnol Bioeng (68) 602.

van Gulik WM, Antoniewicz MR, de Laat WTAM, Vinke JL, Heijnen JJ (2001) Energetics of growth and penicillin production in a high-producing strain of *Penicillium chrysogenum*. Biotechnol Bioeng (72) 185.

Heijnen JJ, Roels JA, Stouthamer AH (1979) Application of balancing methods in modeling the Penicillin fermentation. Biotechnol Bioeng (21) 2175.

Heijnen JJ, Terwisscha van Scheltinga AH, Straathof AJJ (1992) Fundamental bottlenecks in the application of continuous bioprocesses. J Biotech (22) 3.

Henriksen CM, Holm SS, Schipper D, Jørgensen HS, Nielsen J (1997) Villadsen, J. Kinetic studies on the carboxylation of 6-amino-penicillanic acid to 8-hydroxy-penillic acid. Process Biochem (32) 85.

Jingkang W and Yue L (2003) Semi-batch crystallisation of 7-Amino-desacetoxycephalosporanic acid. Chin J Chem Eng (11) 399.

Jørgensen H, Nielsen J, Villadsen J (1995) Metabolic flux distributions in *Penicillium chrysogenum* during fed-batch cultivations. Biotechnol Bioeng (46) 17.

Kramer HJM, Bermingham SK, van Rosmalen GM (1999) Design of industrial crystallisers for a given product quality. J Cryst Growth (198/199) 729.

Kheirolomoom A, Kazemi-Vaysari A, Ardjmand M, Baradar-Khoshfetrat A (1999) The combined effects of pH and temperature on penicillin G decomposition and its stability modeling. Process Biochem (35) 205.

Kohsaka M, Demain AL (1976) Conversion of penicillin N to cephalosporins by cell-free extracts of Cephalosporium acremonium. Biochem Biophys Res Commun (70) 465.

Nys PS, Abramova EE, Koligina TS, Savitskaya EM (1977) Acid-base equilibrium of D-α-aminophenylacetic acid. Antibiotiki (22) 405.

Penalva MA, Rowlands RT, Turner G (1998) The optimization of penicillin biosynthesis in fungi. Trends Biotechnol (16) 483.

Peters, M. S. and Timmerhaus, K. D. *Plant design and economics for chemical engineers.* 5th ed.; Mc Graw Hill: Boston, 2003.

Robin J, Jakobsen M, Beyer M, Noorman H, Nielsen J (2001) Physiological characterisation of *Penicillium chrysogenum* strains expressing the expandase gene from *Streptomyces clavuligerus* during batch cultivations. Growth and adipoyl-7-aminodeacetoxycephalosporanic acid production. Appl Microbiol Biotechnol (57) 357.

Robin J, Bruheim P, Nielsen ML, Noorman H, Nielsen J (2003) Continuous cultivations of a *Penicillium chrysogenum* strain expressing the expandase gene from *Streptomyces clavuligerus*: Kinetics of adipoyl-7-aminodeacetoxycephalosporanic acid and by-product formations. Biotechnol Bioeng (83) 353.

van de Sandt EJAX (2005) Process intensification in a fermentation production process: a new direct fermentation route to an antibiotic intermediate. Sustainable (Bio)Chemical Process Technology, Incorporating the 6th International Conference on Process Intensification, Delft, the Netherlands. BHR Group Limited. Jansens, P.; Stankiewicz, A.; Green. A. The Fluid Engineering Centre. Cranfield, United Kingdom. pp 271.

Seider WD, Seader JD, Lewin DR (1999) *Process design principles, synthesis, analysis and evaluation*. John Wiley & Sons, Inc. New York.

Schroën CGPH, van de Wiel S, Kroon PJ, DeVroom E, Janssen AEM, Tramper J (2000) Equilibrium position, kinetics, and reactor concepts for the adipyl-7-ADCA hydrolysis process. Biotechnol Bioeng (70) 654.

Schroën CGPH, Nierstrasz VA, Bosma R, Dijkstra ZJ, van de Sandt EJAX, Beeftink HH, Tramper J (2002) Process design for enzymatic adipyl-7-ADCA hydrolysis. Biotechnol Progr (18) 745.

Schroën CGPH, Nierstrasz VA, Bosma R, Kroon PJ, Tjeerdsma PS, de Vroom E, van der Laan JM, Moody HM, Beeftink HH, Janssen AE, Tramper J (2002) Integrated reactor concepts for the enzymatic kinetic synthesis of Cephalexin. Biotechnol Bioeng (80) 144.

Spieß A, Schlothauer RC, Hinrichs J, Scheidat B, Kasche V (1999) pH Gradients in Immobilized amidases and their influence on rates and yields of β-lactam hydrolysis. Biotechnol Bioeng (62) 267.

Švedas VK, Margolin AL, Borisov IL, Berezin IV (1980) Kinetics of the enzymatic synthesis of benzylpenicillin. Enzyme Microb Technol (2) 313.

Swinkels PLJ, van der Weijden RD, Ajah AN, Arifin Y, Loe HL, Manik MH, Siriski I, Reuter MA (2004) Conceptual process design as a prerequisite for solving environmental problems; a case study of molybdenum removal and recovery from wastewater. Miner Eng (17) 205.

Tewari YB, Goldberg RN (1988) Thermodynamics of the conversion of penicillin G to phenylacetic acid and 6-aminopenicillanic acid. Biophys Chem (29) 245.

Weast RC (1971) editor. *Handbook of chemistry and physics*; The Chemical Rubber Company: Cleveland. USA.

van der Wielen LAM, van Buel MJ, Straathof AJJ, Luyben KCHAM (1997) Modelling the enzymatic deacylation of Penicillin G: equilibrium and kinetic considerations. Biocatal Biotransform (15) 121.

Yamana T, Tsuji A (1974) Kanayama, K; Nakano, O. Comparative stabilities of cephalosporins in aqueous solution. J Antibiot (27) 1000.

Yamana T, Tsuji A (1976) Comparative stability of cephalosporins in aqueous solution: Kinetics and mechanisms of degradation. J Pharm Sci (65) 1563.

CHAPTER 7

Outlook and concluding remarks

In this thesis, recovery of fumaric acid and 7-aminodeacetoxycephalosporanic acid (7-ADCA) by direct cooling crystallisation from fermentation broth was studied. It was proven at lab scale that fumaric acid can be produced via fermentation using integrated recovery by cooling crystallisation enhancing then productivities and yields during the fermentation. In the case of 7-ADCA the product recovery was not experimentally proven but predicted using a detailed model showing the fermentation and deacylation can be coupled and cooling crystallisation can be applied to recover the final product after cell removal. In general, this research has contributed to extend the application of crystallisation as a direct recovery technique in the fermentative production of chemicals.

Irrespective of the verification of the integrated process for both cases, process yields are still quite low. In the case of fumaric acid, with our integrated process we could not achieve more than 20% w/w recovery of all the fumaric acid produced. Additionally, despite that our fermentation productivities and yields were not affected by shifting the pH during the batch time, our maximum yields and productivity values (at pH 4.5 – 5.0) were not as high as the ones reported previously in literature with the same strain. It was quite difficult to get uniform pellets up to 1 mm diameter size, which would allow good oxygen penetration so that the fungi could produce fumaric acid at high yields and rates. It was also not possible to avoid growth of the fungi on the stirrer, and big clumps were formed on this part of the fermentor. Because of the size of the clumps on the stirrer, the fermentation inside the clumps might be anaerobic, enhancing the production of ethanol during the fermentation at the expense of the conversion of glucose to fumarate. Furthermore, the low pH during fermentation decreases the fermentation yield and productivity compared to the performance of the fermentation at more neutral values. To overcome this problem it is recommended to metabolically engineer the strain for more resistance at low pH values.

As was shown in this thesis, CO_2 can increase fumaric acid fermentation productivities and yields only when the oxygen levels are not compromised. However, supply of CO_2 was not tested in mixtures with pure oxygen.

We also tried to understand the solubility behaviour of fumaric acid together with its sodium salts and the influence of fermentation co-solutes on them. However, the effect of different concentrations of glycerol, which is also a fermentation by-product was not tested. It was observed during the metastability experiments that the obtained glycerol fermentation titers were not affecting the solubility behaviour of fumarate at pH 3.5. Nonetheless, it is highly recommended for further studies on this topic to analyse deeply the effect of different glycerol concentrations at different pH on the fumarate solubility.

The lab scale concept developed for the recovery of fumaric acid by cooling crystallisation proved that this technique can recover the undissociated acid without any pH shift between the main operations. However, the concept developed at lab scale is a repeated batch system. A continuous process, where fumaric acid is removed in the crystallisation unit while it is being produced in the fermentation vessel might improve not only the recovery but also process yields. In addition, the integrated option to produce fumaric acid did not use a cell recovery/retention unit. The way that fungal pellets were kept into the fermentor was very simple (pellets decantation for few minutes) and implies that a cell removal unit has to be added for continuously running the system. Furthermore, the sterility has to be handled more carefully for a continuous system. In our repeated batch mode not only the fermentor but also the crystalliser and all other equipment were sterilised for the every batch. However, recovery of fumaric acid crystals from the crystalliser was done via vacuum filtration of the mother liquor, and was not a sterile procedure. This crystal recovery has to be developed in a sterile way if the process is to be performed in a continuous mode.

Advantages of product removal by crystallisation to avoid product inhibition during fermentation have been tested not only in this thesis but also in previous ISPR works (Buque-Taboada et al., 2006; Cuellar, 2008). Additional to genetic modifications in order to improve the resistance of the strain to low pH during fermentation, the evaluation of the system's window of operation to determine when product removal can be an effective solution, is mandatory as a starting procedure for ISPR research. Also, any product removal/integration study is incomplete until the scaling up of the concept is tested. Scaling up to the level of pilot plant evaluates the robustness of the process and determines whether the process can be implemented at industrial levels.

Comparing the two systems evaluated in this thesis, an important issue to address is the fact that the 7-ADCA process configurations were not evaluated experimentally and problems like the fungal morphology and the interaction of the cells with the crystals were not considered in the process model. Fungal morphology plays a very important role in the fermentation performance, as was shown for the fumaric acid case, so the production of 7-ADCA by fermentation/conversion might be affected by fungal morphology as well. In addition, for the 7-ADCA production, low pH values were assumed to decrease the yield and productivity of the fermentation and, moreover, to degrade the penicillin that is produced. Furthermore, the kind of crystals formed might play a role in the case of 7-ADCA crystallisation, like for fumaric acid crystallisation. The solubility of 7-ADCA and its sodium salts was evaluated merely with a thermodynamic model and solubility experiments were not performed and included in the 7-ADCA crystallisation calculations. To enable more detailed predictions of 7-ADCA solubility behaviour in the presence of sodium ions and of the crystal

amounts obtained by 7-ADCA cooling crystallisation, an experimental solubility study has to be performed.

In the case of the integration system for fumaric acid, we tried to find the fermentation conditions necessary to integrate with the crystallisation unit. A pH strategy was found to run the batch fermentation in a way that the desired final pH for crystallisation was obtained. In the case of the 7-ADCA system, the methodology was the opposite; we adapted the crystallisation system to the obtained fermentation/conversion results, which implied in this case a pH shift between the two units. In this case, having only cooling crystallisation, the residence time was very long getting then more crystallisation units and higher production costs. It is preferred to avoid the pH shifting between the units for the reasons given before (pH shift implies waste-salts production), then the methodology of adapting the fermentation to the desired crystallisation conditions might be preferred.

Finally, as the integration system concept is proven to work, one can think of the implementation of the same integration set up for the production of other carboxylic acids. There, it is recommended to evaluate in the first place the window of operation in detail and to study what kind of crystals might be obtained.

References

Buque-Taboada EM, Straathof AJJ, Heijnen JJ, van der Wielen LAM (2006) In situ product recovery (ISPR) by crystallization: basic principles, design, and potential applications in whole-cell biocatalysis. Appl Microbiol Biotechnol (71) 1.

Cuellar Soares MC (2008) Towards the integration of fermentation and crystallization. A study on the production of L-phenylalanine. PhD Thesis. TU Delft, Delft, The Netherlands. pp 163.

CHAPTER 8

Summary, Samenvatting

Summary

Fermentation products are gaining more attention in the last years due to the fact that the metabolic and genetic engineering field has been developing techniques to enhance fermentation yields and make biochemical processes competitive compared to traditional chemical production. However, as fermentation productivities are becoming higher, many fermentation processes suffer from product inhibition and/or toxicity. Moreover, besides the inhibition/toxicity problem, the complexity of the fermentation media makes the process recovery an important step in the development of the whole production process. In this thesis, product recovery applying crystallisation techniques was studied for two organic acids: fumaric acid and 7-aminodeacetoxycephalosporanic acid (7-ADCA).

In the case of fumaric acid one of the main problems of the conventional fermentation is that it is carried out at a pH in the range of 4.5–6.5, leading to fumarate salts instead of undissociated fumaric acid. Stoichiometric amounts of bases such as $NaOH$ and $CaCO_3$ are added during fermentation to control the pH. To recover fumaric acid, the supernatant has to be acidified, for example with stoichiometric amounts of sulphuric acid, so that undissociated fumaric acid can precipitate. Stoichiometric amounts of waste salts such as sodium or calcium sulphate are formed in this manner. A similar problem is present in the 7-ADCA production. Here the fermentation and deacylation are working in a pH range of 6.0 − 8.0 while the crystallisation recovery needs to be at pH 4.0. This implies the addition of mineral acids to decrease the pH, and hence waste salts are produced. To overcome these problems, we integrated fermentation and cooling crystallisation to recover the product. At lower temperature the fermentation product should become partly insoluble, so that it can be filtered off, thus avoiding acidification and waste salts production.

In this thesis Chapter 1 presents general aspects of the In-Situ Product Recovery (ISPR) techniques and their development as process integration tools. Additionally, a general overview of the fumaric acid and 7-ADCA systems is presented to show the concept that is developed in this research. Chapters 2-5 deal with the fumaric acid system and chapter 6 with the 7-ACDA system.

Chapter 2 reviews the production of fumaric acid by fermentation. Here the metabolism of *Rhizopus oryzae* (the strain used in this study for fumaric acid production) and the importance of CO_2 fixation in this mechanism are described. Future options for improvement in the fermentation and recovery are also discussed here.

Fermentation development for low pH values is presented in Chapter 3. This chapter shows that delay of pH control during the fermentation until a low pH has been reached at the end of the batch cycle does not affect fermentation productivities and allows the fermentation unit to be integrated with product crystallisation without pH shifting. Nonetheless, because it is very important to understand the conditions leading to crystallisation of fumaric acid or its sodium salts, the solubility behaviour of fumaric acids and its sodium salts are studied and presented in Chapter 4. The findings here showed that the integration should be performed in a pH range of 2.5 – 3.5 in order to get only fumaric acid crystals and avoid the crystallisation of one of the sodium fumarate salts.

Integration of fumaric acid production by fermentation and cooling crystallisation is proven to work in an experimental set-up that is described in Chapter 5. In this chapter it is also shown that the integration of these two units can be done while avoiding pH shifting. Consumption of neutralising agent is reduced as compared to the base case system, which uses sulphuric acid to precipitate the fumaric acid out of the fermentation broth thus reducing the associated production of waste salts. A perspective of industrial scale-up of the experimental set up is presented, showing that the studied process may become competitive at industrial levels if the some elements in the concept (like lower pH) are improved further.

In Chapter 6 the production of 7-ADCA is investigated. A new integrated process option for β-lactam nuclei production is proposed, which is an integration of fermentative production and enzymatic deacylation of adipyl-7-aminodeacetoxycephalosporanic acid (adADCA) in one reactor, thus producing 7-ADCA directly from glucose. The outcome of this study proves that according to mathematical modelling it is possible to recover 7-ADCA via cooling crystallisation and in this way the number of downstream steps can be reduced. This new process option avoids the use of mineral acids and bases for pH shifts and leads to a reduction in waste salt production.

In Chapter 7 the outlook of this thesis and recommendations for future work are presented.

Samenvatting

Fermentatieproducten komen de laatste jaren in een groeiende belangstelling te staan doordat er technieken ontworpen worden in het veld van metabolische en genetische modificatie die fermentatieopbrengsten verhogen en biochemische processen concurrerend maken met traditionele chemische productie. Als de productiviteit van fermentaties hoger wordt, beginnen inhibitie en/of toxiciteit van het eindproduct echter een limiterende rol te spelen. Daarnaast wordt de scheiding van het product uit het complexe fermentatiemedium een belangrijke stap in het gehele productieproces. In dit proefschrift is een studie uitgevoerd naar productscheiding met kristallisatietechnieken van twee organische zuren: fumaarzuur en 7-aminodesacetoxycefalosporinezuur (7-ADCA).

In het gaval van fumaarzuur is een van de grootste problemen van de gebruikelijke fermentatie dat deze uitgevoerd wordt bij een pH tussen de 4,5 en 6,5, waardoor fumaraatzout geproduceerd wordt in plaats van fumaarzuur. Om de pH te beheersen worden stoechiometrische hoeveelheden NaOH en $CaCO_3$ toegevoegd tijdens een fermentatie. Om het fumaarzuur van het medium te scheiden wordt het supernatant verzuurd, bijvoorbeeld met stoechiometrische hoeveelheden zwavelzuur, waardoor het ongedissocieerde fumaarzuur kan neerslaan. Hierdoor worden stoechiometrische hoeveelheden afvalzout gevormd zoals natrium- of calciumsulfaat. Er treedt een vergelijkbaar probleem op bij de productie van 7-ADCA. Hier worden de fermentatie en deacylering uitgevoerd tussen pH 6,0 en 8,0 terwijl de scheiding door kristallisatie bij een pH van 4,0 uitgevoerd moet worden. Daardoor moeten minerale zuren toegevoegd worden om de pH te verlagen en worden er dus afvalzouten gevormd. Om dit probleem te verhelpen hebben we het fermentatieprocess en het koelingsproces geïntegreerd om het product te scheiden. Bij lagere temperaturen moet het fermentatieproduct gedeeltelijk onoplosbaar worden, waardoor het afgefiltreerd kan worden, waardoor verzuring en afvalzoutproductie voorkomen kunnen worden.

In dit proefschrift worden in hoofdstuk 1 algemene In-Situ productverwijdering (ISPV) technieken en hun ontwikkeling als procesintegratietechniek gepresenteerd. Daarnaast wordt er een algemene beschouwing van fumaarzuur en 7-ADCA systemen gepresenteerd om het concept dat in deze studie ontwikkeld is te tonen. Hoofdstukken 2-5 gaan over het fumaarzuursysteem en hoofdstuk 6 gaat over het 7-ADCA systeem.

Hoofdstuk 2 geeft een beschouwing over fumaarzuur-productie door fermentatie. Hier worden het metabolisme van *Rhizopus oryzae* (de stam die in deze studie voor fumaarzuurproductie

gebruikt wordt) en het belang van CO_2 fixatie in dit mechanisme beschreven. Toekomstige mogelijkheden om de fermentatie en productscheiding te verbeteren worden bediscussieerd.

Fermentatie-ontwikkelingen bij lage pH waarden worden gepresenteerd in hoofdstuk 3. Dit hoofdstuk laat zien dat een vertraging van de pH beheersing tijdens de fermentatie tot een lage pH bereikt is geen effect heeft op de fermentatieproductiviteit and hierdoor kan de fermentatie-eenheid geïntegreerd worden met productkristallisatie zonder pH aanpassing. Omdat het erg belangrijk is om de condities die tot kristallisatie van fumaarzuur tot zijn natriumzout leiden te begrijpen, wordt het oplosbaarheidgedrag van fumaarzuur en zijn natriumzout bestudeerd en gepresenteerd in hoofdstuk 4. De bevindingen lieten zien dat integratie moet worden uitgevoerd bij pH waarden tussen de 2,5 en 3,5 om alleen maar fumaarzuurkristallen te krijgen en te voorkomen dat een van de natriumzouten van fumaraat kristalliseert.

Integratie van fumaarzuur en productie door fermentatie en kristallisatie door koeling worden bewezen in een experimentele opstelling die beschreven wordt in hoofdstuk 5. In dit hoofdstuk wordt ook getoond dat integratie van deze twee onderdelen uitgevoerd kan worden zonder de pH te veranderen. Consumptie van neutralisatiestoffen wordt verminderd vergeleken met het base systeem, waarin fumaarzuur met zwavelzuur wordt geprecipiteerd uit het fermentatiebeslag waardoor minder afvalzout wordt geproduceerd. Een industriëel opschalingperspectief van deze experimentele opstelling wordt gepresenteerd, dat laat zien dat het bestudeerde proces concurrerend kan worden op industriëel niveau als sommige elementen uit het concept (zoals lagere pH waarden) verbeterd worden.

In hoofdstuk 6 wordt productie van 7-ADCA bestudeerd. Een nieuwe geïntegreerde procesoptie voor productie van β-lactam kernen wordt voorgesteld, die bestaat uit integratie en enzymatische deacylering van adipyl-7-aminodesacetoxycefalosporinezuur (adADCA) in één reactor, waardoor 7-ADCA direct uit glucose geproduceerd wordt. De uitkomst van deze studie bewijst dat volgens het mathematische model de scheidingsstappen beperkt kunnen worden. Deze nieuwe procesoptie voorkomt het gebruik van minerale zuren en bases om de pH te beheersen en zorgt voor een beperking van de hoeveelheid geproduceerd afvalzuur.

In hoofdstuk 7 worden de discussie van dit proefschrift en de aanbevelingen gepresenteerd.

CHAPTER 9

Curriculum Vitae, Publications,
Acknowledgements

Curriculum Vitae

Carol Andrea Roa Engel was born on 22th of January 1977 in Bogotá, Colombia. In 1993 she completed her high school studies and graduated from Colegio Nuestra Señora del Pilar (Bogotá). She studied Chemical Engineering at America University (Bogotá) and developed her thesis project "Bioethanol production in Cundinamarca Region" at Cundinamarca Liquors Company in Bogotá. She graduated in 2000.

From 2000 to 2002 she worked as a project engineer for a Bogota River remediation project at the NGO "Al Verde Vivo". In October 2002 she enrolled in the Environmental Science and Technology Master Programme at IHE Delft (Institute for water education). After completing her Master studies she joined the PDEng Trainee Programme on Bioprocess Design at Delft University of technology in September 2004. Her PDEng project "Conceptual process desing for the integration of fermentation, deacylation and crystallisation to produce β-lactam antibiotics" was carried out in cooperation between Delft University of Technology and DSM Anti-infectives (Delft). She completed the PDEng Programme in September 2006 and graduated on September 2007.

In September 2006 she started as a PhD student at the Biotechnology Department of Delft University of Technology under the supervision of Prof. Luuk van der Wielen and Dr. Adrie Straathof. As a PhD she studied the production of organic acids by fermentation and their recovery from the fermentation broth by cooling crystallisation. The results of that work are described in this thesis. Currently she is following a post-doctoral research for the production of bio-ethylene at Delft university of Technology in cooperation with State University of Campinas (Brazil).

Publications

Roa Engel CA, Straathof AJJ, Zijlmans TW, van Gulik WM, van der Wielen LAM (2008) Fumaric acid production by fermentation. Appl Microbiol Biotechnol (78) 379.

Roa Engel CA, Straathof AJJ, van Gulik WM, van de Sandt EJAX, van der Does T, van der Wielen LAM (2009) Conceptual process design of integrated fermentation, deacylation, and crystallization in the production of β-Lactam antibiotics. Ind Eng Chem Res (48) 4352.

Roa Engel CA, van Gulik WM, Marang L, van der Wielen LAM, Straathof AJJ. Development of low pH fermentation strategy for fumaric acid production by *Rhizopus oryzae*. *Submitted.*

Roa Engel CA, ter Horst JH, Pieterse M, van der Wielen LAM, Straathof AJJ. Solubility of fumaric acid and its sodium salts in the presence of fermentation co-solutes. *In preparation.*

Roa Engel CA, van Gulik WM, van der Wielen LAM, Straathof AJJ. Integration of fermentation and crystallisation in the production of fumaric acid. *In preparation*.

Acknowledgements

Firstly, I wish to thank my Promotor Prof. Luuk van der Wielen for giving me the opportunity to undertake this PhD research and for all his support and guidance. Luuk, thanks for believing in me and what I am capable of. You opened doors for me and I will always be thankful for those opportunities.

I also want to thank to my dearest and dedicated supervisor Adrie Straathof. Adrie, thanks very much for always being there to answer questions (despite the distance) and sharing with me all your knowledge. All those discussions we had have helped me to find the best solutions to the many different challenges I faced during my work. Thanks for all the time you spent reading my papers and for correcting my English. I learned a lot from you!

I wish to thank the sponsors of this project (B-Basic) and the user's committee Henk Noorman and Emile van de Sandt from DSM, Delft. Henk and Emile, thanks for your interest, contributions and the many interesting discussions during our B-Basic meetings. I also thank Ruud van der Pool from DSM, Delft for his technical support during the initial phase of my fermentation experiments. The B-Basic in-situ product removal team, Mark, Louise, Corjan and Jan Harm generated useful discussions and scientific ideas.

I would also like to thank all the Bachelors students that decided to carry out their projects under my supervision. Guido, thanks a lot for your good ideas, enthusiasm and pragmatism. Your results were very decisive for understanding the crystal formation in the fumarate system. Jan-Hein, thanks for your perseverance and for working hard with the metastable set up. Leonie, thanks a lot for all your dedication and interest in the project. I admire your discipline and self-sufficient way of working. Your fungi pellet study made an enormous contribution to the Chapter 3 of this thesis. Claire, thanks for your work on the crystal growth kinetics, and for being patient at stressful moments.

Many staff members also helped me during the development of my thesis. Susan, thank you very much for your help to start the fermentation experiments. And thanks for your positive energy. Mervin, thanks for all your valuable help in the crystallisation experiments, but also assistance, friendship and for your enthusiasm. Dirk, Rob, Cor, Angie, Stef, Max, Astrid, Apilena, Jos, Arno, Herman and Ronald, thanks for all the time, the patience, and for always being there to help me so kindly during my experiments. Sjaak, thanks for arranging so many things for me, for singing to me, smiling at me and making my day much better! Ginie, Robbert, Hans and Marcel, thanks for all support, help and kindness. Kawieta, thanks for all the time you spent arranging things for me and for sharing your energy and smile all time. Lies, Janine and Ger, thank you very much for the

opportunities, supporting talks, care and for your endless interest in my professional and personal life.

I want to thank to my TwAIO collegues Edwin, Paula, Jolanda, Beckley, David, Marco, Victor, Anil, Christos, Marta and Ines for all the discussions, support, friendship and so many good moments. To my BST people Çağri (dear brother), Beckley, Marijana (dear compañera), Marija, Marcel, Rob, Tangir, Arjen, Kedar, Xionan, Hermen and Arjan, thanks a lot for all the support, time, friendship, motivating talks and scientific inputs and discussions. Also I want to thank to my Kluyver collegues Marjan (thanks for all the water!), Lodewijk, André, Zheng, Rob, Aljoscha, Hilal, Sergio, Emrah, Michiel, Roeland, Jasper (thanks for the nice Colombian trip), Raymon, Leon, Wouter, Katja, Jiang, Marlies, Merle, Joost, Lucie, Sander and Jean Paul for the support, nice conversation and making a very pleasant working environment. Roelco, thanks for the friendship, supportive talks, good times and all the gezelligheid. *María, gracias por los buenos momentos que compartimos en la oficina (las carcajadas y el compañerismo), por compartir lo bueno y lo malo sin pedir nada a cambio construyendo asi nuestra amistad. Esteban, gracias por tu amistad y por ser siempre tu mismo*. Rutger, thanks for your unconditional support, presence, care, patience, serious and non-serious talks, laughs, criticism and for being always the loyal friend you are.

To my dear friends, Ewen, Lies, Marcos, Carla, Ljiljana, Erik, Emma, Angela, Gaetano, Maribel, Wim, Stef, Andreas, Taise, Nick and Marijke, thanks for being my daily life, my family and my wonderful moments in the Netherlands. John, Aga and Robbie, thanks for the great moments and constant support despite the distance. *Para meus queridos amigos ibéricos, Marta, Paulo, Margarida, Pedro, Julieta e Filipe, obrigada pelo tempo compartilhado, pela amizade e fazer-me sentir sempre em casa. Gracias a mis amigos, Paty, Cristhian, Sandra, Leo, Carlitos, Nathasja, Arlex y Edgar por el apoyo y las sonrisas compartidas. A minha comunidade Brasileira em Santos, Martha, Andrés, Eva e Nikolas obrigada pela amizade, apoio e os momentos bons durante a última etapa de minha tese. Claudia, mi hermana, gracias por siempre estar ahí escuchándome, apoyándome y dándome ánimos para seguir caminando. Bibis, gracias por el amor, la amistad y compinchería desde siempre y desde cualquier lugar. Teresa, Sandro y Marce, gracias por el apoyo, la energía positiva y los buenos momentos. Andresito, Liz y Javi, gracias por toda la fuerza, la familia, el coraje, por construir con amor cada segundo de mi vida hasta llegar aquí. Pilar, madre mía, decirte gracias nunca será suficiente para agradecer cada uno de tus esfuerzos y luchas por ayudarme a ser la mujer que soy. Pedrito, desde mi corazón, donde siempre estas y donde quiera que estés, te agradezco la lucha incansable y el amor inagotable que siguen llenando mi vida.*

Diego, mi leal compañero, gracias por tu amor, tu dedicación y por creer en mí cada día, cada momento. Sin tu apoyo y presencia en mi vida nunca hubiera logrado alcanzar mis sueños. Gracias por hacerme feliz!